This information product has been peer reviewed and approved for publication as a preprint by the U.S. Geological Survey.

Prepared in cooperation with Virginia Department of Environmental Quality

Investigation of Drivers and Sources of Potential Harmful Algal Blooms in Lake Anna, Virginia, 2023–24

By Carly M. Maas,[1] Brendan M. Foster,[1] Aliyah Downing[2], Margaret Mulholland[2]

[1]U.S. Geological Survey

[2]Old Dominion University

Acknowledgments

The authors want to give a special thanks to the numerous U.S. Geological Survey (USGS) staff that have contributed to the design, maintenance, and operation of this study. Special thanks to Douglas Chambers on the design of this project. This report was greatly improved by review comments from U.S. Geological Survey staff. Feedback from Alejandra Flota also greatly improved the report.

Outline

Figures

Figure 6. Bar charts of absolute (A, B, C) and relative abundance (D, E, F) of the potentially toxigenic cyanobacterial community across all three monitored Lake Anna stations from June 2023 to December 2024. Samples shown here were collected by both USGS and ODU. Refer to Table 1 for additional station information.
Figure 7. Time series of cyanobacteria toxin concentrations that were above the reporting limit from June 2023 until December 2024. Microcystin, Anatoxin-a, Cylindrospermopsin, and Saxitoxin were all analyzed, but only samples over the reporting limit are displayed. Microcystin (MCY) and Anatoxin-a (ATX-A) concentrations were the only two that exceeded their reporting limit of 0.15 μg/L. Refer to Table 1 for additional station information.
Figure 8. Time series of discrete chlorophyll-a samples at *A,* North Anna River (016701405), *B,* Pamunkey Creek (01670200), *C,* North Anna arm (01670144), *D,* Pamunkey Creek arm (01670209), *E,* the Confluence (016702576; U.S. Geological Survey, 2026) in the Lake Anna watershed in central Virginia, 2023–2024. Refer to Table 1 for additional station information.
Figure 9. Graphs showing the parametric linear relation between chlorophyll-a and total nitrogen (TN) and dissolved inorganic nitrogen (DIN) concentrations at *A,* North Anna River (016701405), *B,* Pamunkey Creek (01670200), *C,* North Anna arm (01670144), *D,* Pamunkey Creek arm (01670209), *E,* the Confluence (016702576; U.S. Geological Survey, 2026) in the Lake Anna watershed in central Virginia, 2023–2024. Refer to Table 1 for additional station information.
Figure 10. Graphs showing the parametric linear relation between chlorophyll-a concentration and total phosphorus (TP) and OP at *A,* North Anna River (016701405), *B,* Pamunkey Creek (01670200), *C,* North Anna arm (01670144), *D,* Pamunkey Creek arm (01670209), *E,* the Confluence (016702576; U.S. Geological Survey, 2026) in the Lake Anna watershed in central Virginia, 2023–2024. Refer to Table 1 for additional station information.
Figure 11. Graphs showing the time series of the total nitrogen to total phosphorus ratio of discrete samples collected at *A,* North Anna River (016701405), *B,* Pamunkey Creek (01670200), *C,* North Anna arm (01670144), *D,* Pamunkey Creek arm (01670209), *E,* the Confluence (016702576; U.S. Geological Survey, 2026) in the Lake Anna watershed in central Virginia, 2023–2024. A TN:TP ratio less than 9 (red dashed line) indicates that the water body is nitrogen limited. In between the dashed lines is when the TN:TP ratio is co-limiting. A sample with a TN:TP ratio greater than 22 is when the body of water is phosphorus limited. Refer to Table 1 for additional station information.
Figure 12. Results of global and pairwise permutational multivariate analysis of variance (PerMANOVA) statistical tests on relative abundance of cell densities for the total community (all taxa; top row), all cyanobacteria (cyanobacteria taxa only; middle row), and pTOX cyanobacteria (potentially toxic cyanobacteria taxa only; bottom row). Refer to Table 1 for additional station information. [* indicates a significant result with p-values ranging from <0.01–0.05, ** indicates a significant result with p-values ranging from <0.001–0.01 , *** indicates a significant result with p-values <0.001, ns indicates a non-significant result with p-values ≥ 0.05]
Figure 13. Bar chart showing the statistically significant drivers from the conditional random forest (CRF) and generalized additive model (GAM). The stacked bars show the number of models for which each driver was statistically significant, and the colors identify the model in which the driver was identified as statistically significant. The drivers included alkalinity (Alk), sodium (Na), total nitrogen (TN), total phosphorus (TP), suspended sediment concentration (SSC), wind speed, water temperature (WT), copper (Cu), iron (Fe), molybdenum (Mo), and nickel (Ni). Additional information is available about the stations used in these models in Table 1. Data used in these models are available at USGS Water Data for the Nation (U.S. Geological Survey, 2026).
Figure 14. Conceptual diagram of the environmental drivers associated with each of the five distinct algal community modeling approaches. The ellipses represent those key drivers of each model (i.e., algal

biomass, cyanobacteria, pTOX genera, *Raphidiopsis*, and pTOX excluding *Raphidiopsis*, in order from the most influential to the least influential driver. The percentages indicate the amount variance explained by the model. Additional information is available about the stations used in these models in Table 1. Data used in these models are available at USGS Water Data for the Nation (U.S. Geological Survey, 2026).

Figure 15. Partial effects plots from the generalized additive models of algal biomass (chlorophyll-a), cyanobacteria, pTOX genera, pTOX excluding *Raphidiopsis*, and *Raphidiopsis*. *A*, Alkalinity; *B*, Sodium (Na); *C*, Copper (Cu); *D*, Iron (Fe); *E*, Molybdenum (Mo); *F*, Nickel (Ni); *G*, Total Nitrogen (TN); *H*, Total phosphorus (TP); *I*, Suspended Sediment Concentration (SSC); *J*, Wind speed; *K*, Water temperature. The units are in milligrams per liter (mg/L) or micrograms per liter (µg/L), kilometers per hour (km/hr), and degrees Celsius (°C). Variables that were not statistically significant were not included in each model and were therefore not included in every plot. If the fitted value is above zero, the predictor is contributing more than its average contribution. If the fitted value is less than zero, the predictor is contributing less than its average contribution. The average contribution is at zero. Station information for the stations included in these models is found in Table 1. Data used in these models are available at USGS Water Data for the Nation (U.S. Geological Survey, 2026).

Figure 16. Time series of the discrete water quality data from North Anna River and Pamunkey Creek tributaries during 2023 –2024. Circle points represent baseflow and triangle points represent stormflow. Refer to Table 1 for additional station information.

Figure 17. Time series of discharge (in cubic feet per second, ft^3/s) with storm peaks identified as points (top); and estimated accumulated loads of suspended sediment, total nitrogen, and total phosphorus exported to Lake Anna from the North Anna River and Pamunkey Creek from June 1, 2023, through December 31, 2024 (bottom). Refer to Table 1 for additional station information.

Figure 18. Baseflow and stormflow load contribution percentages of suspended sediment, total nitrogen, and total phosphorus exported by the North Anna River and Pamunkey Creek from June 1, 2023, through December 31, 2024. Bar magnitudes represent the total load of each constituent at each station, and the percentages within each bar represent the proportion of each constituent load delivered during baseflow (yellow) and stormflow (purple). Refer to Table 1 for additional station information.

Figure 19. Time series of estimated suspended sediment load (top), total nitrogen load (middle), and total phosphorus load (bottom) at the North Anna River (grey) and Pamunkey Creek (orange). All plots show total cell densities (green points) and potentially toxic cell counts (blue points) at their respective lake stations (North Anna arm and Pamunkey Creek arm). Refer to Table 1 for additional station information.

Figure 20. Estimated constituent yields at North Anna River and Pamunkey Creek during water year 2024 from October 1, 2023, through September 30, 2024. Refer to Table 1 for additional station information.

Figure 21. Stable isotope of nitrogen ($\delta^{15}N\text{-}NO_3^-$) and oxygen ($\delta^{18}O\text{-}NO_3^-$) from the North Anna River (grey Points) and Pamunkey Creek (orange points) from 2023 – 2024. Characteristic source ranges (bounding boxes) referenced from Kendall and others (2007), Granger and others (2010), and Snow (2018). Refer to Table 1 for additional station information.

Figure 22. Boxplots of estimated nitrate apportionment from stable isotope mixing model from the North Anna River (grey boxplots) and Pamunkey Creek (orange boxplots) during 2023–2024. Refer to Table 1 for additional station information.

Figure 23. Boxplot showing the bed-sediment concentrations of select constituents identified from the GAMs to have a potential relation with algal biomass and community composition from the three locations in Lake Anna in central Virginia. The n = 30 for all parameters. The boxes represent the interquartile range, with the bottom part of the box at the 25th percentile and the top part of the box at the 75th percentile. The whiskers extend from the minimum, at lower concentrations, and the maximum, at higher concentrations. The points outside the box and whiskers are outliers. Refer to Table 4 for additional station information.

Figure 24. Bottom shear stress versus maximum wave height by station and season across calendar year 2024. Data points represent 15-minute interval bottom shear stress and maximum wave height data. Gray points indicate that the bottom shear stress was less than or equal to the critical shear stress (i.e., no sediment resuspension) and red points indicate that bottom shear stress was greater than the critical shear stress (i.e., sediment resuspension). Data from Vande Pol and others (2026).
Figure 25. The proportion of days in each season and at each station in which at least one wave was generated that could resuspend lake-bottom sediment (i.e., lake-bottom shear stress was greater than critical shear stress). Refer to Table 1 for additional station information.
Figure 26. Graphs showing the 15-minute interval lake-bottom shear stress versus average wind speed. Red points show waves where lake-bottom shear stress was greater than critical shear stress and grey points when a wave that were less than or equal to critical shear stress. Refer to Table 1 for additional station information.
Figure 27. Plots of 15-minute interval lake-bottom shear stress versus maximum wave heights by station during the high residential occupancy and boating activity (HROB) and low residential occupancy and boating activity (LROB) water quality sampling events. The dashed lines represented the critical shear stress value for each station. Grey points represent wave were estimated to not resuspend lake bed sediments and red points represent waves that were estimated to resuspend lake bed sediments. Refer to Table 1 for additional station information.
Figure 28. Boxplots of suspended sediment concentrations during the high residential occupancy and boating activity (HROB) and low residential occupancy and boating activity (LROB) water quality sampling events. [* indicates a significant results with p-values ranging from <0.01-0.05, ** indicates a significant result with p-values ranging from <0.001-0.01 , *** indicates a significant result with p-values <0.001, ns indicates a non-significant result with p-values ≥ 0.05]. Refer to Table 1 for additional station information.
Figure 29. Differences in water temperature per meter of vertical profile plotted as a function of depth and longitudinal distance from the mouth of the tributary for the North Anna arm, Pamunkey Creek arm, and Confluence across six sampling periods (Summer 2023, Fall 2023, Winter 2024, Spring 2024, Summer 2024, and Fall 2024). The y-axis is depth, with 0 m at the surface of the lake. Refer to Table 4 for additional station information.
Figure 30. Dissolved oxygen (DO) profiles plotted as a function of depth and longitudinal distance from the mouth of the tributary for the North Anna arm, Pamunkey Creek arm, and Confluence across six sampling periods (summer 2023, Fall 2023, Winter 2024, Spring 2024, Summer 2024, and Fall 2024). The black line indicates areas of hypoxic conditions. The y-axis is the depth, with 0 m at the surface of the lake. Refer to Table 4 for additional station information.
Figure 31. Absolute abundance and relative abundance of phyla for agricultural, residential, and forested land use during low- and high-occupancy periods from the lake shore at 0 m to the mid-channel. Sample collected along the transect during the low-occupancy period were collected on 4/30/2024 and 5/01/2024. Sample collected along the transect during the high occupancy period were collected on 8/13/2024. Refer to Table 3 for additional station information.
Figure 32. Absolute abundance and relative abundance of pTOX for agricultural, residential, and forested land use during low- and high-occupancy periods. Sample collected along the transect during the low-occupancy period were collected on 4/30/2024 and 5/01/2024. Sample collected along the transect during the high occupancy period were collected on 8/13/2024. Refer to Table 3 for additional station information.
Figure 33. Graphs showing the total concentrations for agricultural, residential, and forested land use during low- and high-occupancy periods across the transects. The x-axis represents the distance from shoreline. Sample collected along the transect during the low-occupancy period were collected on 4/30/2024 and 5/01/2024. Sample collected along the transect during the high occupancy period were collected on 8/13/2024. Refer to Table 3 for additional station information.

Tables

in each model were identified using conditional random forest and generalized additive models. Superscripted values next to each parameter indicated the variance explained by each parameter. The R^2 value indicates the total variance explained by each model. Station information for the stations included in these models is found in Table 1. Data used in these models are available at USGS Water Data for the Nation (U.S. Geological Survey, 2026).

Appendix Table 3.1. Summary of the median analyte concentrations of the Lake Anna bed sediment within the North Anna River arm, Pamunkey Creek arm, Confluence, and the entire lake. Refer to Table 4 for additional site information.

Appendix Table 3.2. Summary of the median and standard deviation for the near-shore transects during low- and high-occupancy periods across agricultural, forested, and residential land uses. Refer to Table 3 for additional information.

Conversion Factors

U.S. customary units to International System of Units

Multiply	By	To obtain
	Length	
foot (ft)	0.3048	meter (m)
mile (mi)	1.609	kilometer (km)
	Area	
square mile (mi^2)	259.0	hectare (ha)
square mile (mi^2)	2.590	square kilometer (km^2)
	Volume	
acre-foot (acre-ft)	1,233	cubic meter (m^3)
acre-foot (acre-ft)	0.001233	cubic hectometer (hm^3)
	Flow rate	
mile per hour (mi/h)	1.609	kilometer per hour (km/h)
	Mass	
pound, avoirdupois (lb)	0.4536	kilogram (kg)

International System of Units to U.S. customary units

Multiply	By	To obtain
	Length	
millimeter (mm)	0.03937	inch (in.)
meter (m)	3.281	foot (ft)
kilometer (km)	0.6214	mile (mi)
kilometer (km)	0.5400	mile, nautical (nmi)
meter (m)	1.094	yard (yd)
	Area	
square kilometer (km^2)	247.1	acre
square kilometer (km^2)	0.3861	square mile (mi^2)
	Volume	
liter (L)	33.81402	ounce, fluid (fl. oz)
liter (L)	2.113	pint (pt)
liter (L)	1.057	quart (qt)

Multiply	By	To obtain
liter (L)	0.2642	gallon (gal)
liter (L)	61.02	cubic inch (in^3)
	Mass	
gram (g)	0.03527	ounce, avoirdupois (oz)
	Pressure	
kilopascal (kPa)	0.009869	atmosphere, standard (atm)
kilopascal (kPa)	0.01	bar
kilopascal (kPa)	0.2961	inch of mercury at 60°F (in Hg)
kilopascal (kPa)	0.1450	pound-force per inch (lbf/in)
kilopascal (kPa)	20.88	pound per square foot (lb/ft^2)
kilopascal (kPa)	0.1450	pound per square inch (lb/ft^2)

Temperature in degrees Celsius (°C) may be converted to degrees Fahrenheit (°F) as follows:

°F = (1.8 × °C) + 32.

Temperature in degrees Fahrenheit (°F) may be converted to degrees Celsius (°C) as follows:

°C = (°F – 32) / 1.8.

Datums

Vertical coordinate information is referenced to the [insert datum name (and abbreviation) here; for example, North American Vertical Datum of 1988 (NAVD 88)].

Horizontal coordinate information is referenced to the [insert datum name (and abbreviation) here; for example, North American Datum of 1983 (NAD 83)].

Supplemental Information

Specific conductance is in microsiemens per centimeter at 25 degrees Celsius (µS/cm at 25 °C).

Concentrations of chemical constituents in water are in either milligrams per liter (mg/L) or micrograms per liter (µg/L).

A water year is the 12-month period from October 1 through September 30 of the following year and is designated by the calendar year in which it ends.

Abbreviations

CAAS	Cube automated ELISA System
CCM	Carbon concentrating mechanisms
CRF	Conditional random forest
Cu	Copper
CVI	Conditional variable importance
DCLS	Division of Consolidated Laboratory Services
DEQ	Virginia Department of Environmental Quality
DIC	Dissolved organic carbon
DIN	Dissolved inorganic nitrogen
DO	Dissolved oxygen
ELISA	Enzyme linked immunosorbent assay
EPA	U.S. Environmental Protection Agency
Fe	Iron
GAM	Generalized additive model
HAB	Harmful algal bloom
HDPE	High density polyurethane
HROB	High residential occupancy and boating activity
LROB	Low residential occupancy and boating activity

MBAS	Methylene blue active substances
Mo	Molybdenum
N	Nitrogen
Ni	Nickel
NO_3^-	Nitrate
ODU	Old Dominion University
OP	Orthophosphate
P	Phosphorus
PEP	Partial effect plots
PerMANOVA	Permutational multivariate analysis of variance
ppb	Parts per billion
ppt	Parts per thousand
pTOX	Potentially toxigenic cyanobacteria genera
REML	Restricted maximum likelihood
SC	Specific conductance
SIMM	Stable isotope mixing model
SSC	Suspended sediment concentrations
TB	Turbidity
TN	Total nitrogen

TP	Total phosphorus
USGS	U.S. Geological Survey
VDH	Virginia Department of Health
YSI	Yellow Springs Instrument
τ_b	Lake bottom shear stress
τ_{cr}	Critical shear stress

Abstract

Algal blooms in freshwater reservoirs are an increasing concern because of the risk to aquatic ecosystem health, recreational use, and water quality. Among the taxa that comprise an algal bloom, cyanobacteria are of particular concern due to the potential to produce toxic compounds which can cause acute and chronic illness in humans if ingested through contaminated water or shellfish. When toxins are above a toxin-specific threshold in the water column, the Commonwealth of Virginia categorizes the bloom as a harmful algal bloom (HAB), distinguishing it from an algal bloom without toxins present. Toxins are of particular concern in bodies of water which serve as major recreational areas, such as Lake Anna in central Virginia. Lake Anna is a 27 km-long and 47 km^2 reservoir in central Virginia. Since the Commonwealth of Virginia revised the HAB monitoring framework in 2018, algal bloom advisories for potentially toxigenic blooms have been issued in the western, riverine zone of the reservoir. There were detections of microcystin and anatoxin production but no detections of cylindrospermopsin and saxitoxin production in Lake Anna; however, toxin concentrations were low, at values less than 0.65 µg/L.

In 2023, the U.S. Geological Survey, in cooperation with Virginia Department of Environmental Quality, initiated a 19-month intensive and extensive study of western Lake Anna and its tributaries (North Anna River and Pamunkey Creek) to (1) characterize the algal community, biomass, and toxin production; (2) identify potential drivers leading to algal bloom initiation, persistence, and decline; and (3) assess the primary sources of the drivers contributing to algal blooms. Continuous and discrete monitoring of water quality within the lake, watershed inputs, meteorological conditions, and algal communities were monitored.

Multiple modeling scenarios identified that the formation and persistence of algal blooms in Lake Anna are driven by interactions among chemical, macro- and micronutrient, and physical factors. Key drivers include total nitrogen, total phosphorus, water temperature, suspended sediment concentration, wind speed, copper, iron, molybdenum, nickel, sodium, and alkalinity. During this study, winter stormflow events delivered the highest loading of macro- and micronutrients from the tributaries to the lake. The lake is a sink for these nutrients in the water column or in the lake-bed sediments. During high-occupancy and recreation periods on the lake in the summer months, boating activity can promote internal loading by the resuspension of the lake-bed sediments, thereby increasing the nutrient availability for algal uptake. Thermal stratification and hypoxic conditions were observed, which can contribute to the passive release of nutrients into the water column, further facilitating algal bloom proliferation. These processes may create a positive feedback loop that supports the formation, persistence, and annual recurrence of algal blooms in the western region of Lake Anna. Continued water-quality monitoring of early warning indicators may improve the detection and forecasting of algal growth in the lake and help managers proactively manage water quality and algal growth.

Plain Language Summary

Algal blooms are an increasingly global threat to freshwater lakes and reservoirs due to their adverse effects on aquatic organisms, recreation, drinking water resources, agriculture, and local economies. Additionally, algal blooms can produce toxic compounds that are harmful to human health when ingested and have been linked to the deaths of pets and livestock. Algal blooms often occur during warm, summer months when human recreation is at its highest, which poses a threat to public health and safety.

Located in central Virginia, the Lake Anna reservoir has experienced potentially toxic algal blooms since monitoring began in 2018. To address this issue, the U.S. Geological Survey, in cooperation with Virginia Department of Environmental Quality, conducted a 19-month study beginning in May 2023 to investigate local factors contributing to these recurring algal blooms. Monitoring the water quality at multiple stations in the Lake Anna watershed facilitated analyses to (1) characterize the algal community, biomass, and toxin production; (2) identify potential drivers leading to algal bloom initiation, persistence, and decline; and (3) assess the primary sources of the drivers contributing to algal blooms.

The study found that key drivers of algal growth include nitrogen, phosphorus, water temperature, wind speed, suspended sediment, alkalinity, sodium, and trace metals. Heavy precipitation during winter months transported nutrients and other materials into the lake from the tributaries which settled into the lake-bed sediment. During the summer months, boating activity, wind, and waves stirred the nutrients and trace metals back into the water, helping algal blooms develop and persist. Low dissolved oxygen and changes in water temperature from the surface of the lake to the bottom of the water column can promote the release of nutrients from the sediment. Together, these processes can provide favorable conditions for algal blooms to thrive. Implementing continuous monitoring of water quality may support early warning systems of HABs and facilitate proactive management for public health safety.

Introduction

Algal blooms are increasingly recognized as a global environmental threat to aquatic resources. Across marine and freshwater settings, algal blooms cause ecological, economic, and public health concerns (Igwaran and others, 2024; Leiker and others, 2021). Algal blooms can degrade drinking water supplies, limit agricultural use, reduce property value, discolor water, produce foul odors, and be exported to adjacent terrestrial ecosystems (Dodds and others, 2008; Feng and others, 2024a; Gorney and others, 2023b; Graham and others, 2016; Griffith and Gobler, 2020; Igwaran and others, 2024; Lee and others, 2017; Mishra and others, 2023; Moy and others, 2016). In freshwater systems, cyanobacteria, also called blue-green algae, can dominate algal blooms in systems with a high concentration of nutrients, low water clarity, and warm waters (Beaver and others, 2018; O'Neil and others, 2012; Paerl and others, 2001; Wiltsie and others, 2018). Some bloom-forming genera of cyanobacteria can release toxic secondary metabolites called cyanotoxins that can cause acute and chronic effects in mammals which affect the liver, digestive, endocrine, dermal, and nervous systems (Feng and others, 2024a; Paerl and Otten, 2013). In the Commonwealth of Virginia, a harmful algal bloom (HAB) is defined as algae and cyanobacteria that produce toxins which may adversely affect human health through ingestion of contaminated water or shellfish (Commonwealth of Virginia, 2021). Therefore, these ecological, economical, and potential human health effects emphasize the need to understand and monitor algal bloom formation, persistence, and decline in freshwater bodies.

Excess nutrients from anthropogenic sources, warm water temperatures, and light availability are well-established drivers of freshwater algal biomass occurrence and intensity (Feng and others, 2024b; Murphy and others, 2025; O'Neil and others, 2012). There are several different drivers that have been attributed to the growth and proliferation of algal biomass, including organic matter, iron and trace elements, conductivity and salinity, turbulence, residence times, stratification, water column stability, interactions with the food web, human introduction and displacement of species, and climate change (Paerl and others, 2001). In lakes, the growth and accumulation of potential HAB-forming algae and cyanobacteria depend also on sources of macronutrients and micronutrients, inputs from external delivery pathways, and passive and active internal (or, within lake) processes (Iiames and others, 2021). External delivery of macro- and micronutrients from the watershed to the lake can depend upon precipitation duration and intensity, varying runoff pathways, and sediment delivery (Busse and others, 2006; Iiames and others, 2021; Mrdjen and others, 2018). Near-shore nutrient sources, including septic systems, lawn fertilizers, and agricultural activities, might contribute to proliferation of algal communities. Internal, in-lake processes can also affect lake macro- and micro-nutrient concentrations. Internal loading of nutrients generally occurs through either passive nutrient diffusion across the lake-bed sediment-water interface during thermal stratification or hypoxia events, or through active sediment resuspension caused by physical turbulence, including wind-induced mixing, bioturbation, and boat wakes (Anthony and Downing, 2003; Gautreau and others, 2020; Gerhardt and Schink, 2005; Tang and others, 2020).

Lake Anna, a heavily recreated, shallow reservoir located in central Virginia, has had consistently elevated cell counts of potentially toxigenic planktonic cyanobacteria genera resulting in swimming advisories from the Virginia Department of Health (VDH). Since monitoring began in 2018, cyanobacteria cell counts of potentially toxigenic taxa have been reported above the threshold of 100,000 cells/mL that the Virginia Department of Health (VDH) used prior to 2025 for issuing recreational advisories (Department of Environmental Quality, 2021). These elevated counts have prompted annual HAB advisories, or “No Swim” recreational advisories recommended by VDH. Despite these recurring issues, relatively little published literature is available on the composition and the potential toxicity of the blooms at Lake Anna.

From May 2023 through December 2024, the U.S. Geological Survey, in cooperation with Virginia Department of Environmental Quality, began a study to collect and analyze meteorological, water quality, water quantity, chemical, and biological data from the western portion of Lake Anna and two major tributaries (North Anna River and Pamunkey Creek). The study also investigated driver inputs from external watershed sources as well as internal passive and active sediment-nutrient loading, stratification, and hypoxia.

Purpose and Scope

Despite extensive research on algal and cyanobacterial blooms, there is a limited understanding of the complex interactions that cause potentially toxic cyanobacterial taxa to dominate in shallow, highly recreated reservoirs such as Lake Anna. Additionally, the roles of internal and external loading, storm driven inputs, trace metal availability, and physical mixing on cyanobacterial community composition in algal bloom development are often studied independently. This report collectively identifies and describes the drivers and sources influencing potentially toxigenic cyanobacterial bloom events in the western region of Lake Anna, Virginia. This study spans May 2023 through December 2024 with data collected by federal (U.S. Geological Survey), state (Virginia Department of Environmental Quality), and academic (Old Dominion University) collaborators. Potential drivers of cyanobacterial dominance were identified using conditional random forest and generalized additive models. The mechanistic processes influencing these drivers were identified through studies targeting specific internal and external loading processes.

The purpose of this report is to:

(1) Characterize the algal community, biomass, and toxin production;

(2) Identify potential drivers leading to algal bloom initiation, persistence, and decline; and

(3) Assess the primary sources of the drivers contributing to algal blooms

The scope of the work at Lake Anna includes an intensive, multi-method monitoring program that integrates continuous instruments and discrete sampling in the tributaries and on the lake itself. The study area encompasses the western area of Lake Anna where recreational advisories occurred from 2018 through 2024, which includes the watershed up-lake of the confluence of the North Anna and Pamunkey arms of the reservoir and the North Anna River and Pamunkey Creek watersheds.

Description of Study the Area

Lake Anna is a 0.60 km^3, 27-km long and 47 km^2 reservoir located in central Virginia (Figure 1). Lake Anna was created in 1972 when the North Anna River was impounded by a 30.5-m-tall earthen dam (U.S. Army Corps of Engineers, 2024) to form a cooling-water supply for the North Anna Power Station (NAPS) and recreational areas (Odhiambo and Ricker, 2012). Lake Anna is a relatively shallow reservoir, with the maximum depth in the entire reservoir at 24 m and the mean depth is 8 m (Parker and Voshell Jr., 1983). The reservoir spans Orange, Spotsylvania, and Louisa Counties and is within the York River watershed. The Lake Anna watershed is situated within the Piedmont physiographic province of Virginia (Odhiambo and Ricker, 2012). The bedrock in this region includes granite, metamorphic granite gneiss, and mica schist bedrock (Odhiambo and Ricker, 2012).

The land use in the Lake Anna study area is dominated by forest (61 percent) and agriculture (26 percent) (U.S. Geological Survey, 2019). Historically, many of the forests were cleared for cropland and other agricultural activities. There is also significant mining history in the area, including mining for pyrite (1834–1920), copper, and sulfur (until 1877) but mining operations in the watershed ceased in the early 1990s (Odhiambo and others, 2013). More recently, some of the land is now being converted from farmland into residential and commercial centers (7 percent) (Odhiambo and others, 2013; U.S. Geological Survey, 2019). Lake Anna is a heavily recreated lake, with five marinas and many pontoon, ski boat, and jet ski rental operations across the lake (Phillips, 2017; Lake Anna, 2026). The peak recreation season is from June through August, with the peak around July 4th and Labor Day (Lake Anna, 2026).

The study area included the North Anna River and its watershed, the Pamunkey Creek River and its watershed, and the lake from the mouth of those rivers to the confluence of the North Anna and Pamunkey arms in the western portion of Lake Anna. The study area matches the area that has historically been subjected to recreational advisories by VDH (Robertson, 2025). The drainage area for the entire study area is 665 km^2 (U.S. Geological Survey, 2019). There are six USGS continuous monitoring locations throughout the watershed: 1 meteorological station, 2 tributary stations, and 3 lake stations (Figure 1).

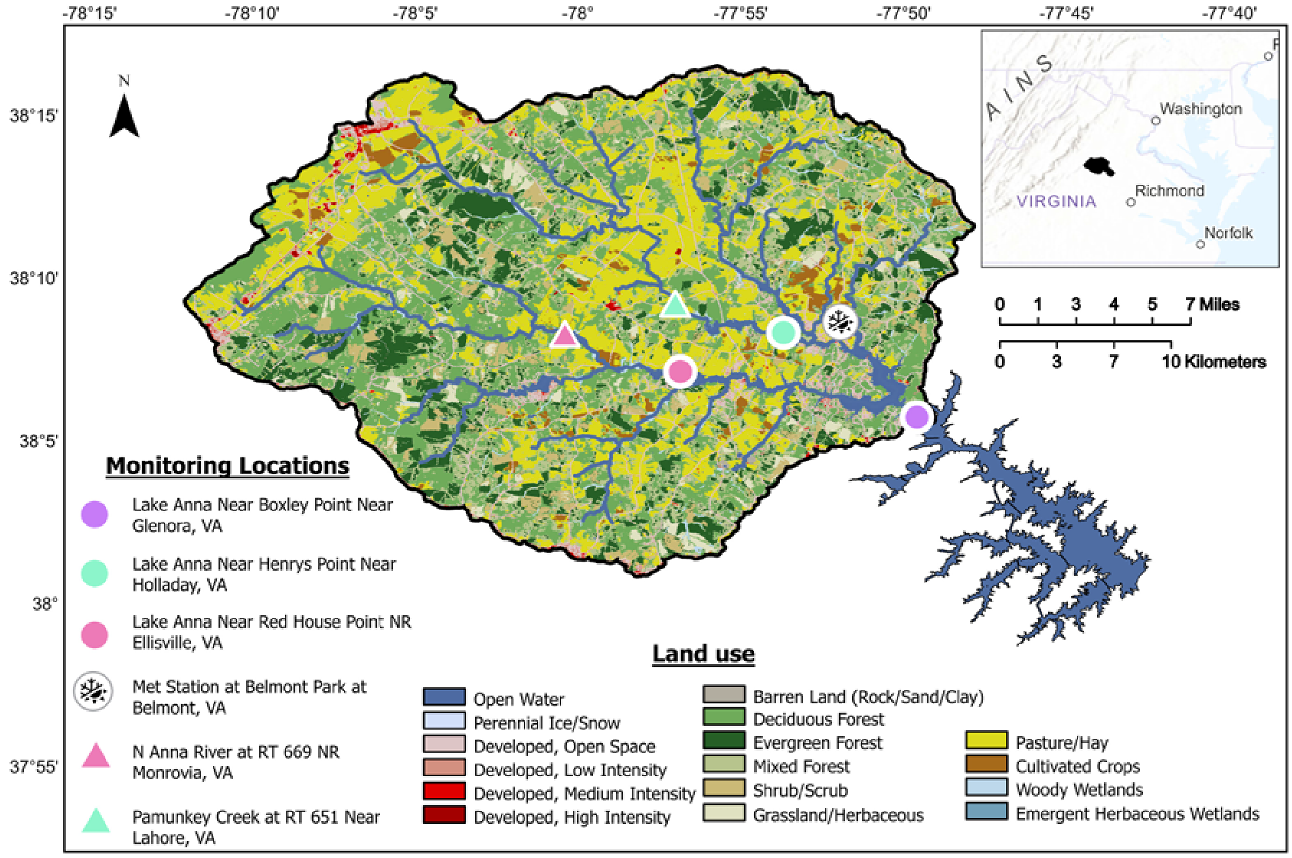

Base map from ESRI; National Land Cover Data from Multi-Resolution Land Characteristics Consortium; Watershed boundary from USGS Water for the Nation; Streams from Streamstats and USGS Water for the Nation; Outline of Lake Anna from DEQ.

Index map base from ERSI, Watershed boundary from USGS Water for the Nation; Outline of Lake Anna from DEQ.

Geographic Coordinate systems

North American Datum of 1983

Figure 1. Map of U.S. Geological Survey (USGS) water-quality and meteorological monitoring stations within the Lake Anna watershed in central Virginia. Station names and numbers are defined in table 1. Additional station information is available through the USGS Water Data for the Nation (U.S. Geological Survey, 2026). Land cover data from U.S. Geological Survey (2024).

Table 1. Description of the six U.S. Geological Survey water-quality and meteorological monitoring stations (U.S. Geological Survey, 2026) within the Lake Anna watershed in central Virginia.

[PAR, Photosynthetic Active Radiation; WT, water temperature; TB, turbidity; DO, dissolved oxygen; SC, specific conductance; CYAN, cyanobacteria; GA, green algae; CRY, cryptophytes; DIA, diatoms; UP, unbound phycocyanin]

USGS Station number	USGS station name	Shortened station name	Instrument	Measurement	Measurement Interval
380839077515701	Met Station at Belmont Park at Belmont, VA	Belmont Met Station	Ott Pluvio2L Apogee ePAR Sensor R.M. Young Wind Monitor	Precipitation PAR Wind Speed, Wind Direction	5-minutes
016701405	N Anna River at RT 669 NR Monrovia, VA	North Anna River	Sutron constant flow bubbler YSI EXO3 Seabird SUNA	Stage WT, pH, TB, DO, SC, Nitrate	15-minutes
01670200	Pamunkey Creek at RT 651 near Lahore, VA	Pamunkey Creek	Sutron constant flow bubbler YSI EXO3 Seabird SUNA	Stage WT, pH, TB, DO, SC, Nitrate	15-minutes
01670144	Lake Anna Near Red House Point nr Ellisville, VA	North Anna arm	RBRsolo3 R.M. Young Wind Monitor YSI EXO3 bbe Moldanke PhycoProbe	Depth, Pressure Wind Speed, Wind Direction WT, pH, TB, DO, SC CYAN, GA, CRY, DIA, UP	0.25-seconds 5-minutes 15-minutes 15-minutes
01670209	Lake Anna Near Henrys point Near Holladay, VA	Pamunkey Creek arm	RBRsolo3, YSI EXO3, bbe Moldanke PhycoProbe	Depth, Pressure, WT, pH, TB, DO, SC, CYAN, GA, CRY, DIA, UP	0.25-seconds 15-minutes 15-minutes
016702576	Lake Anna Near Boxley Point Near Glenora, VA	Confluence	RBRsolo3, YSI EXO3, bbe Moldanke PhycoProbe	Depth, Pressure WT, pH, TB, DO, SC CYAN, GA, CRY, DIA, UP	0.25-seconds 15-minutes 15-minutes

Data Collection and Statistical Methods

Data were collected using a combination of continuous meteorological, water-quality, streamflow, and biological sensors; discrete data collected for water-quality, phytoplankton, and toxins; near-shore transects; and in-lake synoptic surveys. All data are publicly available through Vande Pol and others (2026) and in the USGS Water Data for the Nation (U.S. Geological Survey, 2026).

Characterization of Algal Community, Biomass, and Toxins

A combination of continuous algal monitoring and year-round, high-frequency discrete sampling was used to characterize algal community, biomass, and toxins over time in Lake Anna. All analytes from discrete sample collection were analyzed by Old Dominion University. Descriptive statistical analyses were conducted between the chlorophyll-a concentrations and nutrients. Statistical analysis was applied to determine if the algal community was statistically similar throughout the watershed.

Data Collection and Laboratory Analysis

A photosynthetic pigment fluorometer (bbe Moldanke, Raisdorf, Germany, PhycoProbe), an *in situ* sensor that characterizes algal community concentrations every 15-minutes, was deployed on November 16, 2023, at the North Anna and Pamunkey arms and on November 17, 2023 at the Confluence (Stauffer and others, 2019). The PhycoProbe uses multichannel excitation and fluorescence to differentiate algal classes, including blue-green algae, green algae, cryptophytes, diatoms, and unbound phycocyanin, based on the pigment signature (Stauffer and others, 2019). A detailed analysis of the bbe Moldanke PhycoProbe continuous data results is not included in this report.

Discrete samples were collected at the three continuous monitoring stations on Lake Anna by both USGS and ODU from June 2023 through December 2024 to produce a high-frequency dataset of phytoplankton community, biomass, and toxins. Samples were collected on the lake on a seasonally variable schedule. From May through September, USGS and ODU both collected samples twice per month on alternating weeks, yielding a weekly interval dataset. From October through April, samples were collected once per month, alternating bi-weekly, yielding a two-week interval dataset. However, the sample collection methodology and analytes analyzed differed between USGS and ODU. USGS collected field parameter depth profiles and obtained discrete samples that were either integrated throughout the entire water column or two separate samples near the surface and the bottom, depending on whether thermal stratification was present. The samples were analyzed for water-quality and biological parameters. ODU identified the location of the peak algal biomass in the water column and collected samples at that depth for the analysis of biological parameters.

USGS Field Sampling Methods: Phytoplankton and Toxin Sample Collection

Discrete biological samples were collected in the field at each station on a dock near the continuous monitoring stations. Before sample collection, the Secchi disk depth and the depth to the bed sediments were determined. Due to the shallow nature of each station, a depth profile was collected with a YSI Inc. (Yellow Springs, Ohio) EXO3 water quality sonde at three equidistant locations within the water column for water temperature (WT), specific conductance (SC), dissolved oxygen (DO), pH, and turbidity (TB). Each station was assessed for thermal stratification, defined here as the presence of a temperature change greater than 1.0 degree

Celsius per meter (°C/m; Wetzel, 2001). When the lake station was not stratified, water samples were collected at the three depths for which the field parameters were collected using a 1.2-liter (L) acid-rinsed Kemmerer sampler and composited in a 14-L churn splitter. When the lake station was stratified, discrete hypolimnetic and epilimnetic samples were collected, processed, and analyzed in separate 14-L churns. The biological analytes include photosynthetic pigments, algal identification, algal enumeration, and cyanotoxin (*e.g.*, anatoxin, saxitoxin, microcystin, and cylindrospermopsin) concentrations (Appendix Table 1.1). All samples were immediately processed in the field. Sample bottles were triple rinsed with deionized (DI) water and native rinsed once. All samples were stored on ice and in the dark until they were transported to the laboratory. At each station, 3 replicates and 2 blanks were collected throughout the duration of the study.

Supplemental Phytoplankton and Toxin Sample Collection

Discrete water was collected for phytoplankton and toxin samples at each station near the dock by boat using acid-cleaned 10-L high density polyurethane (HDPE) carboys and a peristaltic pump. The pump tubing was flushed for 2 minutes prior to sample collection to minimize contamination. Before use, carboys were rinsed three times with station water to remove residual acid. At each lake station, one discrete water sample was collected at the depth with maximum chlorophyll-a concentration determined using a YSI EXO2 sonde and YSI Total Algae probe. From each station's carboy, a phytoplankton sample was poured into a 500 mL HDPE bottle with Lugol's iodine with a final concentration of about 1 percent. Preserved samples were stored at room temperature with minimum light exposure to avoid photo-oxidation. For toxin sample collection, station water from each station carboy was transferred into glass amber bottles, placed on ice packs in a cooler (less than or equal to 10°C), and transported back to the Phytoplankton Analysis Laboratory at ODU. At ODU, manufacturer's instructions for the Cube Automated ELISA System (CAAS Cube; Gold Standard Diagnostics Horsham, Inc., Horsham, Pennsylvania) and ABRAXIS Enzyme-Linked Immunosorbent assays (ELISA) toxin kits were followed to analyze samples for each cyanotoxin, including anatoxin-a (ABRAXIS, 2023a), saxitoxin (ABRAXIS, 2023d), microcystin (ABRAXIS, 2023c), and cylindrospermopsin (ABRAXIS, 2023b) .

Phytoplankton and Toxin Laboratory Analysis

Upon arrival at ODU, USGS and ODU toxin samples were stored for ≤ 149-days in a -80 °C freezer until batch analysis could be conducted. To prepare samples for total toxin analysis prior to analyses, which includes intra- and extra- cellular toxins, the cells were lysed using the freeze-thaw method to free cell-bound (intra-cellular) toxins into the liquid matrix (Loftin and others, 2008). Sample preparation required reducing the sample size by 25 percent of the container capacity and freeze then thaw samples three times in an approximately 35°C water bath, making sure all samples were completely thawed before re-freezing until the cycle was complete. After completion of the freeze-thaw method, toxin samples were then decanted into 3.7 mL amber glass vials and loaded into the CAAS Cube for toxin analysis. Algal toxins, including saxitoxin, anatoxin-a, microcystins, and cylindrospermopsin were analyzed in duplicates and plates were analyzed according to manufacturer suggestions (Storm User's Manual for the CAAS Cube, 2021).

Each toxin assay has specific method detection limits (MDL) and method reporting limits (MRL): microcystins (0.10/0.15 μg/L), anatoxin-a (0.10/0.15 μg/L), cylindrospermopsin (0.04/0.05 μg/L), and saxitoxin (0.015/0.02 μg/L). The concentrations of each test are determined by using a standard curve that is run with each assay. To validate and accept results from each toxin assay run (1) the coefficient of determination (R^2) for the standard curve was greater than or equal to 0.98; (2) the laboratory reagent blank and control were in a detectable range; and (3) the coefficient of variation for samples was less than 15 percent and the standard curve coefficient of variation was less than 10 percent for each test (ABRAXIS 2023a–d). Only toxin results meeting these criteria were retained for reporting and interpretation. Samples that did not pass all three criteria were rejected and rerun on a new assay. There were no samples that exceeded the highest standard; therefore, dilution was not necessary (Karlson and others, 2010).

The phytoplankton community composition was estimated using discrete whole water samples. Enumeration was performed using an Olympus Corporation (Tokyo, Japan) CKX41 inverted microscope equipped with phase contrast and a Palmer-Maloney counting cell (Karlson and others, 2010). Phytoplankton were identified to the lowest taxonomic level using features described by Komárek (2008), Komárek (2013), Komárek and Anagnostidis (2005), and Wehr and Sheath, (2015). Samples were determined to be potentially toxigenic genera (pTOX) of cyanobacteria based on a list compiled by the Virginia Department of Health (VDH; Table 2) and reviewed by state and federal HAB experts (Chorus and Welker, 2021a).

Table 2. Adapted Regional list of potentially toxigenic (pTOX) taxa from the Virginia Department of Health (Virginia Department of Health, 2021).

Genus
Anabaena
Anabaenopsis
Aphanizomenon
Chrysosporum
Cuspidothrix
Dolichospermum
Lyngbya
Microcoleus
Microcystis
Microseira
Nodularia
Nostoc
Oscillatoria
Phormidium
Planktothrix
Raphidiopsis
Sphaerospermopsis
Woronichinia

Phytoplankton abundances were analyzed microscopically using natural counting unit criteria and enumerated and reported in cells per milliliter (Karlson and others, 2010). A natural counting unit is defined as a natural grouping of algae, including a filament (such as *Pseudanabaena*), a single cell (such as centric diatoms), or a colony (such as *Microcystis*). Cells per milliliter were calculated as the number of cells within each natural counting unit, and broken cells were excluded. For consistency with concurrent DEQ and VDH sample analysis, the concentration of the sample bottle was not increased prior to enumeration (Charles and others, 2002; Karlson and others, 2010). A minimum of 300 natural counting units were enumerated per sample. If there were less than 300 natural counting units in a single Palmer-Maloney chamber, additional chambers were counted until the target was reached (Charles and others, 2002).

Statistical Methods for Characterizations of Nutrients and Algal Pigments over Space and Time

To assess the differences in taxonomic richness among sampling locations in Lake Anna, the richness at the three stations (North Anna arm, Pamunkey Creek arm, and Confluence; Table 1) were compared in both 2023 and 2024 using a one-way Analysis of Variance (ANOVA). An ANOVA is a parametric test to determine whether there is significant difference in the means among three or more independent groups. Prior to analysis, the assumptions normality and homogeneity of variance must be met (Helsel and others, 2020; R Core Team, 2025). When there was a statistical difference among stations (p-value less than [<] 0.05), a Tukey's honestly significant difference (HSD) post hoc test was conducted to determine which stations differed significantly (R Core Team, 2025; Tukey, 1953).

Descriptive statistics were evaluated for chlorophyll-a, total nitrogen (TN), total phosphorus (TP), dissolved inorganic nitrogen (DIN), and orthophosphate (OP) at each of the five discrete monitoring stations, which are the three lake stations and the two tributary stations. The relation between chlorophyll-a and TN, TP, DIN, and OP were evaluated using parametric linear regressions. The TN:TP ratio was evaluated at each station as well. A TN:TP ratio below 9 indicates nitrogen limitation, values above 22 indicate phosphorus limitation, and ratios between 9 and 22 indicate potential co-limitation, where algal growth may respond to the addition of either nitrogen or phosphorus (Sterner, 2008).

Identifying the Potential Drivers of Algal Biomass and Cyanobacteria Proliferation

Continuous meteorological and water-quality parameters were recorded. Discrete water-quality samples were collected in conjunction with the algal samples for USGS using the same methodology as explained in the Characterization of Algal Community, Biomass, and Toxins.

Data Collection and Laboratory Analysis

Meteorological conditions in the Lake Anna watershed were monitored at two stations: Belmont Park meteorological station near Belmont, VA (USGS 380839077515701) and Lake Anna near Red House near Ellisville, VA (USGS 01670144; U.S. Geological Survey, 2026). All parameters were recorded continuously at 5-minute intervals (Table 1). The meteorological station at Belmont Park was located in a county park approximately 0.56 kilometers from the lake and recorded precipitation, photosynthetically active radiation (PAR), air temperature, wind direction, and wind speed from June 2023 through December 2024. Wind speed and wind direction were recorded continuously on the lake at USGS-01670144 from October 2023 through December 2024.

Continuous water quality monitoring data was collected at the three lake stations through 11:45 PM on December 31, 2024. A stationary YSI EXO3 (YSI Inc., 2017) was deployed at each lake station within the photic zone attached to a dock. The YSI EXO3 recorded water temperature (WT), specific conductance (SC), pH, dissolved oxygen concentration (DO), and turbidity (TB) every 15 minutes. The EXO3 was installed at the Pamunkey Creek arm and the Confluence on May 17, 2023, and at the North Anna arm on May 18, 2023. A detailed analysis of the continuous data was not included in this report. All data were collected and quality assured in accordance with USGS guidelines and standard procedures (Sauer and Turnipseed, 2010; Wagner and others, 2006).

Discrete water-quality samples were collected at the three monitoring stations on the lake using isokinetic sampling methods as described in the "USGS Field Sampling Methods" section. Samples were collected year-round from June 2023 through December 2024 at all stations. Each sample was analyzed for nutrients, major ions, metals, trace elements, and ash-free dry mass using standard analytical methods (Appendix Table 1.2). All data were collected and quality assured in accordance with the USGS Guidelines and standard procedures (U.S. Geological Survey, 2015).

Statistical Methods for Determining Drivers of Algal Biomass and Proliferation

There are many definitions of HABs depending on the management context, the organism of concern, and the effects being evaluated (Gorney and others, 2023a). Because algal blooms may be characterized by biomass, toxin production, taxonomic composition, or indicator groups, multiple metrics are necessary to capture the complexity; therefore, five response variables were evaluated using a consistent modeling framework (Figure 2):

1. Algal biomass as chlorophyll-a concentration (µg/L),
2. Cyanobacteria (cells/mL),
3. pTOX genera (cells/mL),
4. *Raphidiopsis* (cells/mL),
5. pTOX genera excluding *Raphidiopsis* (cells/mL).

This multi-metric approach allows the comparison of model performance across different biological indicators. Chorophyll-a (a proxy for algal biomass) and cyanobacteria were selected because analyses will help identify overall drivers of algal biomass and cyanobacterial abundance. pTOX genera were selected to better understand drivers of the abundance of potentially toxic cyanobacteria, and *Raphidiopsis* was selected because it was the dominant cyanobacterial and pTOX genera in Lake Anna during the study period. pTOX genera excluding *Raphidiopsis* was included to help determine the influence of *Raphidiopsis* on the overall pTOX relation. Three-day medians were used for continuously monitored explanatory variables, such as water temperature and wind speed.

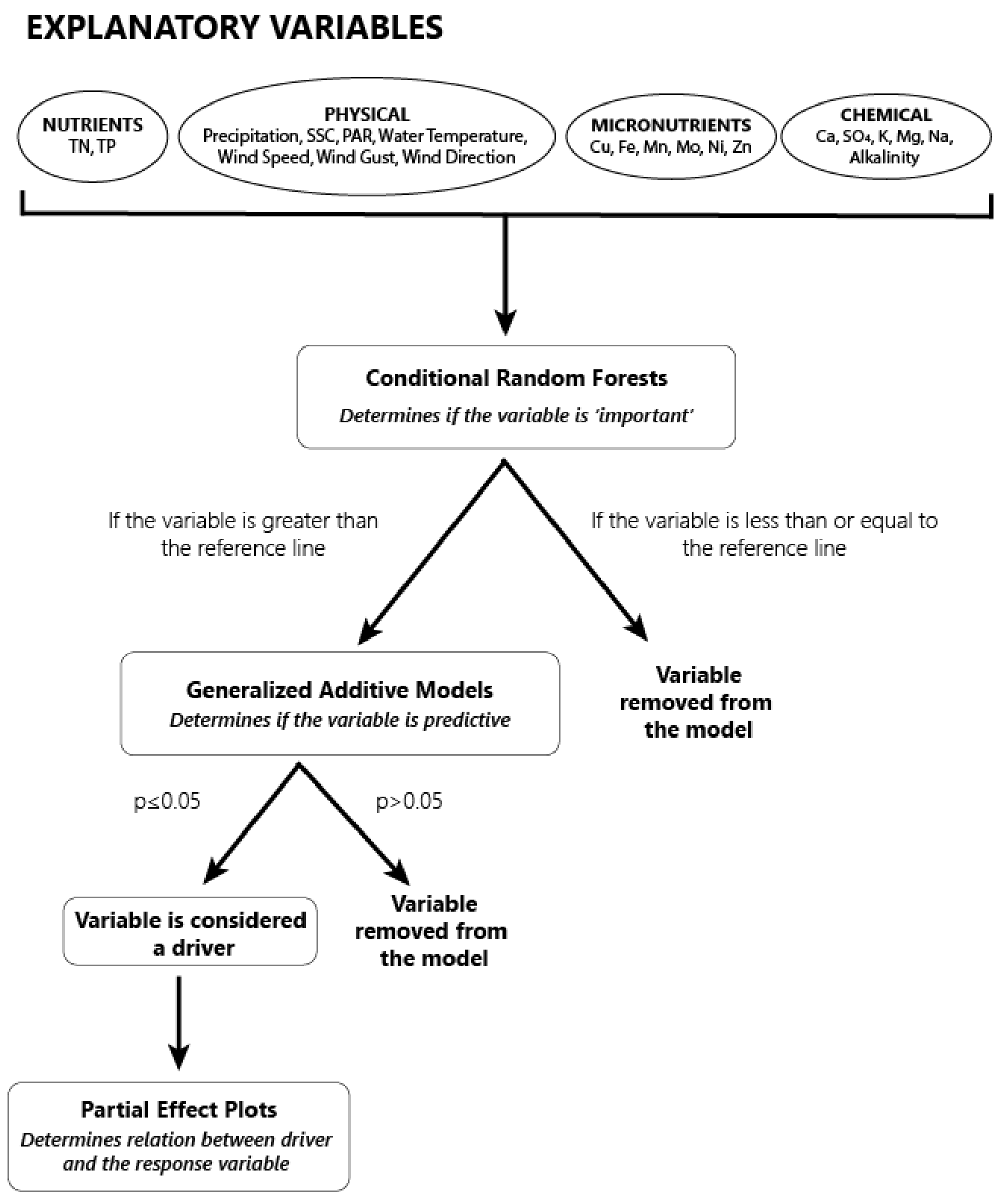

Figure 2. Flowchart showing the sequential process for selecting the drivers that are used in each model.

Station, Season, and Year Effects

Permutational multivariate analysis of variance (PerMANOVA) is a non-parametric test that compares matrices of dissimilarity distances and tests the null hypothesis that there are no differences in relative magnitude of a set of variables between different groups. The PerMANOVA was used to test whether there is at least one difference among station, seasons, and years in the algal community composition. If a difference was identified, then a post-hoc pairwise PerMANOVA test was further applied to test whether each pair of groups are different.

Global PerMANOVA tests were used to determine if the composition of the total algal community on the phyla level, all cyanobacteria genera, and potentially toxigenic (pTOX) cyanobacteria genera varied spatially, seasonally, or annually. The results were used to evaluate whether it was appropriate to group all stations into a single lake model. A post-hoc pairwise PerMANOVA test was then applied to any variables that yielded a significant result ($p < 0.05$) from the global PerMANOVA tests. The pairwise PerMANOVA test was statistically significant, meaning there was a significant difference in a particular pair of groups, if the p-value was < 0.05.

All PerMANOVA and pairwise PerMANOVA testing and plotting were performed in R version 4.5.2 (R Core Team, 2025). Packages used for PerMANOVA and pairwise PerMANOVA testing were *vegan* (Oksanen and others, 2026) and *pairwiseAdonis* (Arbizu, 2026).

Variable Importance of Predictors: Conditional Random Forest

A conditional random forest (CRF) was used to quantify the importance of each potential driver among a chosen biological predictor, such as the concentration of pTOX genera. CRF is a non-parametric statistical method used in datasets with small numbers of samples and many more variables than samples (small n, large p), non-linearity, and highly intercorrelated predictors (Levshina, 2020). CRFs produce more accurate predictions than single conditional inference trees (Levshina, 2020) because multiple trees are “grown,” and the predictions are averaged together (Levshina, 2020). Subsampling without replacement was used to reliably detect the informative variables and to obtain unbiased variable importance measures (Strobl and others, 2007).

The overall importance of water quality variables at predicting biological parameters was determined using conditional variable importance (CVI) scores (Filbee-Dexter and Scheibling, 2017). A CVI score quantifies the contribution of each water quality predictor to a model and can account for all other variables and interactions (Levshina, 2020). This score is calculated by averaging the results from the trees and measuring the decrease in prediction power if the predictor is randomly permuted. The algorithm reduces the impact of high multicollinearity among the predictor variables (Fenberg and others, 2015). Predictors that are strongly associated with the response will have a decrease in prediction accuracy (Levshina, 2020). The variable is considered ‘important’ if the score is greater than a reference score and ‘unimportant’ if less than or equal to the reference score (Levshina, 2020). The reference score is the absolute value of the smallest importance value. The CRF models were fit in R version 4.5.2 (R Core Team, 2025) using the packages *partykit* (Hothorn and others, 2025; Hothorn and Zeileis, 2011) and *cforest* (Strobl and others, 2007).

The Deviance Explanation and Covariate Behaviors: GAMs and Partial Effect Plots

Separate multivariate generalized additive models (GAM) were developed to characterize the relation between the environmental variables identified through the CVI analysis and algal biomass (chlorophyll-a concentration), cyanobacteria cell counts, pTOX genera cell counts, *Raphidiopsis* cell counts, and pTOX genera excluding *Raphidiopsis* cell counts. GAMs can accommodate non-normally distributed data, handle nonlinear relations between predictor and response variables, and assess the additive effects of multiple, co-occurring predictors (Schulte and others, 2022; Tao and others, 2012). Penalized restricted maximum likelihood (REML) estimation was used to avoid overfitting and an extra penalty was added to each term so that the GAM penalized the terms to zero (Schulte and others, 2022; Wood, 2025). All models were fit using a negative binomial distribution, best used for count data, with a log-link function (Greene, 2008). If a response variable was significant, a partial effects plot was used to assess the response between the driver and the response variable. A partial effect plot shows the effect of the statistically significant response variable while holding all other variables constant (Schulte and others, 2022). The coefficient of determination (R^2) decomposition from *mgcv* was also identified for each significant variable. The GAMs were completed in R version 4.5.2 (R Core Team, 2025) using package *mcgv* (Wood, 2025).

Methods for Assessing Potential Sources of the Drivers

External load assessments included evaluating the potential load from the tributaries and examining the water-quality and algal community at the near-shore on the lake (Figure 3). Internal nutrient loading was characterized by the presence of thermal stratification ($\Delta 1$ °C m^{-1}) and hypoxia (DO ≤ 2 mg L^{-1}), assessing lake-bed sediment chemistry, and quantifying sediment resuspension from wave action.

Data Collection and Laboratory Analysis

Both continuous and discrete data were collected and analyzed to assess the potential sources of the drivers at Lake Anna. The sources of drivers investigated include external loading from the tributaries to the lake as well as passive and active internal loading from the lake bed sediments.

Tributary Load Analysis

Two tributaries were continuously monitored in the watershed for streamflow and water quality. Streamgages were installed on May 16, 2023 at both the North Anna River and Pamunkey Creek (Table 1). Discrete measurements of discharge were measured throughout the study period, and a rating curve between water-level and discharge was constructed to enable computation of continuous discharge dataset (Rantz, 1982). YSI, Inc. (Yellow Springs, Ohio) YSI EXO3 sensors, which measured WT, SC, pH, DO, TB every 15-minutes, were installed at Pamunkey Creek on May 16, 2023, and at the North Anna River on May 18, 2023. Sea-Bird Scientific (Bellevue, Washington) SUNA nitrate sensors (Seabird Scientific, 2018), which recorded nitrate concentration at 15-minute intervals, were installed on July 27, 2023 at Pamunkey Creek and August 3, 2023 at the North Anna River. Data collection was completed at 11:45 PM on December 31, 2024. Sensors were maintained and operated in accordance with USGS standards (Sauer and Turnipseed, 2010; Wagner and others, 2006).

Discrete water-quality samples were collected at the streamgage locations monthly and during targeted stormflow conditions following published USGS sampling methods (U.S. Geological Survey, 2015). A multiparameter YSI EXO3 was used to measure WT, SC, pH, DO, and TB at each station during sample collection. The discrete water-quality samples were collected using the equal width integration method with a weighted bottle sampler or a DH-95 sampler, depending on flow conditions. Samples were collected in a 1-liter (L) Teflon bottle, which was triple rinsed with DI water and single rinsed with native water before sample collection. All samples were composited in a 14-L churn splitter for processing to ensure that each subsample accurately represented a composite sample (Barr, 2018). All samples were immediately processed in the field. Sample bottles were triple rinsed with deionized (DI) water and single rinsed with native water before filling. All samples were stored on ice and in the dark. Each sample was analyzed for nutrients, sediment, major ions, photosynthetic pigments, alkalinity, and stable isotopes of nitrate and oxygen (Appendix Table 1.3). At each station, 2 replicates and 1 blank were collected for monthly samples, and 1 replicate and 1 blank were collected for storm samples.

Potential near-shore sources of nutrients

To determine potential near-shore nutrient sources, three transects from the shoreline to the mid-channel of the lake were established at stations that represent residential, agricultural, and forested land use (Figure 3; Table 4). Samples were collected twice during the duration of the study during a low-occupancy period on April 30, 2024 and May 1, 2024, and during a high-occupancy period on August 13, 2024. Samples were collected during two different occupancy periods to determine the effect of occupancy levels on near-shore source influence. Samples were collected from a canoe at the shore (0 m), 10 m, 25 m, and from a boat at the mid-channel.

At each station, field parameters were collected (WT, DO, pH, TB, and SC), and the Secchi disk depth was recorded. At 0 m, a 1-L HDPE bottle was collected via grab sample or dipping the bottle in the water. At 10 and 25 m and at mid-channel, a 1-L high density polyethylene (HDPE) weighted bottle was used. Seven dips were collected at each station. There were different analytes that were collected at each station, which required different churn sizes. Nutrients, major ions, stable isotopes, and methylene-blue active substances were collected at 0 m, 10 m, and 25 m from shore. Algal community and toxins were collected at 0 m, 25 m, and the mid-channel (Appendix Table 1.4). A 14-L churn was used for 0 m and 25 m, and an 8-L churn was used for 10 m and the mid-channel. Samples were analyzed on station and put on ice in the dark. Replicates were collected at 25 m during the low-occupancy period and at 0 m during the high-occupancy period. Blanks were collected once per sampling period.

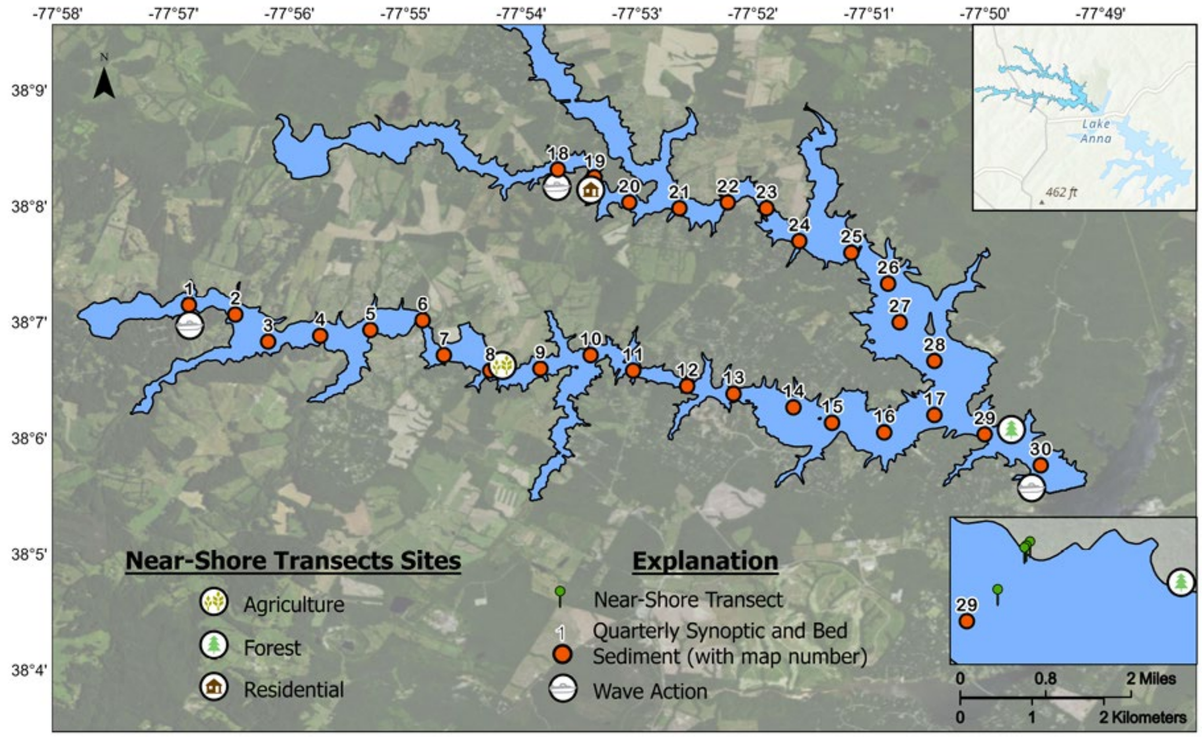

Base map from ESRI; Data from USGS Water for the Nation; Outline of Lake Anna from DEQ.

Index map base from ERSI, Watershed boundary from USGS Water for the Nation; Outline of Lake Anna from DEQ.

Geographic Coordinate systems

North American Datum of 1983

Figure 3. Map showing U.S. Geological Survey wave action, quarterly synoptics, near-shore transects, and bed sediment stations. Wave action stations are the USGS continuous lake monitoring stations identified in Table 1; near-shore transect stations are identified in Table 3, and quarterly synoptic and bed sediment transects are identified in Table 4.

Table 3. Description of the 12 U.S. Geological Survey near-shore transect stations in Lake Anna, central Virginia (U.S. Geological Survey, 2026). Samples were collected in 2024. The location of the near-shore transects are shown in Figure 3.

[locations of near-shore transect stations are shown in an inset in Figure 3. DEQ, Virginia Department of Environmental Quality; ID, identifier; USGS, U.S. Geological Survey]

Distance (m)	Transect	USGS station number
0	Forest	380606077495601
10	Forest	380606077495602
25	Forest	380606077495605
Mid-channel	Forest	380603077495801
0	Residential	380756077523901
10	Residential	380756077523903
25	Residential	380756077523801
Mid-channel	Residential	380809077531901
0	Agriculture	380642077534801
10	Agriculture	380642077534702
25	Agriculture	380642077534704
Mid-channel	Agriculture	360634077541201

Lake-Bed Sediments as a Source of Nutrients

To characterize potential internal nutrient sources, lake-bed sediments were collected once (August 10–11, 2023) at 30 evenly spaced stations in the mid-channel of Lake Anna. The top 10 cm of lake-bed material was sampled from a boat using a petite PONAR dredge, and approximately 500 g of each grab sample were passed through a 2 mm-sieve. The remaining sieved material was placed into sample jars and analyzed for nutrients, metals, and trace elements at RTI Laboratories in Livonia, Michigan (Appendix Table 1.5). Two replicates were collected on each day of sample collection.

Table 4. Description of the 30 U.S. Geological Survey quarterly water quality synoptic and bed sediment locations (U.S. Geological Survey, 2026). The location of the map numbers are shown in Figure 3.

[USGS, U.S. Geological Survey]

Map number	USGS station number	USGS station name
1	380709077565201	Lake Anna Synoptic Sample Location 1
2	380704077562801	Lake Anna Synoptic Sample Location 2
3	380650077561101	Lake Anna Synoptic Sample Location 3
4	380653077554401	Lake Anna Synoptic Sample Location 4
5	380656077551801	Lake Anna Synoptic Sample Location 5
6	380701077545101	Lake Anna Synoptic Sample Location 6
7	380643077544001	Lake Anna Synoptic Sample Location 7
8	380635077541601	Lake Anna Synoptic Sample Location 8
9	380636077535001	Lake Anna Synoptic Sample Location 9
10	380643077532401	Lake Anna Synoptic Sample Location 10
11	380635077530201	Lake Anna Synoptic Sample Location 11
12	380627077523401	Lake Anna Synoptic Sample Location 12
13	380623077521001	Lake Anna Synoptic Sample Location 13
14	380616077513901	Lake Anna Synoptic Sample Location 14
15	380608077511901	Lake Anna Synoptic Sample Location 15
16	380603077505201	Lake Anna Synoptic Sample Location 16
17	380612077502601	Lake Anna Synoptic Sample Location 17
18	380819077534101	Lake Anna Synoptic Sample Location 18
19	380815077532201	Lake Anna Synoptic Sample Location 19
20	380802077530401	Lake Anna Synoptic Sample Location 20
21	380753077523801	Lake Anna Synoptic Sample Location 21
22	380802077521301	Lake Anna Synoptic Sample Location 22
23	380759077515301	Lake Anna Synoptic Sample Location 23
24	380742077513601	Lake Anna Synoptic Sample Location 24
25	380736077510901	Lake Anna Synoptic Sample Location 25
26	380720077505001	Lake Anna Synoptic Sample Location 26
27	380700077504401	Lake Anna Synoptic Sample Location 27
28	380640077502601	Lake Anna Synoptic Sample Location 28
29	380602077500001	Lake Anna Synoptic Sample Location 29

30	380546077493101	Lake Anna Synoptic Sample Location 30

Temperature Stratification and Hypoxic Conditions within Lake Anna

To assess the stratification regime and the hypoxic conditions, quarterly synoptic surveys were conducted from August 2023 through November 2024 (Table 5) at the 30 mid-channel stations (Table 4). These surveys quantified spatial, temporal, and vertical variability in water column structure and water-quality conditions at the 30 evenly spaced locations throughout the western portion of Lake Anna (Figure 4). Thirty locations were chosen to ensure statistical power. At each station, the depth to the lake-bed sediment was measured, and the Secchi disk depth was recorded. Vertical profiles were collected at 0.5-m depth intervals from the surface to the bed sediments for field parameters and algal pigments. A YSI EXO3 sonde was used to measure WT, SC, pH, DO, and TB.

Table 5. Description of the sampling dates for the quarterly synoptic surveys. The bed sediment samples were collected during the summer 2023 sampling event.

Season	Sampling Dates
Summer 2023	08/10/2023 – 08/11/2023
Fall 2023	11/30/2023 – 12/1/2023
Winter 2023	2/15/2024 – 2/16/2024
Spring 2024	5/22/2024 – 5/23/2024
Summer 2024	09/03/2024 – 09/04/2024
Fall 2024	11/05/2024 – 11/06/2024

Resuspension of bed sediment through wave action

Each of the continuous monitoring lake stations were equipped with an ultra-high-frequency wave sensor (RBRsolo3; RBR Global, Ottawa, Canada) that measured depth and pressure every 0.25 seconds. The sensors were deployed at all lake monitoring stations from May 2023 through December 2024 and analyzed for calendar year 2024.

At each of the three continuous water-quality monitoring locations, discrete, depth-integrated water-quality samples were collected hourly between 8:00 and 19:00 on July 1, 2024, and between 8:00 and 18:00 on October 15, 2024. These sampling dates were selected to represent high residential occupancy and boating (HROB) on the Fourth of July holiday week and low residential occupancy and boating (LROB) in mid-October (Lake Anna, 2026). Samples were collected at the same location where the discrete water-quality and algal community samples were collected throughout the study period. Before sample collection, a depth profile of field measurements (WT, SC, pH, DO, and TB) was recorded with Secchi disk depth and depth of the water column. Before sample collection, the 1-L HDPE bottle, 8-L churn, and all sample bottleware were triple rinsed with DI water. A 1-L HDPE sampling bottle was used in a weighted bottle holder to collect a depth integrated sample. Prior to filling the churn with the sample, the 1-L HDPE bottle and 8-L churn were rinsed with native water. Six-liters of water were collected and composited into the 8-L churn. The sample bottles were rinsed with native water from the churn prior to filling for analysis. Samples were analyzed for nutrients and sediment. Every station had 2 churns and 2 1-L HDPE sampling bottles that were triple rinsed with DI water and placed in a new churn bag, creating two sets of sampling equipment that was used throughout the day. A blank and a replicate were collected at each station for both the HROB and LROB.

Statistical Methods

External sources of potential driving factors were statistically evaluated by estimating load, determining the sources using the stable isotopes of nitrogen and oxygen, and evaluating the near-shore sources. Bed sediments, wave action, hypoxia, and thermal stratification measurements were examined to increase understanding of internal loading processes. Spatial variability in bed-sediment nutrient and micronutrient concentrations was quantified to identify potential hotspots; statistical differences among stations were determined using the Kruskal-Wallis test. Wave action was evaluated as a potential driver of sediment resuspension by estimating bed shear stress and determining if conditions were sufficient to mobilize the bottom material. Finally, interpretations of the synoptic profile data were used to assess the timing and the spatial distribution of hypoxic conditions and thermal stratification, two processes known to influence nutrient release.

External Nutrient loading

Delivered loads of suspended sediment concentration (SSC), TN, and TP to Lake Anna from the North Anna River and Pamunkey Creek were estimated using a surrogate-regression approach (Miller and others, 2023; Porter, 2025). Multiple linear regressions related the discrete constituents (SSC, TN, and TP) to selected continuously measured parameters, including streamflow, TB, SC, DO, WT, or pH for each tributary. Model exploration was performed to determine the most parsimonious model, that is, the model that explained the greatest amount of variability with the fewest amount of predictor variables. Model outputs were 15-minute interval estimates of concentrations, which were multiplied by streamflows to calculate loads of SSC, TN, and TP. Annual water constituent loads and yields (watershed area normalized loads) were summarized and compared by water year (October 1 through September 30, named for the calendar year in which the period ends). Analysis was performed in R version 4.5.2 (R Core Team, 2025). Multiple linear regressions were formulated and model archive summaries were produced using the *wren* package (Eslick-Huff and Puls, 2025). A baseflow separation was performed using the *hydroEvents* package (Wasko and Guo, 2022) to estimate the contributions of external loads that occurred during baseflow and stormflow. Model inputs and outputs and model archive summaries are published in USGS data release by Vande Pol and others (2026).

Isotopic nitrate sourcing

Within the nitrate molecule (NO_3^-), stable isotope ratios of nitrogen ($\delta^{15}N$-NO_3^-) and oxygen ($\delta^{18}O$-NO_3^-) provide insights about nitrogen sources (Granger and others, 2010; Kendall and others, 2007; Snow, 2018). In freshwater ecosystems, it is common for samples to have $\delta^{15}N$-NO_3^- and $\delta^{18}O$-NO_3^- values that are within multiple sources characteristic end-member intervals (Niu and others, 2021). Here, characteristic ranges of $\delta^{15}N$-NO_3^- and $\delta^{18}O$-NO_3^- (Table 6) were sourced from Kendall and others (2007), Granger and others (2010), and Snow (2018). To facilitate apportionment of nitrate sources, a stable isotope mixing model (SIMM) was applied. The SIMM applies a Bayesian Markov Chain Monte Carlo algorithm and Gibbs Sampler and is expressed in the following mathematical form (Parnell and others, 2010); Equations 1 through 4:

$$X_{ij} = \sum_{k=1}^{k} P_k \left(S_{jk} + C_{jk}\right) + \varepsilon_{ij} \qquad [1]$$

$where$:

X_{ij} is the isotopic signature j $\left(\frac{\delta^{15}N-NO_3-}{\delta^{18}O-NO_3-}\right)$ of mixture i (water sample),

P_k is the estimated proportion of source k, that is, manure and human waste, soil nitrogen, nitrate fertilizer, ammonium fertilizer and precipitation,

$$S_{jk} \sim N\left(\mu_{jk}, \omega_{jk}^2\right) \qquad [2]$$

$where$:

S_{jk} is the normally distributed source value k based on isotope j,

μ_{jk} is the mean of source k on isotopic signature j,

ω_{jk} is the standard deviation of source k on isotopic signature j,

$$C_{jk} \sim N\left(\lambda_{jk}, \tau_{jk}^2\right) \quad [3]$$

$where$:

C_{jk} is the normally distributed fractionation factor of isotope j on source k,

λ_{jk} is the mean of source k on isotopic signature j,

τ_{jk} is the standard deviation of source k on isotopic signature j,

$$\varepsilon_{ij} \sim N\left(0, \sigma_j^2\right) \quad [4]$$

$where$:

ε_{ij} is the normally distributed residual error,

σ_j standard deviation of unquantified variation between individual mixtures.

Input means and standard deviations for source types were referenced from literature (Ji and others, 2022; Niu and others, 2021) (Table 7). The stable isotope mixing model was executed in R version 4.5.2 (R Core Team, 2025) using the *simmr* package (Parnell and others, 2010).

Table 6. Description of the characteristic ranges of $\delta^{15}N\text{-}NO_3^-$ and $\delta^{18}O\text{-}NO_3^-$. Values are referenced from Kendall and others (2007), Granger and others (2010), and Snow (2018).

[$\delta^{15}N\text{-}NO_3^-$, stable isotope of nitrogen; $\delta^{18}O\text{-}NO_3^-$, stable isotope of oxygen; ppt, parts per thousand]

Source	$\delta^{15}N\text{-}NO_3$ (ppt)	$\delta^{18}O\text{-}NO_3$ (ppt)
Manure and Human Waste	0 to 25	-15 to 15
Soil Nitrogen	2 to 8	-15 to 15
Nitrate Fertilizer	-5 to 6.5	17 to 25
Ammonium Fertilizer and Precipitation	-10 to 5	-15 to 15

Table 7. Characteristic means and standard deviations used for inputs to stable isotope mixing model. Values referenced are from Niu and others (2021) and Ji and others (2022).

[$\delta^{15}N\text{-}NO_3^-$, stable isotope of nitrogen; $\delta^{18}O\text{-}NO_3^-$, stable isotope of oxygen; ppt, parts per thousand]

Source	Mean $\delta^{15}N\text{-}NO_3^-$	Standard deviation δ^{15} $N\text{-}NO_3^-$	Mean $\delta^{18}O\text{-}NO_3^-$	Standard deviation $\delta^{18}O\text{-}NO_3^-$
Manure and Human Waste	10.49	4.53	3.45	2.63
Soil Nitrogen	2.87	0.21	2.03	0.21
Nitrate Fertilizer	3.21	0.12	20.1	0.21
Ammonium Fertilizer and Precipitation	-2.25	1.75	4.14	1.89

Near-Shore Sources of Drivers

To assess spatial variability in biological and environmental conditions between the shoreline and middle of Lake Anna, descriptive statistics were analyzed and compared. These samples were compared to land use and occupancy period.

Bed Sediments

Concentration of nutrients, metals, and physical parameters of bed sediments were tested for spatial differences using the non-parametric Kruskal-Wallis test followed by a Dunn's test for multiple comparisons (Sokal and Rohlf, 1995). Results of all analyses were considered statistically significant for p-values < 0.05. The Kruskal-Wallis and Dunn's tests were performed using R version 4.5.3 and the *stats* package (Harvey and Hanson, 2024).

Wave-generated bottom shear stress

Using the RBRSolo3 high-frequency continuous data, the maximum wave height, wave period, and depth were averaged across the 0.25-second observations to match the 15-minute continuous data collection intervals for water-quality parameters. These summarized 15-minute interval data were used to analyze the properties of waves at each of the three continuously monitored lake stations and included a comparison of lake-bottom shear stress (τ_b) versus maximum wave height and analyzing which waves generated τ_b that was greater than each station's critical shear stress (τ_{cr}). Waves where τ_b exceeded τ_{cr} indicated sufficient energy to resuspend the lake-bed sediments at the bottom of the lake. Source attribution of waves where τ_b exceeded τ_{cr} was analyzed by relating τ_b to wind speed. For each of these analyses, τ_b and τ_{cr} at each station were calculated by the following series of equations (Equations 5 through 10). The median grain size was assumed to be 0.000002 m at North Anna arm and Pamunkey Creek arm and 0.0005 m at Confluence based on (1) measurements of sand/fine fractions over the study period in Lake Anna and tributaries, and (2) observations of bottom material during bed sediment sampling. Seasonal summary wave statistics were computed where the seasons were defined astronomically based on the Vernal and Autumnal Equinoxes and Winter and Summer Solstices.

1. Calculate wave number (k) from the linear dispersion equation and solve iteratively (Salmon, 2008):

$$gktanh(kh) = \omega^2 \quad [5]$$

$where$:

$g = gravitational\ acceleration,$ 9.81 $meters\ per\ second\ squared,$

$h = depth, in\ meters\ (measured\ value),$

$k = wave\ number\ (solved\ for\ iteratively),$

$\omega = \ angular\ wave\ frequency, \frac{2\pi}{T}, in\ radians\ per\ second,$

$T = wave\ period, in\ seconds\ (measured\ value).$

2. Calculate near-bed orbital velocity (U_w) from linear wave theory (Salmon, 2008):

$$U_w = \frac{\pi H}{Tsinh(kh)} \quad [6]$$

$where$:

$U_w = near - bed\ wave\ orbital\ veloicty\ amplitude, in\ meters\ per\ second,$

$H = wave\ height, in\ meters\ (measured\ value),$

$T = wave\ period, in\ seconds\ (measured\ value),$

$k = wave\ number$ [from equation 1],

$h = depth, in\ meters\ (measured\ value).$

3. Calculate roughness height based on Manning-Strickler (Yamashita and others, 2022):

$$k_s = 2.5d_{50} \quad [7]$$

$where$:

$k_s = roughness\ height, in\ meters,$

$d_{50} = median\ grain\ size, in\ meters.$

4. Calculate wave friction factor from Grant-Madsen-type quadratic stress law (Myrhaug and others, 2024):

$$f_w = 0.237 \left(\frac{U_w T}{k_s}\right)^{-0.52} \quad [8]$$

$where$:

$f_w = wave\ friction\ factor, dimensionless,$

$U_W = near - bed\ orbital\ velocity$ [from equation 2],

$T = wave\ period, in\ secods\ (measure\ value),$

$k_s = roughness\ height, in\ meters$ [from equation 3].

5. Calculate lake-bottom shear stress based on quadratic law for wave bed shear stress (Metje, 2001):

$$\tau_b = \frac{1}{2}\rho_w f_w U_w^2 \quad [9]$$

$where$:

$\tau_b = lake - bottom\ shear\ stress, in\ Pascals,$

$\rho_w = water\ density, 1000\ kilograms\ per\ cubic\ meter,$

$f_w = wave\ friction\ factor, dimensionless$ [from equation 4],

$U_W = near - bed\ orbital\ velocity$ [from equation 2].

6. Calculate critical shear stress from Shields-based critical stress for motion (Wu and others, 2000):

$$\tau_{cr} = \theta_{cr}(\rho_s - \rho_w)gd_{50} \qquad [10]$$

$where$:

$\tau_{cr} = critical\ shear\ stress\ for\ incipient\ motion, in\ Pascals,$

$\theta_{cr} = critical\ shields\ parameter, 0.03\ was\ used\ (Wu\ and\ others, 2000),$

$\rho_s = sediment\ density, 2650\ kilograms\ per\ cubic\ meter,$

$\rho_w = water\ density, 1000\ kilograms\ per\ cubic\ meter,$

$g = gravitational\ acceleration, 9.81\ meters\ per\ seconds\ squared,$

$d_{50} = median\ grain\ size, in\ meters.$

Evaluation of Thermal Stratification and Hypoxia

The median dissolved oxygen concentration and water temperature were calculated for each synoptic sampling date across the 30 lake sampling stations. For each station, the depth to hypoxia, if present, was identified. Hypoxic conditions were defined as dissolved oxygen concentrations at or below 2 mg/L (Bouffard and others, 2013; Nürnberg, 2004; Palshin and others, 2021). Likewise, at each station, the presence of thermal stratification, that is a temperature change greater than 1°C/m, was determined, and if present, the depth of the thermal stratification was quantified.

Characterizing Chlorophyll-a, Nutrients, and Algal Community Characteristics

The algal community, biomass, and toxin production were assessed across the lake stations and throughout the year. Algal community richness and seasonal variation in abundance were determined. The amount of variance in chlorophyll-a and total nitrogen, DIN, total phosphorus, and OP were evaluated for the two tributary stations and the three lake stations (Table 1). The ratio of TN and TP was determined and evaluated seasonally for the two tributary stations and three lake stations.

Spatial Difference in Algal Communities and Toxin Production at the Lake Stations

Algal community richness differed significantly for the Confluence station compared to the North Anna arm and Pamunkey arm stations in both 2023 and 2024 (Figure 4). The Confluence station showed consistently lower taxonomic richness in both years compared to North Anna and Pamunkey Creek arms. On average, the Confluence station had approximately 10 less taxa in each sample than North Anna arm and Pamunkey Creek arm stations. Median richness was higher in 2024 for all stations and North Anna arm consistently had the most variability in richness over both years. The one-way ANOVA indicated significant differences among stations in both 2023 ($F = 7.17$, $p = 0.0017$) and 2024 ($F = 6.23$, $p = 0.0029$). Post hoc Tukey test revealed that the Confluence station was significantly ($p\text{-value} < 0.05$) lower than the North Anna arm and Pamunkey Creek arm stations.

The observed seasonal pattern generally followed the typical trend of phytoplankton succession from winter through fall. Phytoplankton abundance was lowest during winter, followed by an increase in spring. During summer, abundances peaked before declining through fall (Figure 5). As the season progresses to summer, the total abundance is several orders of magnitude higher, and the largest component of the total abundance is cyanobacteria, making up over 90 percent of the relative abundance during summer (Figure 5).

Seasonal variation in relative abundance of the estimated phytoplankton community showed that cyanobacteria were the dominant taxa during 2023 (June–November) and July through November 2024 at all three stations. The phylum *Heterokontophyta* (diatoms) was most prevalent in winter 2023-2024 at all three stations, and in spring of 2024 at Confluence (Figure 5). Even though *Heterokontophyta* was present during the winter and the spring, the total abundance of *Heterokontophyta* was less than the magnitude of cyanobacteria total abundances. For the pTOX genera, *Raphidiopsis,* a potentially toxigenic species, was the dominant taxon across stations, displaying the highest absolute abundance within the cyanobacteria classification (Figure 6). Each station exceeded the Virginia advisory threshold of 100,000 cells/mL during the study period. The North Anna arm and Pamunkey Creek arm had similar numbers of exceedances, with 25 and 24 samples greater than 100,000 cells/mL of 56 total samples collected, respectively. At the Confluence, 1 sample of 55 total samples collected (1.8 percent) exceeded the 100,000 cells/mL threshold on August 21, 2024.

Over the study period, 732 cyanobacterial toxin analyses were conducted over the four targeted ELISA cyanotoxin assays: cylindrospermopsin, microcystin (MCY), anatoxin-a (ATX-A), and saxitoxin. Cyanotoxin detections in Lake Anna were relatively rare and varied by station. The North Anna arm and Pamunkey Creek arm stations had the highest number of detections (7.6 percent and 11.6 percent of samples, respectively) and the Confluence station had the lowest number of detections (2.2 percent of samples). Cyanotoxins above detection were relatively low

(<0.65 µg/L) over the study. Microcystin and anatoxin-a were the only toxins frequently detected (17.0 percent and 11.7 percent, respectively) above the MDL (0.15 µg/L) (Figure 7).

Microcystin and anatoxin-a were more frequently detected in June and July of 2023 and 2024 when the cyanobacteria community were a mixed assemblage before transitioning into late summer (late July through early September) (Figure 7). *Dolichospermum* were present at this time and are known Microcystin and anatoxin-a producers. Additionally, *Cuspidothrix* and *Chrysosporum* are other genera that were present and are known as anatoxin-a producers. *Raphidiopsis* dominate the cyanobacteria community for the rest of the summer and are known producers of cylindrospermopsin, saxitoxin, and more rarely, anatoxin-a. However, cylindrospermopsin and saxitoxin were not detected above the MDL (0.05 and 0.02 µg/L, respectively).

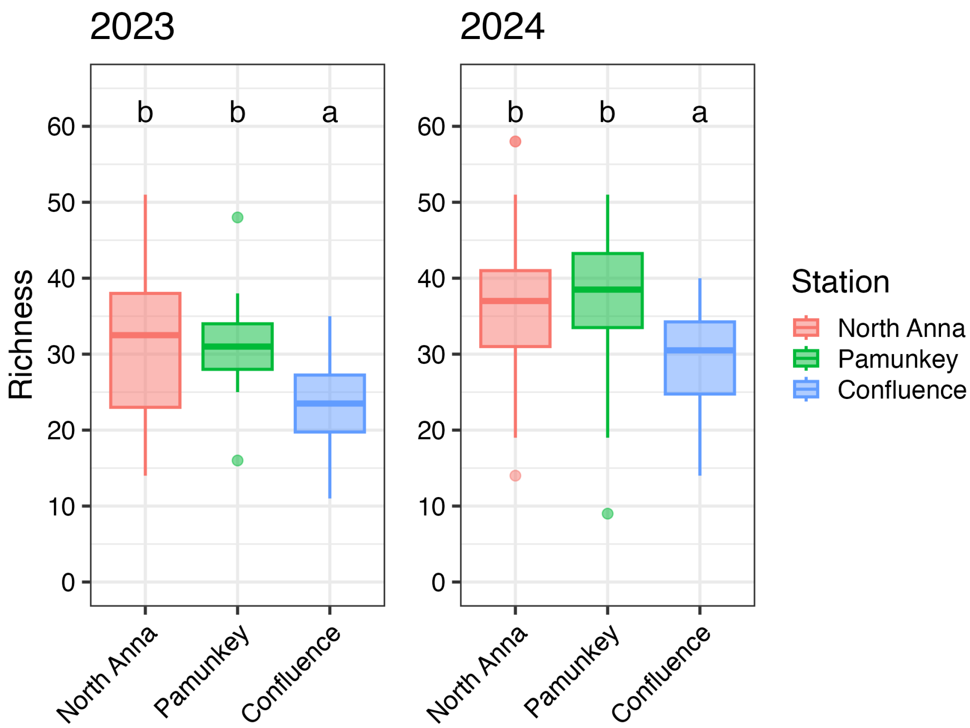

Figure 4. Boxplots showing the variation in phytoplankton community taxonomic richness across the three Lake Anna stations in 2023 and 2024. The boxes represent the interquartile range, with the bottom part of the box at the 25th percentile and the top part of the box at the 75th percentile. The whiskers extend from the minimum, at lower concentrations, and the maximum, at higher concentrations. The points outside the box and whiskers are outliers. A one-way ANOVA indicated a significant difference among stations, followed by Tukey's post hoc test ($p<0.05$) that was used to determine which stations differed, denoted by the letter groupings on the figure; similar letters indicate differences were not statistically significant. Refer to Table 1 for additional station information.

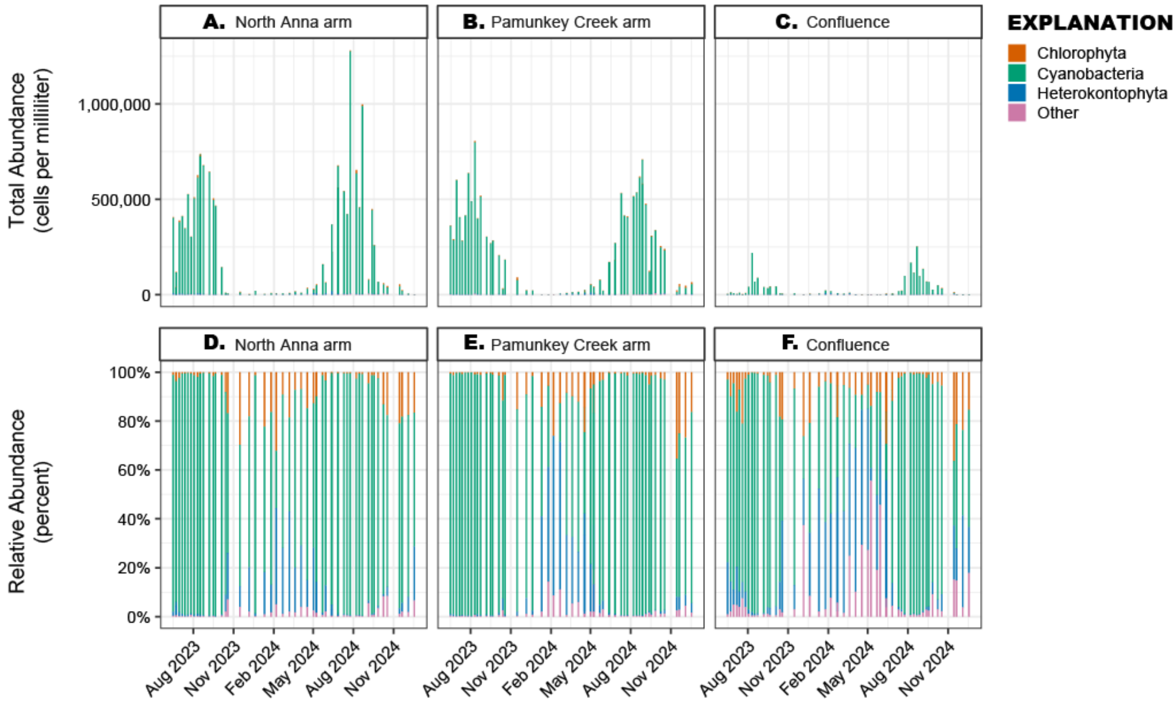

Figure 5. Bar charts of absolute (A, B, C) and relative abundance (D, E, F) of the phytoplankton community across all three monitored Lake Anna stations from June 2023 through December 2024. Samples shown here were collected by both USGS and ODU. Refer to Table 1 for additional station information.

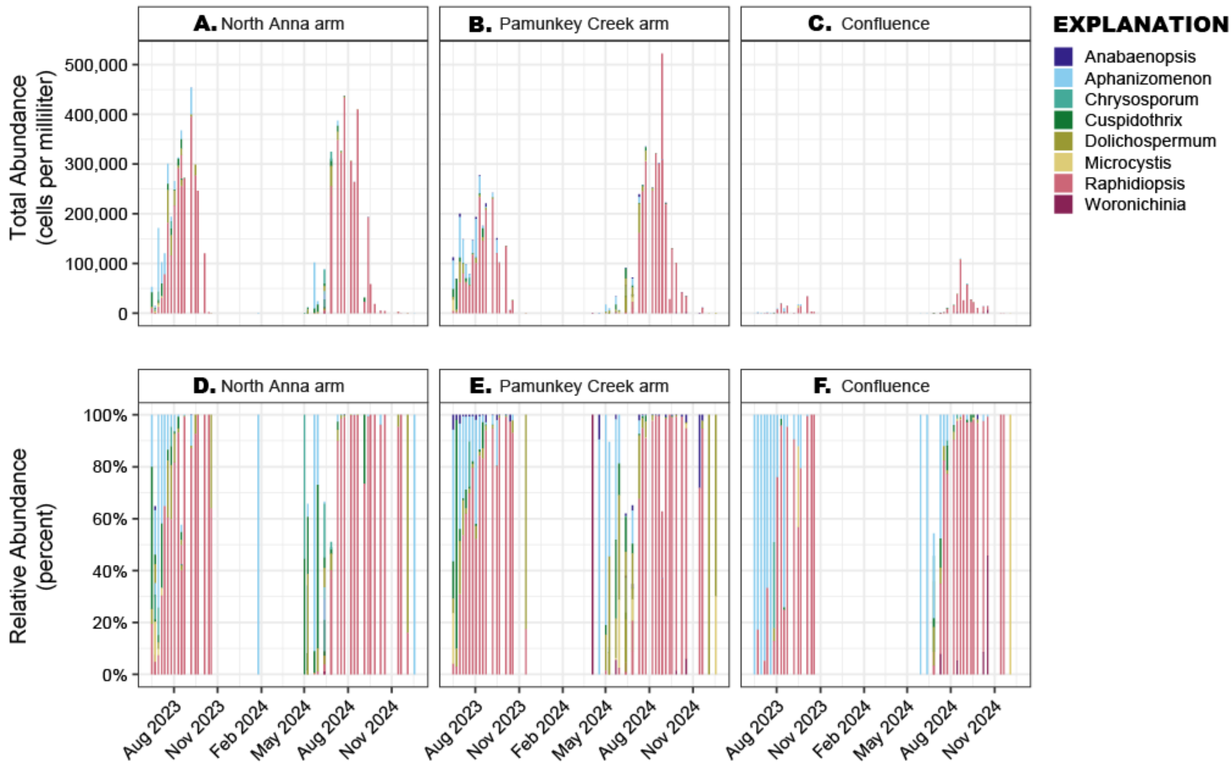

Figure 6. Bar charts of absolute (A, B, C) and relative abundance (D, E, F) of the potentially toxigenic cyanobacterial community across all three monitored Lake Anna stations from June 2023 to December 2024. Samples shown here were collected by both USGS and ODU. Refer to Table 1 for additional station information.

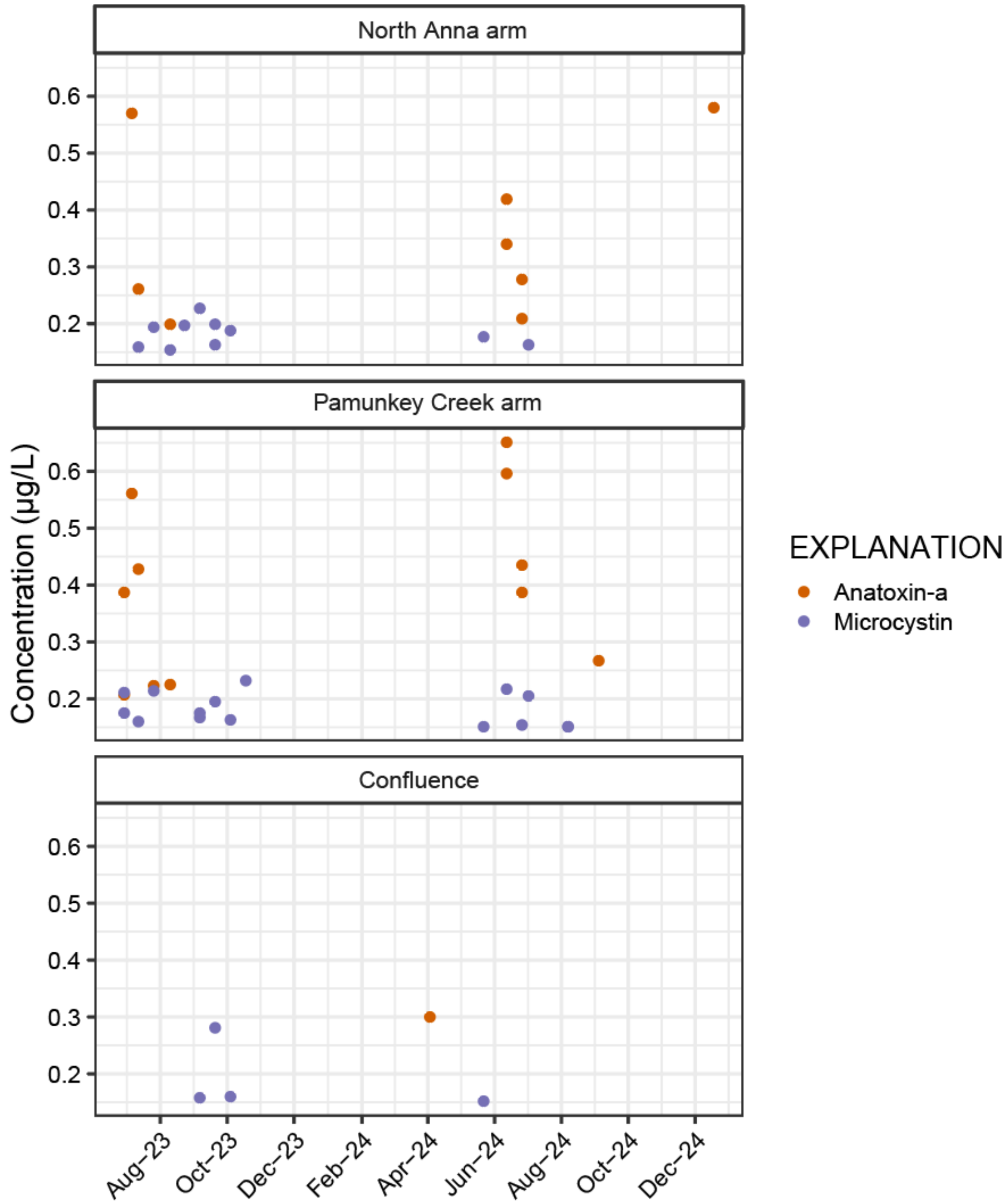

Figure 7. Time series of cyanobacteria toxin concentrations that were above the reporting limit from June 2023 until December 2024. Microcystin, Anatoxin-a, Cylindrospermopsin, and Saxitoxin were all analyzed, but only samples over the reporting limit are displayed. Microcystin (MCY) and Anatoxin-a (ATX-A) concentrations were the only two that exceeded their reporting limit of 0.15 µg/L. Refer to Table 1 for additional station information.

Spatial Characterization of the Chlorophyll-a and Nutrients in the Tributary and Lake Stations

The median chlorophyll-a concentrations at the lake stations were 5 to 35-times higher than the median tributary concentrations (Table 8). Although minimum chlorophyll-a concentrations were similar among the lake stations, the medians and maximum values were 2 to 4 times higher in the North Anna arm and Pamunkey Creek arm than at the Confluence. The North Anna arm had the widest observed range in chlorophyll-a concentration, with both the lowest minimum and the highest maximum of 1.78 and 98.00 μg/L of chlorophyll-a, respectively. Seasonal variability was observed at the lake stations, with chlorophyll-a concentrations peaking from July through September in 2023 and 2024 (Figure 8).

Table 8. Descriptive statistics of chlorophyll-a, total nitrogen, total phosphorus, dissolved inorganic nitrogen, and orthophosphate at each station within the Lake Anna watershed in central Virginia, 2023-2024. Refer to table 1 for additional station information.

[Min, Minimum; Med, Median; Max, Maximum; TN, total nitrogen; TP, total phosphorus; DIN, dissolved inorganic nitrogen, OP, orthophosphate; µg/L, micrograms per liter; mg/L, milligrams per liter]

			Chlorophyll-a			TN			TP			DIN			OP		
			µg/L			mg/L											
Station type	Station name	n	Min	Med	Max	Min	Med	Max	Min	Med	Max	Min	Med	Max	Min	Med	Max
Tributary	North Anna River	29	0.34	0.96	3.88	0.20	0.59	2.17	0.01	0.05	0.40	0.02	0.27	1.08	0.00	0.01	0.12
	Pamunkey Creek	29	0.60	1.46	10.90	0.25	0.85	2.20	0.02	0.08	0.43	0.02	0.38	1.11	0.00	0.02	0.16
Lake	North Anna arm	31	1.78	34.20	98.00	0.35	0.94	1.66	0.02	0.08	0.14	0.01	0.02	0.63	0.00	0.00	0.04
	Pamunkey Creek arm	30	2.46	30.85	53.20	0.54	0.85	1.26	0.02	0.06	0.26	0.01	0.02	0.46	0.00	0.00	0.11
	Confluence	29	2.85	7.19	26.20	0.32	0.40	0.64	0.01	0.02	0.07	0.01	0.03	0.14	0.00	0.00	0.00

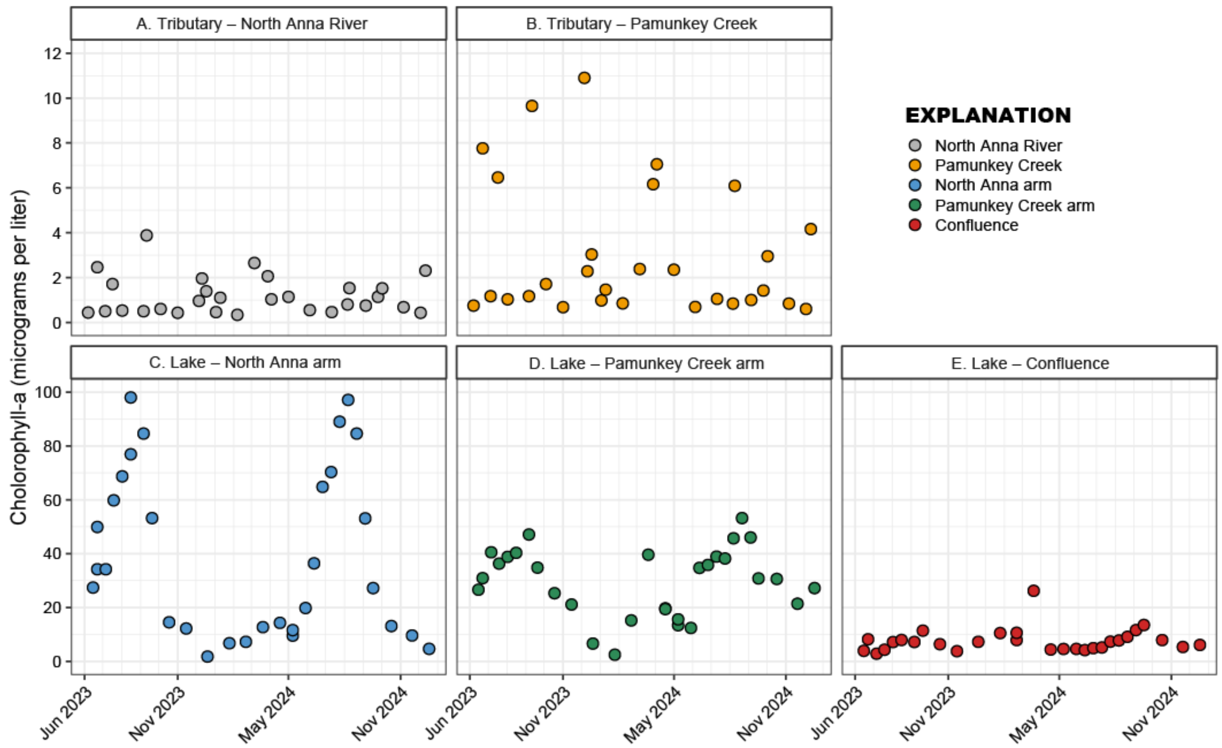

Figure 8. Time series of discrete chlorophyll-a samples at *A,* North Anna River (016701405), *B,* Pamunkey Creek (01670200), *C,* North Anna arm (01670144), *D,* Pamunkey Creek arm (01670209), *E,* the Confluence (016702576; U.S. Geological Survey, 2026) in the Lake Anna watershed in central Virginia, 2023–2024. Refer to Table 1 for additional station information.

The tributary stations exhibited a wider range of TN concentrations compared to the lake stations (Figure 9, Table 8). Median TN concentrations at Lake Anna were 0.5 to 1.6-times higher than the median tributary concentrations. The North Anna arm had the highest minimum TN, with concentrations 1.5 to 2.7-times higher than at the other 4 stations which had minimums of 0.2–0.35 mg/L. The Confluence station had the lowest minimum, median, and maximum TN concentrations, at 0.32, 0.4, and 0.64 mg/L, respectively. However, the median DIN concentration was higher at the tributary stations than at the lake. The median DIN concentrations at the North Anna River and Pamunkey Creek were 13.5 and 19-times higher, respectively, than the median at the lake stations. While the minimum DIN and median concentrations were similar at all stations, the maximum values were 4.5 to 3.3-times higher in the North Anna arm and the Pamunkey Creek arm than the Confluence, respectively. At the tributary stations, TN explains about 50 percent of the variance in chlorophyll-a concentrations at the North Anna River and 30 percent at Pamunkey Creek, and DIN explains about 20 percent at both stations (Figure 9). Relations between chlorophyll-a and nitrogen across the lake were more station specific. TN explained 45 to 86 percent of the variance in chlorophyll-a concentrations at the North Anna arm and Confluence stations, but only 12 percent of the variance at the Pamunkey Creek arm station. In contrast, DIN explained about 25 percent of the variance in chlorophyll-a concentrations at the Pamunkey Creek arm station, 10 percent at the North Anna arm station, and less than 1 percent at the Confluence station. At the North Anna arm and Pamunkey Creek arm stations, there were negative relations between chlorophyll-a and DIN. There was visually one outlier for the North Anna arm and two outliers for the Pamunkey Creek arm for TN that were collected after a high-turbidity inflow event. The exclusion of outliers increased the amount of variance explained by 4 percent for the North Anna arm and 48 percent for the Pamunkey Creek arm.

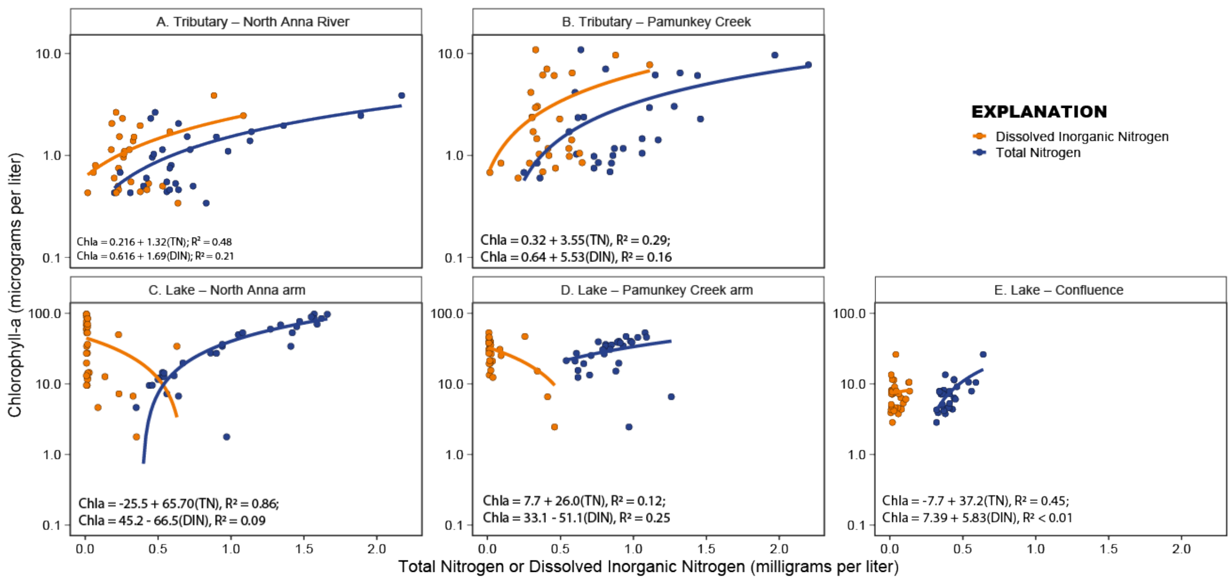

Figure 9. Graphs showing the parametric linear relation between chlorophyll-a and total nitrogen (TN) and dissolved inorganic nitrogen (DIN) concentrations at *A,* North Anna River (016701405), *B,* Pamunkey Creek (01670200), *C,* North Anna arm (01670144), *D,* Pamunkey Creek arm (01670209), *E,* the Confluence (016702576; U.S. Geological Survey, 2026) in the Lake Anna watershed in central Virginia, 2023–2024. Refer to Table 1 for additional station information.

The median TP concentrations at the Lake Anna stations were 0.02–0.08 mg/L, which is similar to the median TP concentrations at the tributary stations of 0.05 mg/L at the North Anna arm and 0.08 mg/L at Pamunkey Creek (Table 8). The minimum and median TP concentrations were similar at the lake and tributary stations. However, the tributary stations had maximum TP concentrations that were 1.5 to 6-times higher than the lake stations. The North Anna arm and Pamunkey Creek arm had TP concentrations that were 2 and 3.7-times higher than the Confluence station, respectively. The minimum and median OP concentrations were similar at both the lake and the tributary stations, ranging from 0.00 - 0.02 mg/L. The maximum OP concentrations were similar at both tributary stations and the Pamunkey Creek arm, with concentrations of 0.11, 0.12, and 0.16 mg/L at the Pamunkey Creek arm, North Anna River, and Pamunkey Creek, respectively. The maximum OP concentrations at the North Anna arm and the Confluence were lower, with concentrations of 0.04 mg/L and 0.00 mg/L. There was one outlier determined visually for the North Anna arm and two outliers determined visually for the Pamunkey Creek arm for TN that were collected after a high-turbidity inflow event. The exclusion of outliers increases the amount of variance explained by 17 percent for the North Anna arm and decreases the amount of variance explained by 15 percent for the Pamunkey Creek arm (Figure 10).

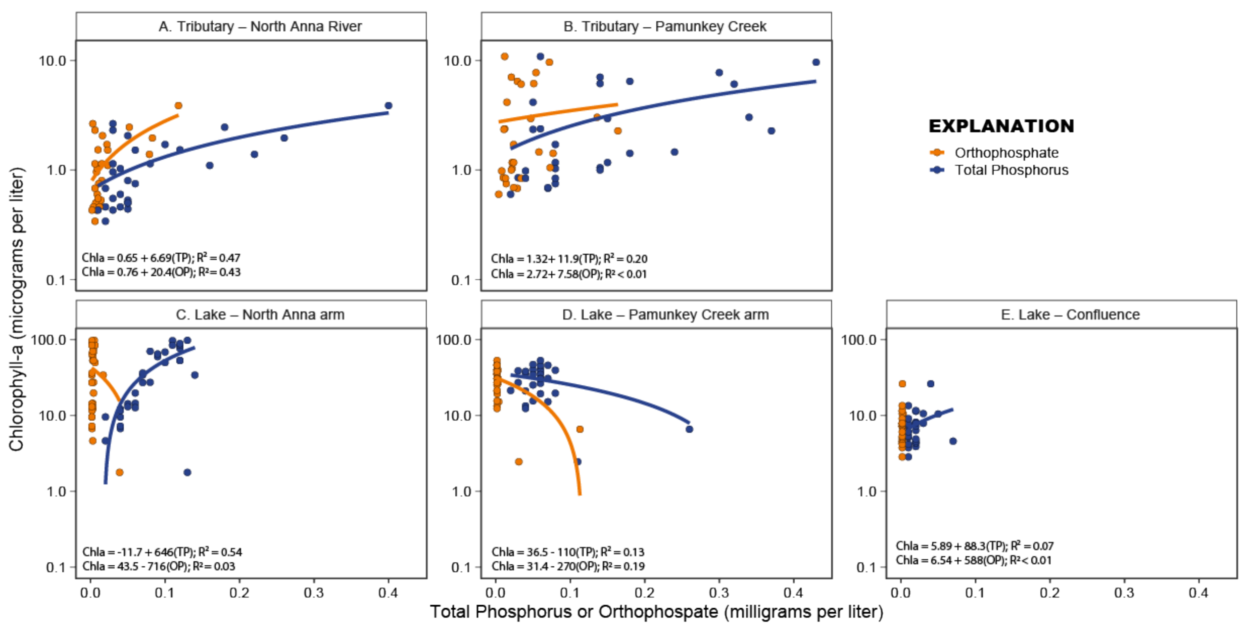

Figure 10. Graphs showing the parametric linear relation between chlorophyll-a concentration and total phosphorus (TP) and OP at *A,* North Anna River (016701405), *B,* Pamunkey Creek (01670200), *C,* North Anna arm (01670144), *D,* Pamunkey Creek arm (01670209), *E,* the Confluence (016702576; U.S. Geological Survey, 2026) in the Lake Anna watershed in central Virginia, 2023–2024. Refer to Table 1 for additional station information.

At the tributary stations, TP and OP explained a greater proportion of variance in chlorophyll-a at the North Anna River than at Pamunkey Creek. At the North Anna River, TP and OP explained 47 and 43 percent of the variation in chlorophyll-a compared to 20 percent and less than 1 percent at Pamunkey Creek. The relations between TP and OP across the lake stations were station specific. TP explained 13 and 54 percent of the variance at the Pamunkey Creek and North Anna arm, respectively, but only 7 percent at the Confluence. OP did not explain much variance at any location, explaining 3, 19, and less than 1 percent at the North Anna arm, Pamunkey Creek arm, and Confluence stations, respectively. There is a negative relation between OP and chlorophyll-a at the North Anna arm and Pamunkey Creek arm, but a positive relation at the Confluence.

The TN:TP ratio varied across stations and over time (Figure 11). At the tributaries, the TN:TP ratios mostly were less than 22. At the North Anna River station, TN:TP ratios were greater than 22 (10.3 percent) for three samples, less than 9 (24.1 percent) for 7 samples, and between 9 and 22 (65.5 percent) for 19 samples. At the Pamunkey Creek station, TN:TP ratios were greater than 22 (3.4-percent) for 1 sample, less than 9 (62.1 percent) for 18 samples, and between 9 and 22 (35.5 percent) for 10 samples. At the Lake Anna stations (Figure 11: C-E), 28 of the 31 samples (90.3-percent) at the North Anna arm, 25 of the 30 samples (83.3 percent) at the Pamunkey Creek arm, and 16 of the 29 samples at the Confluence (55.2 percent) had TN:TP ratios between 9 and 22. However, at the Confluence, 12 of the 29 samples (41.4-percent) were greater than 22. The greatest range in TN:TP conditions were observed at the Confluence, with a minimum of 5.9 and a maximum of 46. The smallest range was observed at the North Anna arm, with a minimum of 7.5 and a maximum of 23.0.

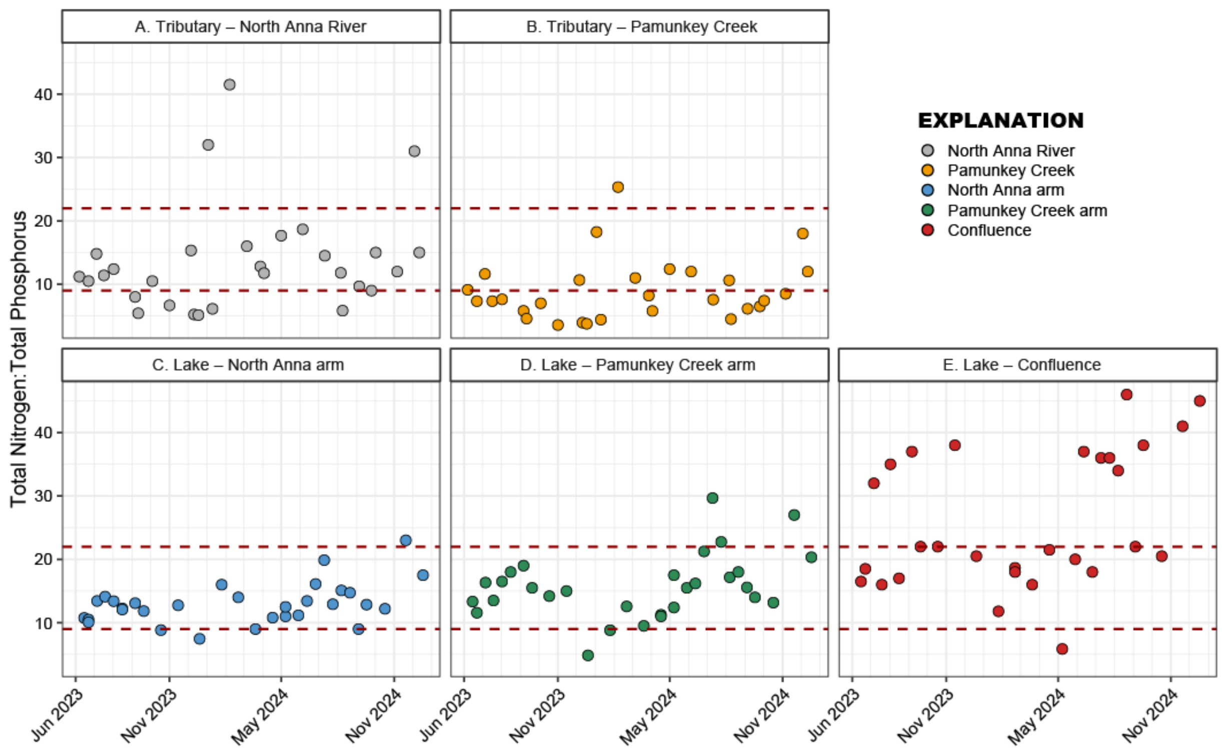

Figure 11. Graphs showing the time series of the total nitrogen to total phosphorus ratio of discrete samples collected at *A,* North Anna River (016701405), *B,* Pamunkey Creek (01670200), *C,* North Anna arm (01670144), *D,* Pamunkey Creek arm (01670209), *E,* the Confluence (016702576; U.S. Geological Survey, 2026) in the Lake Anna watershed in central Virginia, 2023–2024. A TN:TP ratio less than 9 (red dashed line) indicates that the water body is nitrogen limited. In between the dashed lines is when the TN:TP ratio is co-limiting. A sample with a TN:TP ratio greater than 22 is when the body of water is phosphorus limited. Refer to Table 1 for additional station information.

Evaluation and Identification of Algal Bloom Drivers

Due to a lack of detectable toxin concentrations at all three lake stations from May 2023 through December 2024, the drivers of the algal community and algal biomass were modeled and evaluated. The station characteristics of the three continuous monitoring lake stations were assessed. The community composition of the three lake stations were evaluated using a PerMANOVA to determine if the data could be pooled across the three stations. Finally, the drivers of algal biomass were identified, and the directionalities and magnitudes of the relations were assessed.

General Limnological Conditions of Lake Anna Monitoring Stations

Station characteristics varied with depth. The North Anna arm ranges from 1.0 to 1.75 m deep, with a median depth of 1.5 m. The Confluence was deeper, ranging from 1.25 to 2.0 m deep, with a median depth of 1.5 m. Pamunkey Creek was the deepest, ranging from 2.8 m to 4.5 m deep, with a median depth of 4.0 m. Out of the 28 samples collected at each station by the USGS, stratified conditions were recorded at all three stations. Stratified conditions were observed 10.7, 7.14, and 3.6 percent of the time in the North Anna arm, Pamunkey Creek arm, and Confluence, respectively. Secchi disk depths were the lowest on the North Anna arm, ranging from 0.15 to 1.2 m, with a median of 0.4 m. At Pamunkey Creek, the Secchi disk depths ranged from 0.25 to 1.1 m, with a median of 0.7 m. At the Confluence station Secchi disk depths ranged from 0.9 to 1.6 m, with a median of 1.5 m.

Assessing Station, Season, and Year on Algal Community Composition

Of the variables station, season, and year, season explained the most variability in all global tests and was a significant predictor of algal community composition (p-values < 0.05) at all levels tested, that is total community, all cyanobacteria, and pTOX cyanobacteria (Figure 12). Site was also a significant predictor of the total phytoplankton and cyanobacterial community but not the pTOX cyanobacterial community. Year was only a significant predictor of the pTOX cyanobacterial community composition. Combinations of station, season, and year were also significant predictors and generally explained more variability.

Overall, phytoplankton community composition was similar among years but was significantly different between the arms stations and the Confluence station (Figure 12). In addition, summer and winter assemblages were significantly different from assemblages in other seasons. The cyanobacterial community showed similar patterns, indicating their overall dominance in the Lake Anna phytoplankton community. In contrast, the pTOX community was not significantly different among stations but was significantly different between years and among seasons. To help identify drivers of algal biomass and cyanobacterial communities, all data was pooled to incorporate the natural gradients encountered in the western end of Lake Anna.

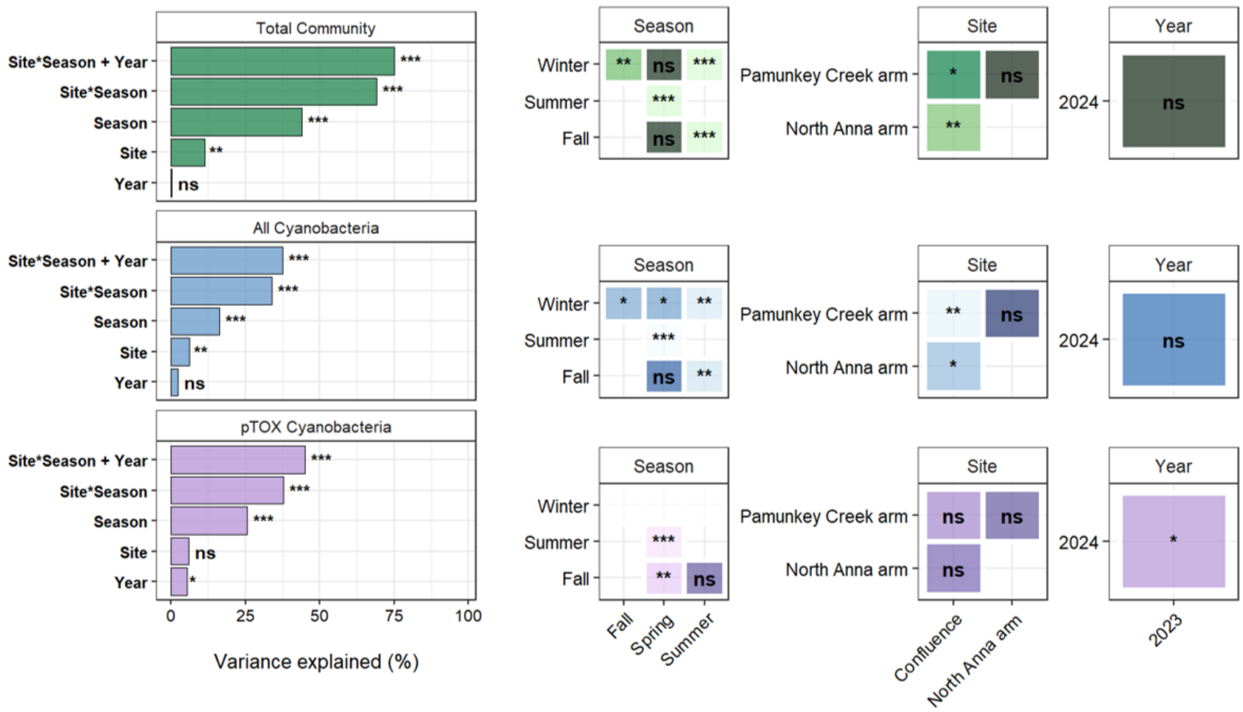

Figure 12. Results of global and pairwise permutational multivariate analysis of variance (PerMANOVA) statistical tests on relative abundance of cell densities for the total community (all taxa; top row), all cyanobacteria (cyanobacteria taxa only; middle row), and pTOX cyanobacteria (potentially toxic cyanobacteria taxa only; bottom row). Refer to Table 1 for additional station information. [* indicates a significant result with p-values ranging from <0.01–0.05, ** indicates a significant result with p-values ranging from <0.001–0.01 , *** indicates a significant result with p-values <0.001, ns indicates a non-significant result with p-values ≥ 0.05]

Identifying Potential Drivers of Algal Biomass and Cyanobacteria Proliferation

The statistically significant drivers differed among the biological response models (Figure 13). Water temperature and total nitrogen were statistically significant in all 5 models. Alkalinity and molybdenum were retained in 4 of the five biological response models. Alkalinity was retained in the algal biomass, cyanobacteria, pTOX, and *Raphidiopsis* models and molybdenum was retained in the algal biomass, cyanobacteria, pTOX excluding *Raphidiopsis*, and *Raphidiopsis* models. The cyanobacteria CRF and GAM model had the largest number of statistically significant drivers at 8, followed by algal biomass, pTOX, and *Raphidiopsis*, with 6 drivers each. Some drivers, such as sodium, TP, and wind speed, were only retained as statistically significant drivers in one model. Sodium was identified as a driver in the pTOX model, and wind speed and TP were both identified as drivers in the pTOX excluding *Raphidiopsis* model.

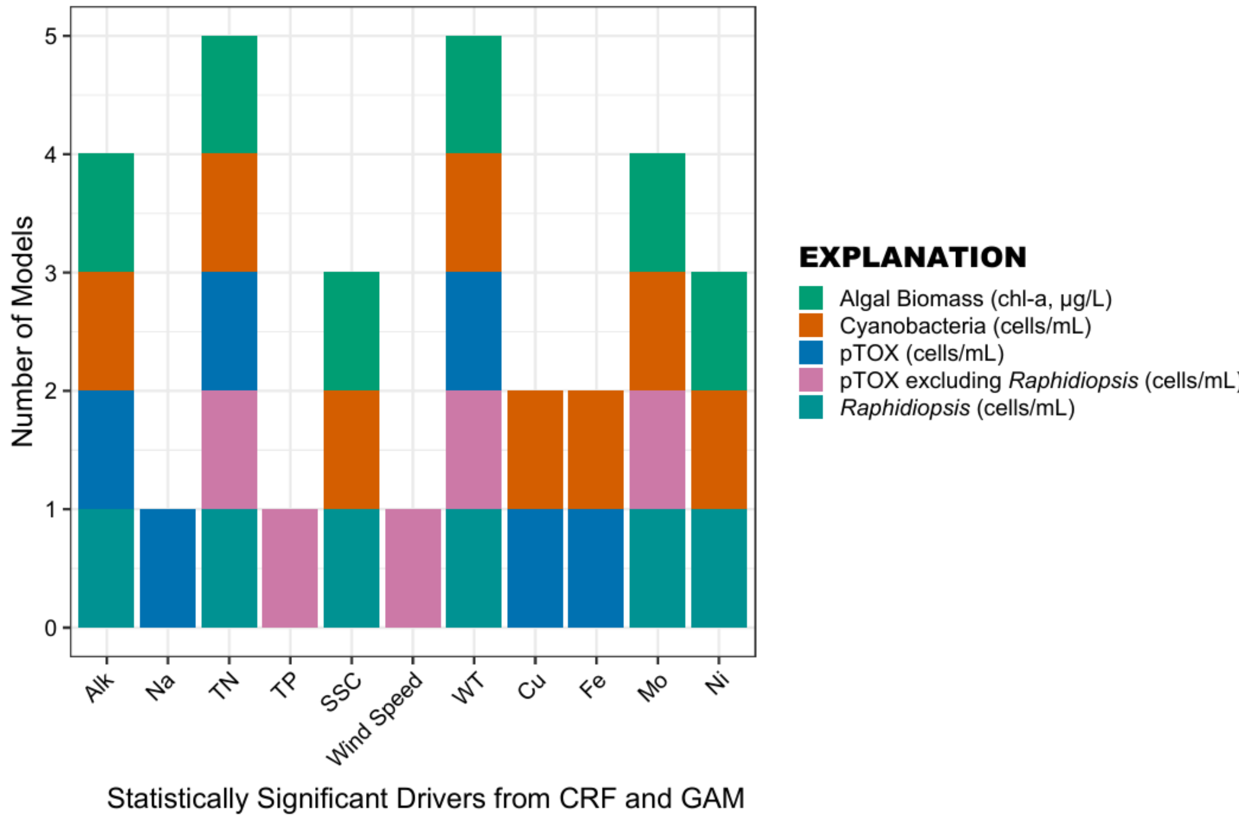

Figure 13. Bar chart showing the statistically significant drivers from the conditional random forest (CRF) and generalized additive model (GAM). The stacked bars show the number of models for which each driver was statistically significant, and the colors identify the model in which the driver was identified as statistically significant. The drivers included alkalinity (Alk), sodium (Na), total nitrogen (TN), total phosphorus (TP), suspended sediment concentration (SSC), wind speed, water temperature (WT), copper (Cu), iron (Fe), molybdenum (Mo), and nickel (Ni). Additional information is available about the stations used in these models in Table 1. Data used in these models are available at USGS Water Data for the Nation (U.S. Geological Survey, 2026).

Because the GAM models focused on increasingly specific biological groups, the proportion of variance explained in each biological group decreased (Figure 14). The algal biomass model, chlorophyll-a concentration, was the most biologically broad model, with driver variables explaining 93.7 percent of the variance. The cyanobacteria model explains 78.7 percent of the variance, followed by the pTOX model (73.1 percent), the *Raphidiopsis* model (69.4 percent), and the pTOX excluding *Raphidiopsis* model (49.7 percent).

In the chlorophyll-a model, water temperature explained the greatest amount of variance (26.6 percent; Appendix Table 2.1) with a bimodal trend. There was a positive effect between 9.14 to 17.2 and 26.4 to 32.8 °C and a negative effect at less than 9.14, 17.2 to 26.4 and greater than 32.8°C (Figure 15). TN and Ni explained 26.2 and 19.1 percent of the variance, respectively, with TN having a positive asymptotic relation above 0.62 mg/L and Ni having a negative asymptotic relation above 0.45 µg/L. Alk, Mo, and SSC explained the remaining 21.8 percent of variability.

In the cyanobacteria model, Ni explains the most variance at 18.8 percent, with a non-monotonic and asymmetric trend where values declined a minimum at 0.61 µg/L and then increased and plateaued. There was a positive effect from 0 to 0.37 µg/L, a negative effect from 0.37 to 0.78 µg/L, and a positive effect after 0.78 µg/L. TN, water temperature, and alkalinity represented 18.2, 10.9, and 10.0 percent of the explained variance, respectively. TN and alkalinity have an increasing asymptotic relation, with a transition to a positive effect at 0.57 mg/L for TN and 19.3 mg/L for alkalinity. The remaining 20.8 percent of the variability is explained by molybdenum, copper, iron, and suspended sediment concentration.

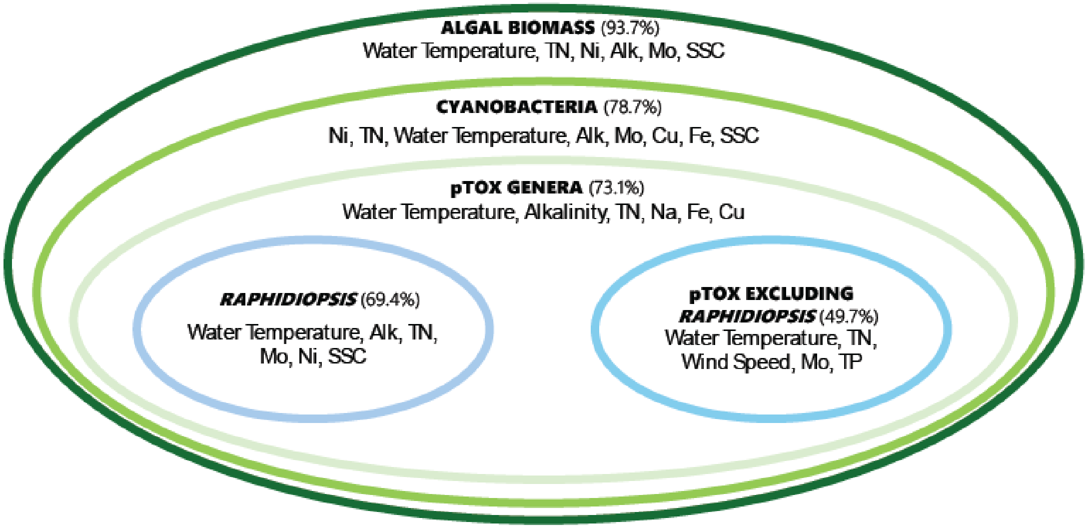

Figure 14. Conceptual diagram of the environmental drivers associated with each of the five distinct algal community modeling approaches. The ellipses represent those key drivers of each model (i.e., algal biomass, cyanobacteria, pTOX genera, *Raphidiopsis*, and pTOX excluding *Raphidiopsis*, in order from the most influential to the least influential driver. The percentages indicate the amount variance explained by the model. Additional information is available about the stations used in these models in Table 1. Data used in these models are available at USGS Water Data for the Nation (U.S. Geological Survey, 2026).

Water temperature explains the most variance in the pTOX genera model (33.1 percent). The water temperature shows a trough at temperatures below 16.3°C, with a minimum at 10°C. Above 16.3°C, there is a positive asymptotic relation. Alkalinity explains 15.9 percent of the variance with a nonlinear positive trend. Below an alkalinity of 18.1 mg/L, there is a negative effect on pTOX cell counts, and above 18.1 mg/L, there is a positive effect. The remaining 24.1 percent of the variance is comprised of TN, Na, Fe, and Cu. TN and Na both have a nonlinear inverted trough-shaped relation, with a peak at around 1.2 mg/L and 5.8 mg/L, respectively. Fe and Cu both have a monotonic, positive relation, that transitions from a lower value of cell counts to a higher value of cell counts at 70.5 and 1.3 µg/L, respectively.

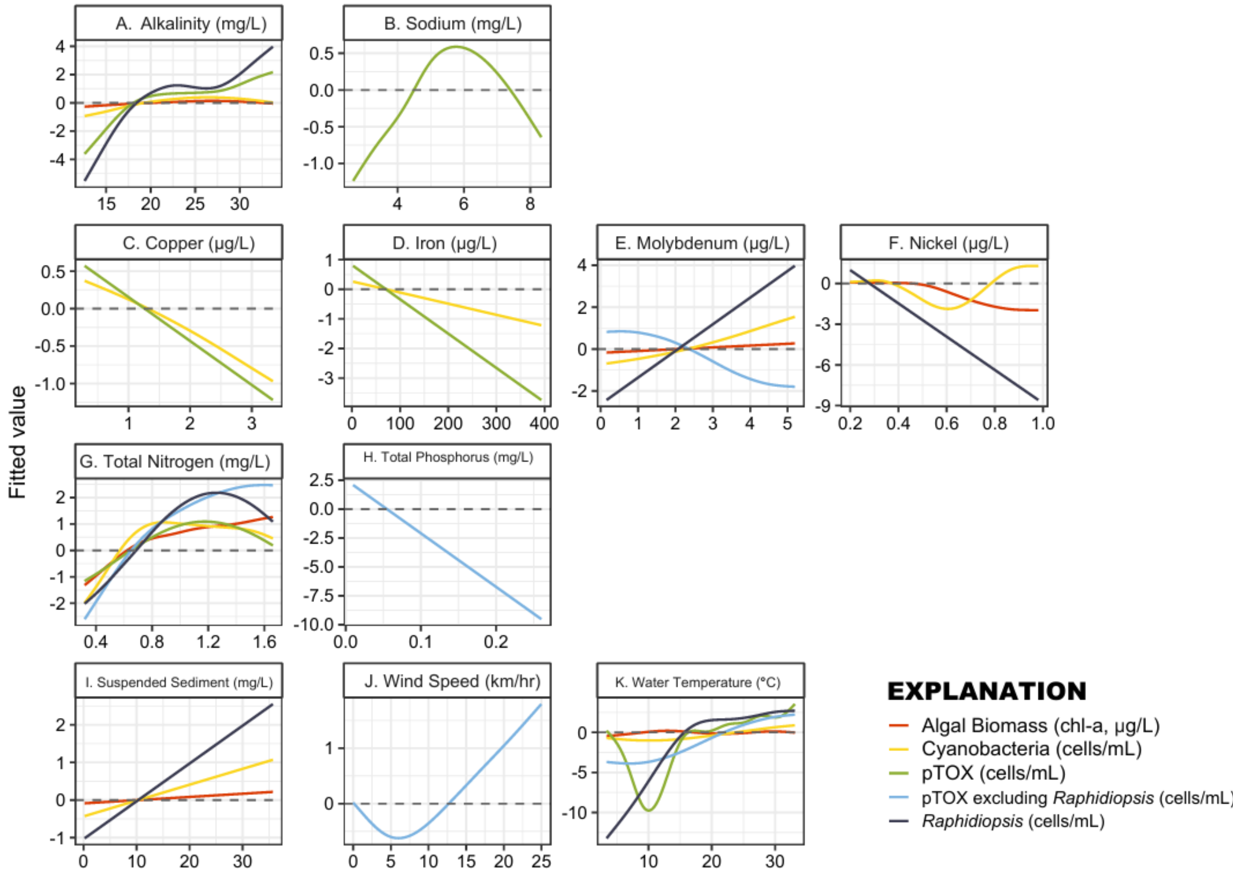

Figure 15. Partial effects plots from the generalized additive models of algal biomass (chlorophyll-a), cyanobacteria, pTOX genera, pTOX excluding *Raphidiopsis*, and *Raphidiopsis*. *A*, Alkalinity; *B*, Sodium (Na); *C*, Copper (Cu); *D*, Iron (Fe); *E*, Molybdenum (Mo); *F*, Nickel (Ni); *G*, Total Nitrogen (TN); *H*, Total phosphorus (TP); *I*, Suspended Sediment Concentration (SSC); *J*, Wind speed; *K*, Water temperature. The units are in milligrams per liter (mg/L) or micrograms per liter (µg/L), kilometers per hour (km/hr), and degrees Celsius (°C). Variables that were not statistically significant were not included in each model and were therefore not included in every plot. If the fitted value is above zero, the predictor is contributing more than its average contribution. If the fitted value is less than zero, the predictor is contributing less than its average contribution. The average contribution is at zero. Station information for the stations included in these models is found in Table 1. Data used in these models are available at USGS Water Data for the Nation (U.S. Geological Survey, 2026).

In the *Raphidiopsis* model, water temperature and alkalinity both explain 21.5 and 20.7 percent of the variation in the model, respectively. Both drivers have a non-linear, positive relation for the partial effect plot. Alkalinity values less than 18.4 mg/L and water temperatures less than 15.7°C have a negative effect, which values greater than 18.4 mg/L and 15.7°C have a positive effect on *Raphidiopsis* cell counts. The remaining 27.2 percent of the variance is explained by TN, Mo, Ni, and SSC. Mo and SSC have a positive linear relation, Ni has a negative linear trend, and TN has a positive asymptotic trend with *Raphidiopsis* cell counts.

In the pTOX excluding Raphidiopsis model, water temperature, total nitrogen, wind speed, and molybdenum explain 13.3, 11.9, 10.2, and 9.4 percent of the variation, respectively. The remaining 4.9 percent is explained by total phosphorus. Water temperature, total nitrogen, and wind speed have asymptotic positive relations that transition from a negative to positive effect at 22°C, 0.7 mg/L, and 12.7 km/hr. Molybdenum has a nonlinear, negative relation that has a positive effect at values less than 2.4 µg/L and a negative effect at values greater than 2.4 µg/L. TP has a negative linear relation; there is a positive effect at low TP concentrations of less than 0.05 mg/L and a negative effect at TP concentrations greater than 0.05 mg/L.

Sources of Algal Bloom Drivers

External and internal sources were evaluated to determine potential pathways for the drivers. The timing, magnitude, and duration of external drivers were analyzed to determine the role that external loading plays in HAB initiation, persistence, and decline. In shallow, eutrophic lakes, such as Lake Anna, internal loading can contribute to the nutrient and micronutrient availability and subsequent cyanobacteria bloom development. Stratification-driven hypoxia and wave-induced resuspension of lake-bed sediments can create multiple pathways for bed sediment and interstitial pore water to release nutrients and trace metals into the water column. Although each pathway was investigated individually, these pathways could be occurring concurrently throughout the Lake Anna watershed.

Evaluating Drivers from Tributaries

Data for six of the 11 drivers of HABs identified within the lake water column were also measured for in the water column of the tributaries: total nitrogen, total phosphorus, suspended sediment concentration, alkalinity, sodium, and water temperature. The timing, magnitude, and duration of exportation of these drivers to Lake Anna are important for understanding the extent these inputs influence HAB development.

Chemical drivers measured in the tributaries include alkalinity and sodium. Mean (± standard deviation) alkalinity concentrations at the tributary stations were 33.1 mg/L ± 10.6 mg/L and 27.6 mg/L ± 9.9 mg/L at Pamunkey Creek and North Anna River, respectively (Table 9). Mean (± standard deviation) sodium concentrations at the tributary stations were 4.1 mg/L ± 1.0 mg/L and 3.9 mg/L ± 1.0 mg/L at Pamunkey Creek and North Anna River, respectively. Lower concentrations of these drivers were observed during stormflow, and higher concentrations were observed during baseflow (Figure 16). Alkalinity concentrations in baseflow conditions were consistently greater than 30 mg/L during the warmer months at Pamunkey Creek with maximum concentrations reaching 50.7 and 42.4 mg/L, respectively (Figure 16; Table 9). Sodium concentrations were generally greater than 4 mg/L during baseflow conditions at both streams, with maximum concentrations reaching about 5.5 mg/L, and generally followed the same seasonal pattern as alkalinity.

Nutrient drivers measured in the water column of the tributaries included total nitrogen and total phosphorus concentrations. These drivers were observed to have enrichment behavior, with higher concentrations during storms and lower concentrations during baseflow (Figure 16). Mean (± standard deviation) total nitrogen concentrations during baseflow were 0.9 mg/L ± 0.4 mg/L and 0.7 mg/L ± 0.4 mg/L in Pamunkey Creek and North Anna River, respectively (Table 9). Maximum measured total nitrogen concentrations during storms were 2.2 mg/L in both Pamunkey Creek and North Anna River. Mean total phosphorus concentrations in baseflow stream conditions were 0.142 mg/L ± 0.112 mg/L and 0.08 mg/L ± 0.088 mg/L at Pamunkey Creek and North Anna River, respectively. Maximum measured total phosphorus concentrations during storms were 0.43 and 0.4 mg/L Pamunkey Creek and North Anna River, respectively.

Physical drivers measured in the tributaries include SSC and water temperature. Mean (± standard deviation) suspended sediment concentrations were 35.4 mg/L ± 46.1 mg/L and 27.4 mg/L ± 37.6 mg/L at Pamunkey Creek and North Anna River, respectively. During baseflow, the mean SSC was 7.90 mg/L and 7.55 mg/L at Pamunkey Creek and North Anna River, respectively. Maximum measured SSC were 157 and 139 mg/L during storms for Pamunkey Creek and North Anna River, respectively. Water temperatures varied seasonally, with the highest temperatures in summer (26.5°C at Pamunkey Creek and 25.2°C at North Anna River) and lowest in winter (0.5°C at Pamunkey Creek and 0.6°C at North Anna River). Water temperatures were similar before, during, and after storm events.

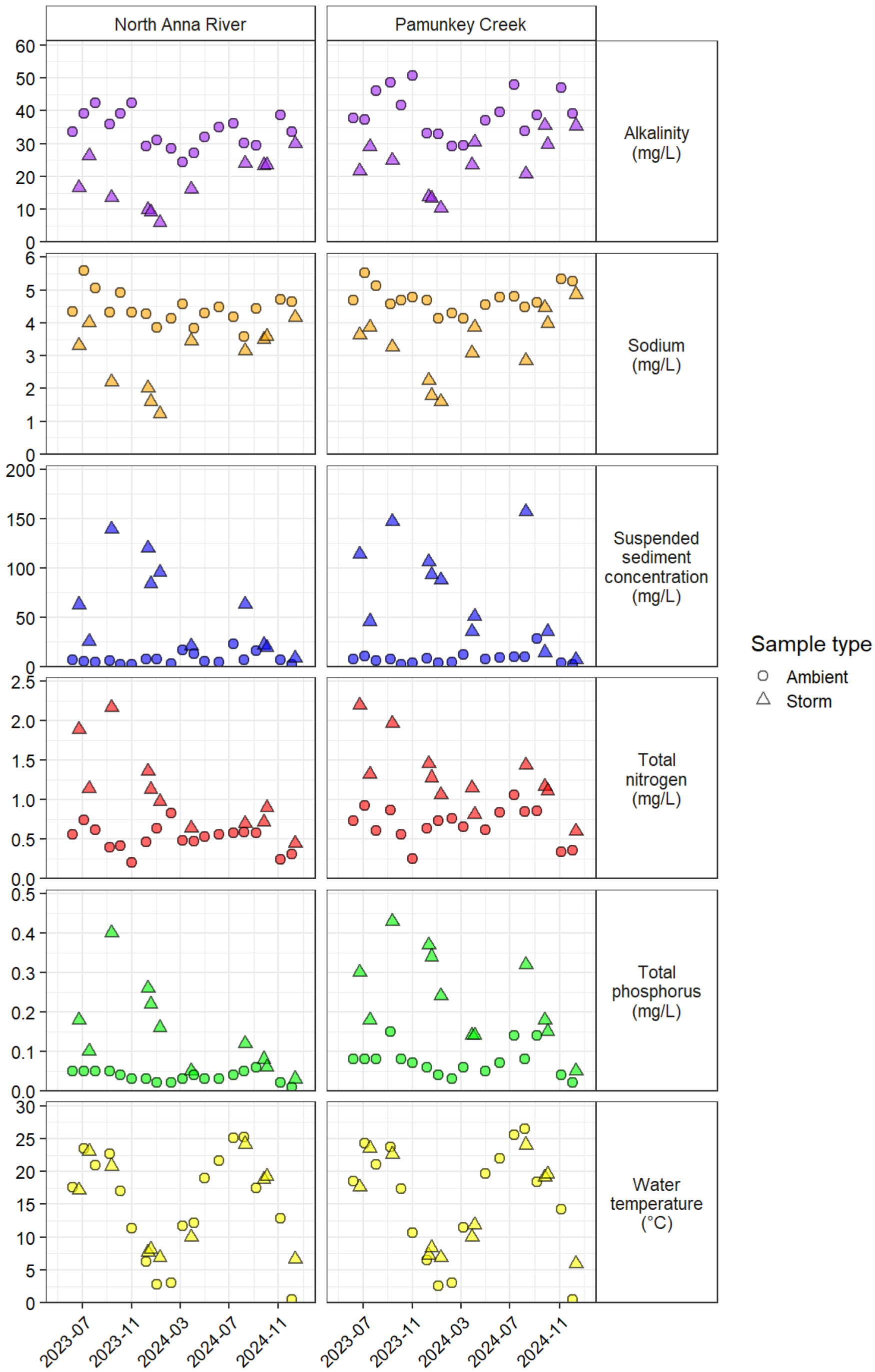

Figure 16. Time series of the discrete water quality data from North Anna River and Pamunkey Creek tributaries during 2023 –2024. Circle points represent baseflow and triangle points represent stormflow. Refer to Table 1 for additional station information.

Table 9. Descriptive statistics of identified drivers that were measured in the tributaries to Lake Anna, Pamunkey Creek and North Anna River. Refer to Table 1 for additional station information.

[n, observations; Min, minimum; SD, standard deviation; Max, maximum]

Parameter	n	Min	Mean	Median	SD	Max
Pamunkey Creek						
Alkalinity (mg/L)	29	10.4	33.1	33.9	10.6	50.7
Sodium (mg/L)	29	1.6	4.1	4.5	1.0	5.5
WT (degrees Celsius)	29	0.5	15.3	17.6	7.8	26.5
SSC (mg/L)	29	2.3	35.4	9.7	46.1	157.0
TN (mg/L)	29	0.3	0.9	0.9	0.4	2.2
TP (mg/L)	29	0.020	0.142	0.080	0.112	0.430
North Anna River						
Parameter	**n**	**Min**	**Mean**	**Median**	**SD**	**Max**
Alkalinity (mg/L)	29	6.0	27.8	29.4	9.9	42.4
Sodium (mg/L)	29	1.2	3.9	4.2	1.0	5.6
WT (degrees Celsius)	29	0.6	14.9	17.2	7.4	25.2
SSC (mg/L)	29	1.8	27.4	8.4	37.6	139.0
TN (mg/L)	29	0.2	0.7	0.6	0.4	2.2
TP (mg/L)	29	0.010	0.080	0.050	0.088	0.400

Accumulated loads of SSC, TN, and TP were higher at Pamunkey Creek compared to the North Anna River. Across water year 2024, the North Anna River delivered an estimated 1,820,891 kilograms of suspended sediment, 32,641 kilograms of TN, and 3,563 kilograms of TP, and Pamunkey Creek delivered an estimated 2,838,414 kilograms of SCC, 40,183 kilograms of TN, and 6,266 kilograms of TP (Table 10). The largest increase in accumulated load over the shortest period occurred from mid-December 2023 through January 2024 (Figure 17). The 4 largest storms were recorded at both stations during this period. At Pamunkey Creek, 47.3 percent of the suspended sediment load, 33.3 percent of the TP load, and 26.9 percent of the TN load were delivered during these storms. These storms lasted for a total duration of 5.73 days and represent 1 percent of the study period. At North Anna River, 39.5 percent of the suspended sediment load, 29.8 percent of the TP load, and 21.3 percent of the TN load were delivered during these storms, which lasted for a total duration of 5.13 days and represented 0.9 percent of the study period.

Table 10. Load of TN, TP, and suspended sediment (SS) delivered into Lake Anna from the North Anna River and Pamunkey Creek. Refer to Table 1 for additional station information.

[TN, total nitrogen; TP, total phosphorus; SSC, suspended sediment concentration; Water Year, October 1st through September 30th]

		Kilograms (kg)		
Source	**Timeframe**	**SS**	**TN**	**TP**
North Anna River	Water Year 2024	1,820,891	32,641	3,563
Pamunkey Creek	Water Year 2024	2,838,414	40,183	6,266
North Anna River	Calendar Year 2024	1,528,448	29,986	3,162
Pamunkey Creek	Calendar Year 2024	2,166,705	35,070	5,064

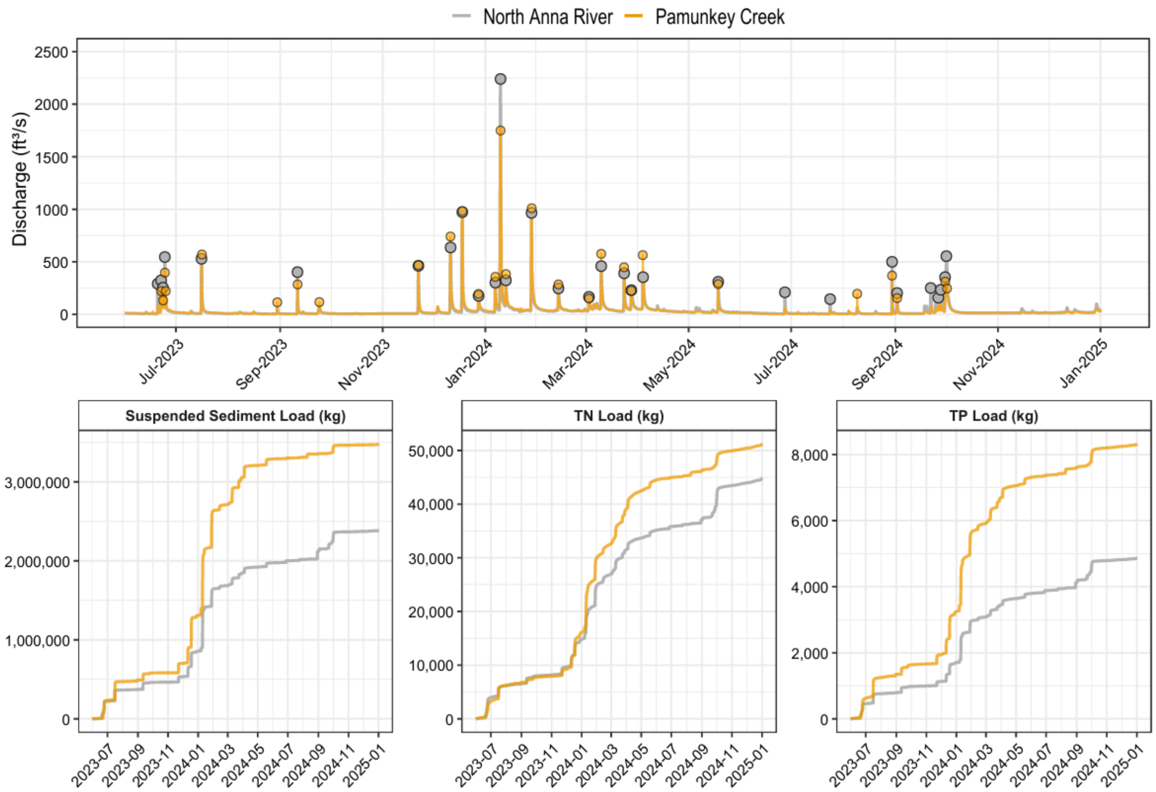

Figure 17. Time series of discharge (in cubic feet per second, ft³/s) with storm peaks identified as points (top); and estimated accumulated loads of suspended sediment, total nitrogen, and total phosphorus exported to Lake Anna from the North Anna River and Pamunkey Creek from June 1, 2023, through December 31, 2024 (bottom). Refer to Table 1 for additional station information.

Suspended sediment, TN, and TP at North Anna River and Pamunkey Creek were primarily delivered during stormflow conditions as determined through baseflow separation analysis. Suspended sediment had the largest proportion of stormflow contribution at both streams, with over 84 percent of the suspended sediment load delivered during stormflow (Figure 18). Stormflow discharge only accounted for 18.6 days at Pamunkey Creek and 19.5 days at North Anna River, representing 3.2 and 3.4 percent of the total study period duration, respectively. Phosphorus loads were also primarily delivered during stormflow. TN had the largest proportion of baseflow contribution, with 34.1 and 37.7 percent of the TN load exported during baseflow from the North Anna River and Pamunkey Creek, respectively; however, like the other constituents, most of the TN load was exported during stormflow.

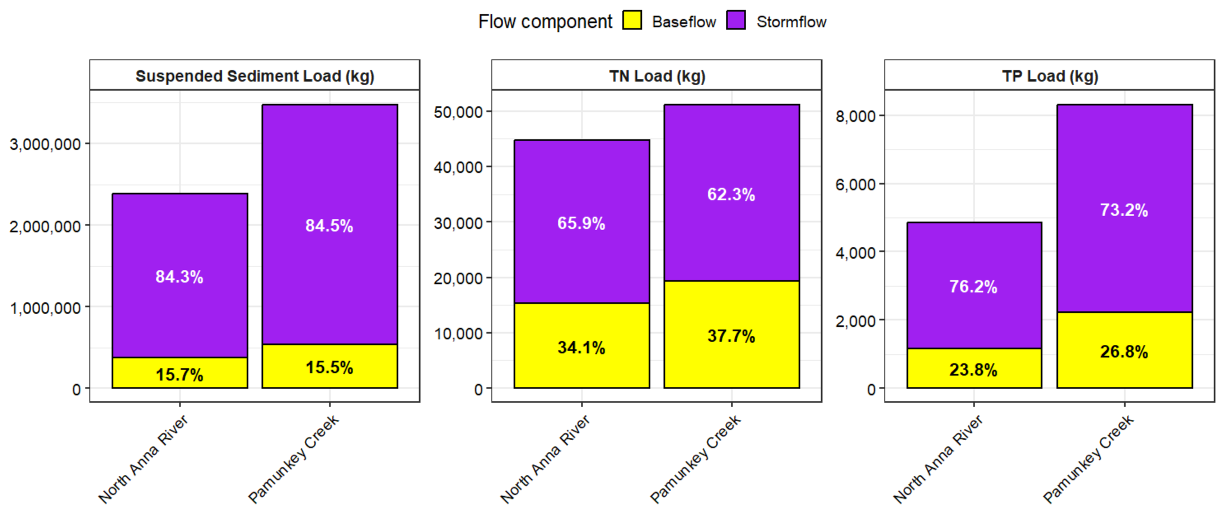

Figure 18. Baseflow and stormflow load contribution percentages of suspended sediment, total nitrogen, and total phosphorus exported by the North Anna River and Pamunkey Creek from June 1, 2023, through December 31, 2024. Bar magnitudes represent the total load of each constituent at each station, and the percentages within each bar represent the proportion of each constituent load delivered during baseflow (yellow) and stormflow (purple). Refer to Table 1 for additional station information.

Tributary loads of suspended sediment, TN, and TP were estimated, and results show exportation of these constituents to Lake Anna at magnitudes that are comparable to other streams in central Virginia (Mason and Soroka, 2026). Both the North Anna River and Pamunkey Creek yields of suspended sediment, TN, and TP in water year 2024 were similar compared to neighboring streams in the area. The North Anna River had the third lowest suspended sediment, TN, and TP yields of the 7 streams compared (Mason and Soroka, 2026; Table 10). Pamunkey Creek had the third highest suspended sediment and TP yields and the second highest TN yields. The 10-year mean constituent yields at the streams were higher or lower than water year 2024, depending on stream and constituent, but were generally similar in magnitude. The water year 2024 suspended sediment, TN, and TP yields at the Lake Anna tributaries were not anomalously high or low when compared to 5 neighboring streams (Table 11).

Table 11. Results of the 10-year mean constituent yields for 5 neighboring streams (Mason and Soroka, 2026) to the Lake Anna tributaries and water year 2024 constituent yields for 5 neighboring streams (Mason and Soroka, 2026) and the Lake Anna tributaries.

Station Name	10-year Mean Constituent Yield (Water Years 2015-2024), in kilograms per hectare (kg/ha)			Water Year 2024 Constituent Yield, in kilograms per hectare (kg/ha)		
	Suspended Sediment	Total Nitrogen	Total Phosphorus	Suspended sediment	Total Nitrogen	Total Phosphorus
Rappahannock River, near Fredericksburg, VA	540	4.73	0.822	384	3.05	0.576
Pamunkey River, near Hanover, VA	140	2.19	0.261	146	2.03	0.242
Mattaponi River, near Beulahville, VA	50.0	2.07	0.187	49.0	1.92	0.177
James River, at Cartersville, VA	402	3.09	0.576	398	2.80	0.560
Appomattox River, at Matoaca, VA	62.0	1.98	0.208	111	2.47	0.310
North Anna River, near Monrovia, VA	—	—	—	137	2.44	0.267
Pamunkey Creek, near Lahore, VA	—	—	—	213	3.02	0.470

In contrast to the high loading rates coming from 4 storms in December 2023 through January 2024, peak algal biomass occurred during the warmer months of July, August, and September, when the loading from the tributaries were low (Figure 19). This pattern was observed for suspended sediment, TN, and TP with both total cell density and pTOX cell density.

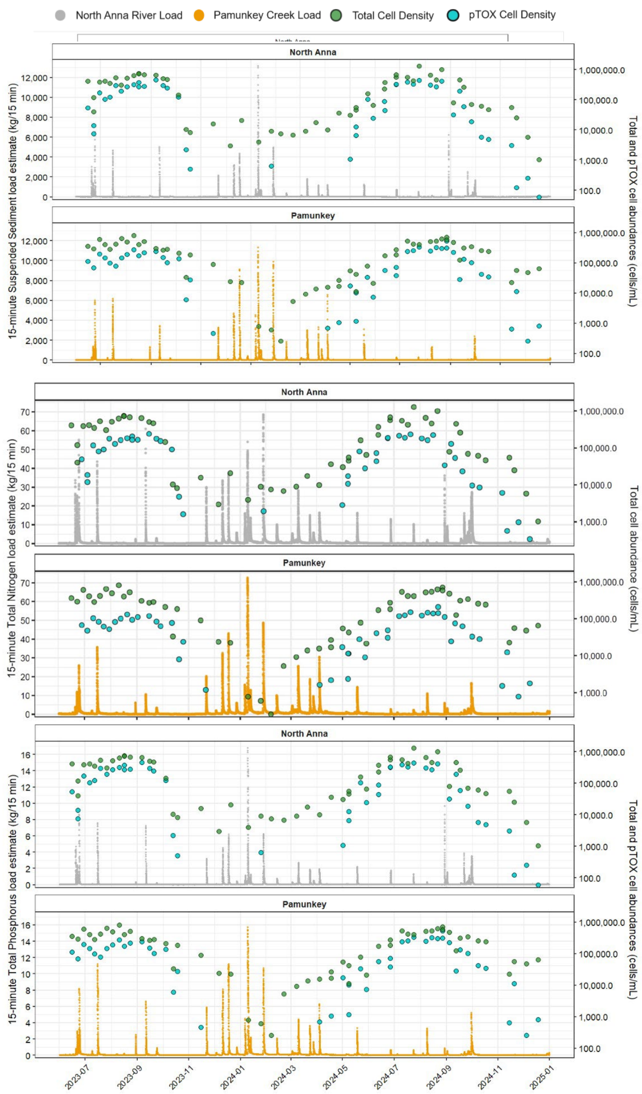

Figure 19. Time series of estimated suspended sediment load (top), total nitrogen load (middle), and total phosphorus load (bottom) at the North Anna River (grey) and Pamunkey Creek (orange). All plots show total cell densities (green points) and potentially toxic cell counts (blue points) at their respective lake stations (North Anna arm and Pamunkey Creek arm). Refer to Table 1 for additional station information.

All estimated constituent yields of water year 2024 were higher at Pamunkey Creek compared to the North Anna River but were similar overall between the two streams (Figure 20). During water year 2024, estimated suspended sediment yields were 136 kg/ha at North Anna River and 213 kg/ha at Pamunkey Creek; estimated total nitrogen yields were 2.4 kg/ha at North Anna River and 3.0 kg/ha at Pamunkey Creek; and estimated total phosphorus yields were 0.3 kg/ha at North Anna River and 0.5 kg/ha at Pamunkey Creek (Table 10).

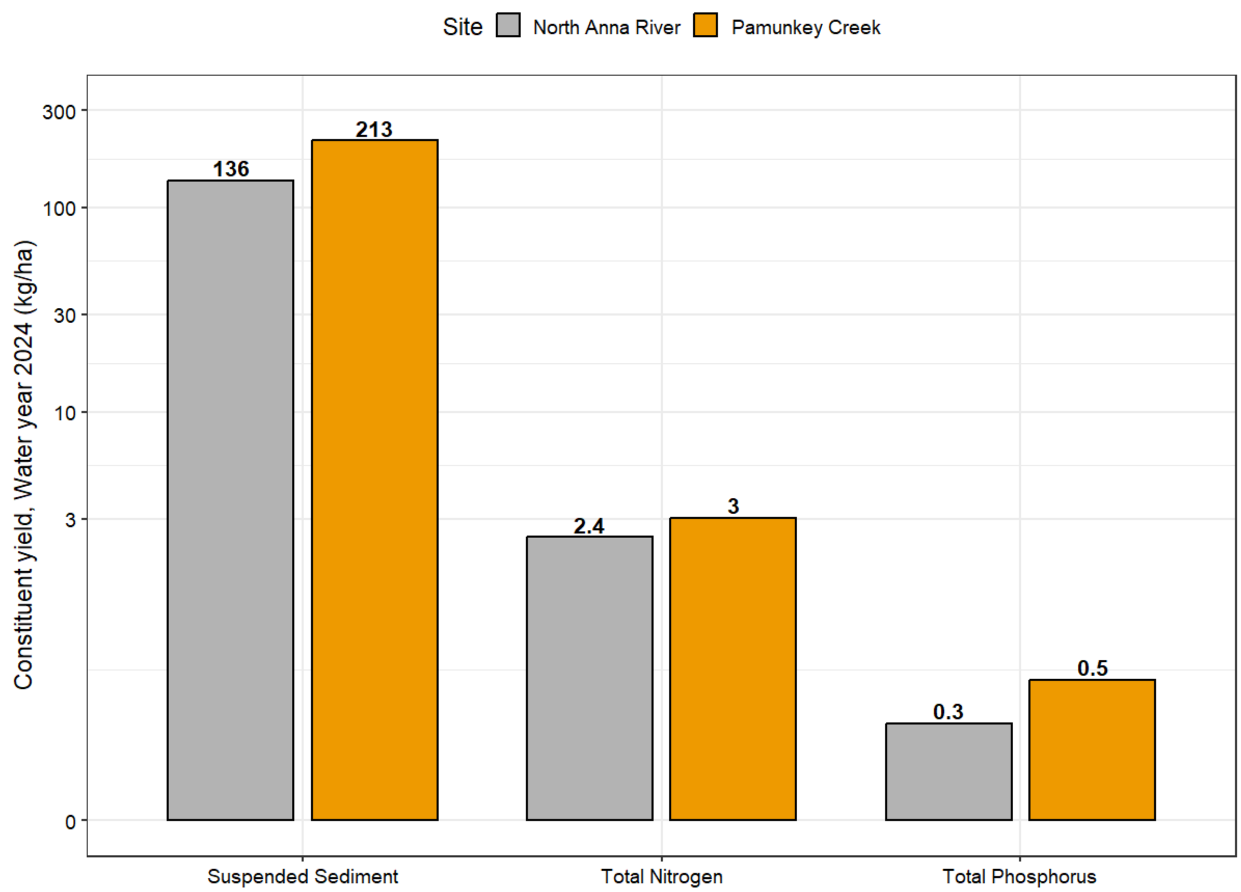

Figure 20. Estimated constituent yields at North Anna River and Pamunkey Creek during water year 2024 from October 1, 2023, through September 30, 2024. Refer to Table 1 for additional station information.

Stable isotope ratios of nitrogen ($\delta^{15}N\text{-}NO_3^-$) and oxygen ($\delta^{18}O\text{-}NO_3^-$) at Pamunkey Creek and North Anna River span multiple source categories. At the North Anna River, 50 percent of the $\delta^{15}N\text{-}NO_3^-$ and $\delta^{18}O\text{-}NO_3^-$ samples indicate manure and human waste as the dominant source of nitrogen, while the other half of the samples contained ratios that indicate multiple sources, including soil nitrogen and ammonium fertilizer and precipitation (Figure 21). At Pamunkey Creek, stable isotope ratios from all samples indicate multiple sources of nitrogen except for one sample that was categorized as a nitrate fertilizer source.

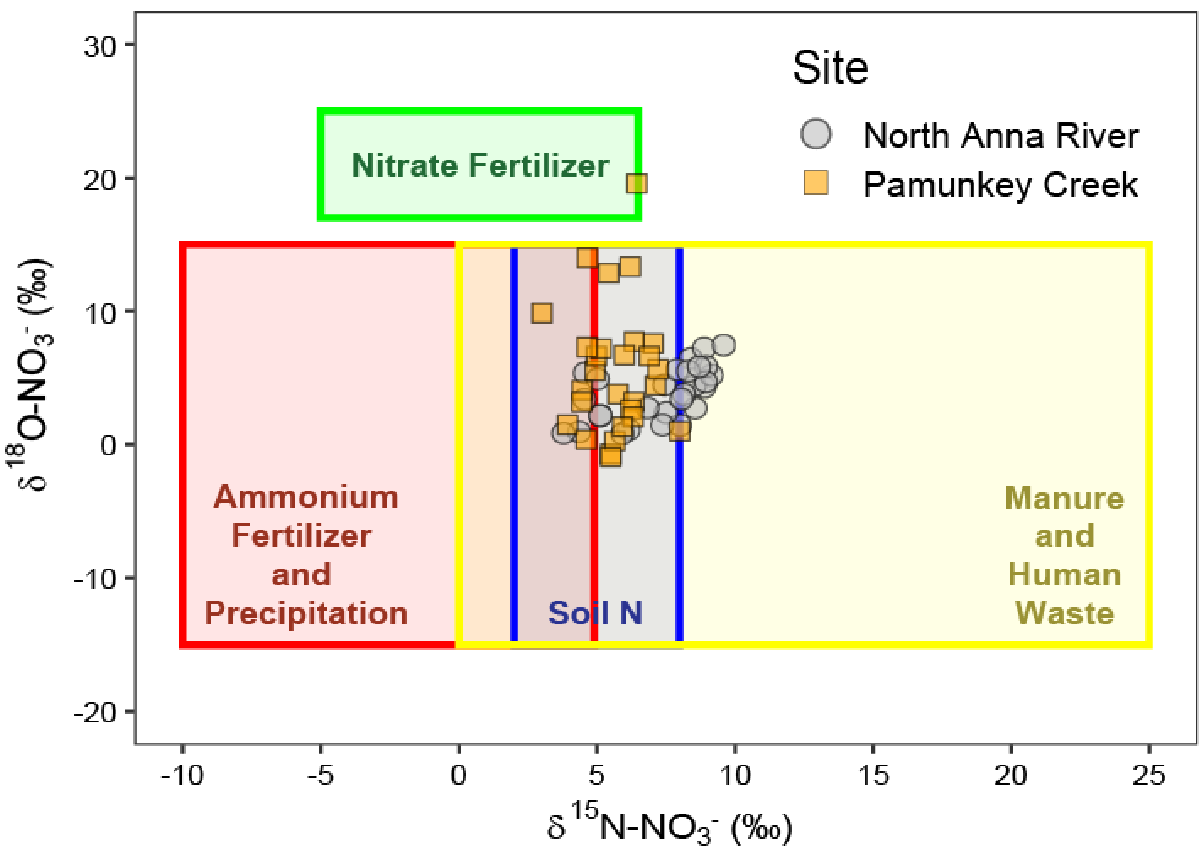

Figure 21. Stable isotope of nitrogen ($\delta^{15}N\text{-}NO_3^-$) and oxygen ($\delta^{18}O\text{-}NO_3^-$) from the North Anna River (grey Points) and Pamunkey Creek (orange points) from 2023 – 2024. Characteristic source ranges (bounding boxes) referenced from Kendall and others (2007), Granger and others (2010), and Snow (2018). Refer to Table 1 for additional station information.

The stable isotope mixing model (SIMM) facilitated apportionment of potential nitrogen sources in the North Anna River and Pamunkey Creek and estimated manure, human waste, and soil nitrogen to likely be the largest sources of nitrogen in both watersheds (Figure 22). At the North Anna River, the SIMM identified manure and human waste as the likely largest contribution of nitrogen and was estimated to range between 42.6 percent and 65.4 percent over the study period (Figure 22). Contributions from soil nitrogen at the North Anna River ranged from 14.1 percent to 48.2 percent, ammonium fertilizer and precipitation from 1.2 percent to 20.6 percent, and nitrate fertilizer from 1.9 percent to 10 percent. At Pamunkey Creek, the SIMM estimated an even contribution of nitrogen sources with soil nitrogen estimated to range from 21.6 percent to 57.4 percent, manure and human waste from 27.5 percent to 44.6 percent, nitrate fertilizer from 5.8 percent to 27.9 percent, and ammonium fertilizer and precipitation from 1.1 percent to 18.5 percent.

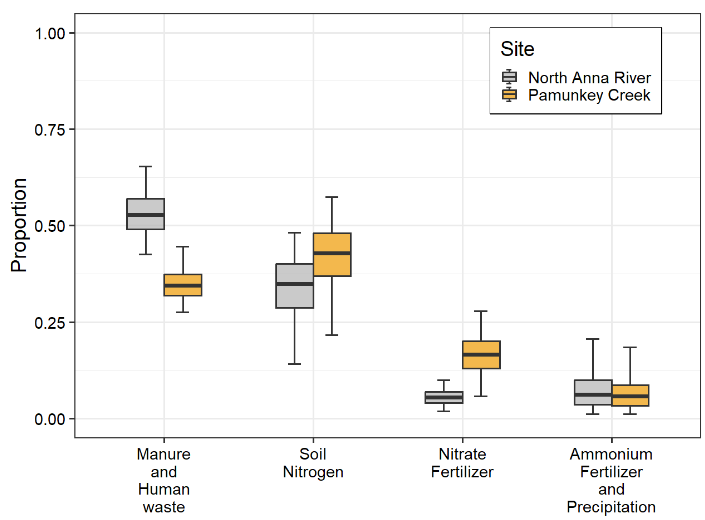

Figure 22. Boxplots of estimated nitrate apportionment from stable isotope mixing model from the North Anna River (grey boxplots) and Pamunkey Creek (orange boxplots) during 2023–2024. Refer to Table 1 for additional station information.

Bed Sediments as a Source of Nutrients and Trace Metals

Bed sediments can be a sink or a source for nutrients and trace metals (Delwiche and others, 2020; Yang and others, 2020). Six of the 11 driving constituents were found to be present in the Lake Anna bed sediments (Figure 23). Across all 3 continuous monitoring stations, analyte concentrations spanned several orders of magnitude, ranging from 0.43 mg/kg for nitrate to 33,000 mg/kg for iron. When ordered from lowest to highest median concentration, the sediment chemistry is NO_3 < Mo < Ni < Cu < Na < Fe.

Lake Anna was divided into three regions to assess spatial patterns in the surficial bed sediment geochemistry within the western lake: the North Anna arm (n = 16; Figure 3, map numbers 1–16), the Pamunkey Creek arm (n = 11; Figure 3, map numbers 18–28), and the Confluence (n = 3; Figure 3; map numbers 17, 29, 30) (Appendix Table 3.1). The North Anna arm had the highest median concentrations for 5 of the 6 drivers, including Fe (33,000 mg/kg), Na (155 mg/kg), Ni (12.5 mg/kg), and nitrate (0.8 mg/kg). The Pamunkey Creek arm had the highest median concentrations for 1 of the 8 drivers, Cu (23 mg/kg). The Confluence had the highest concentration for Mo (1.8 mg/kg). However, the Kruskal-Wallis test did not identify any significant differences in concentrations of the analytes across locations (p-values ≥ 0.05; Figure 23).

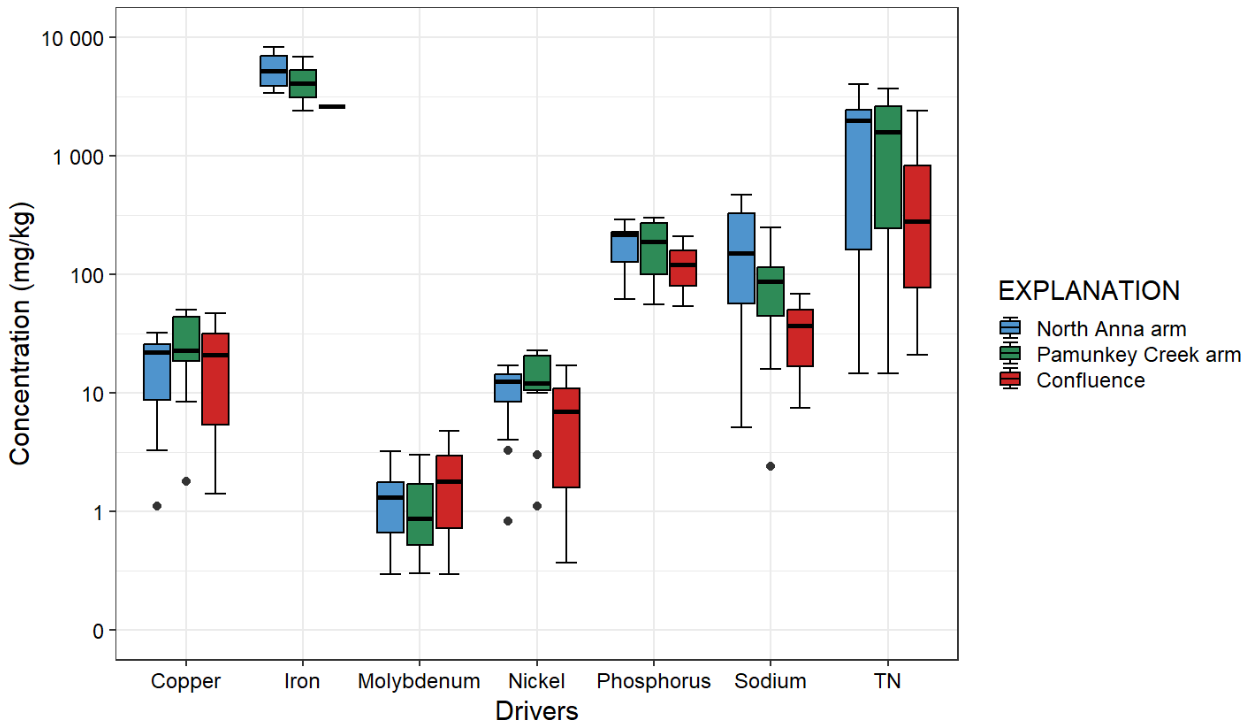

Figure 23. Boxplot showing the bed-sediment concentrations of select constituents identified from the GAMs to have a potential relation with algal biomass and community composition from the three locations in Lake Anna in central Virginia. The n = 30 for all parameters. The boxes represent the interquartile range, with the bottom part of the box at the 25th percentile and the top part of the box at the 75th percentile. The whiskers extend from the minimum, at lower concentrations, and the maximum, at higher concentrations. The points outside the box and whiskers are outliers. Refer to Table 4 for additional station information.

Wave Action Resuspends Lake-Bottom sediments

Maximum wave heights ranged from 0 to 0.457 m at the North Anna arm, 0 to 0.493 m at the Pamunkey Creek arm, and 0 to 0.608 m the Confluence; τ_b ranged from 5.61 x 10^{-9} to 0.023 Pa at North Anna arm, 1.49 x 10^{-14} to 0.006 Pa at Pamunkey Creek arm, and 2.69 x 10^{-7} to 1.12 Pa at Confluence. Critical shear stress was calculated as 9.7 x 10^{-4} at both North Anna arm and Pamunkey Creek arm and 0.24 at the Confluence.

At the North Anna arm, sediment resuspending waves comprise 7.1 percent of the total observed waves in spring, 14.1 percent in summer, 2.4 percent in fall, and 0.5 percent in winter. At the Pamunkey Creek arm, sediment-resuspending waves were estimated to comprise 0.07 percent of spring, 0.2 percent of summer, 0.01 percent of fall, and 0.02 percent of winter. At the Confluence, sediment-resuspending waves were estimated to comprise 0.9 percent of spring, 5.7 percent of summer, 0.4 percent of fall, and 0.03 percent of winter waves (Figure 24). Sediment-resuspending waves were most frequent in the summer across all stations, followed by spring, fall, and winter.

The North Anna arm experienced the highest frequency of sediment resuspending waves, followed by the Confluence and Pamunkey Creek arm. At the North Anna arm, waves that were greater than approximately 0.1 m in height consistently generated sediment resuspension, while at the Confluence, a maximum wave height of 0.5 m was needed. At Pamunkey Creek, no clear wave-height threshold was evident because there was no discernable wave height above which sediment resuspension occurred consistently.

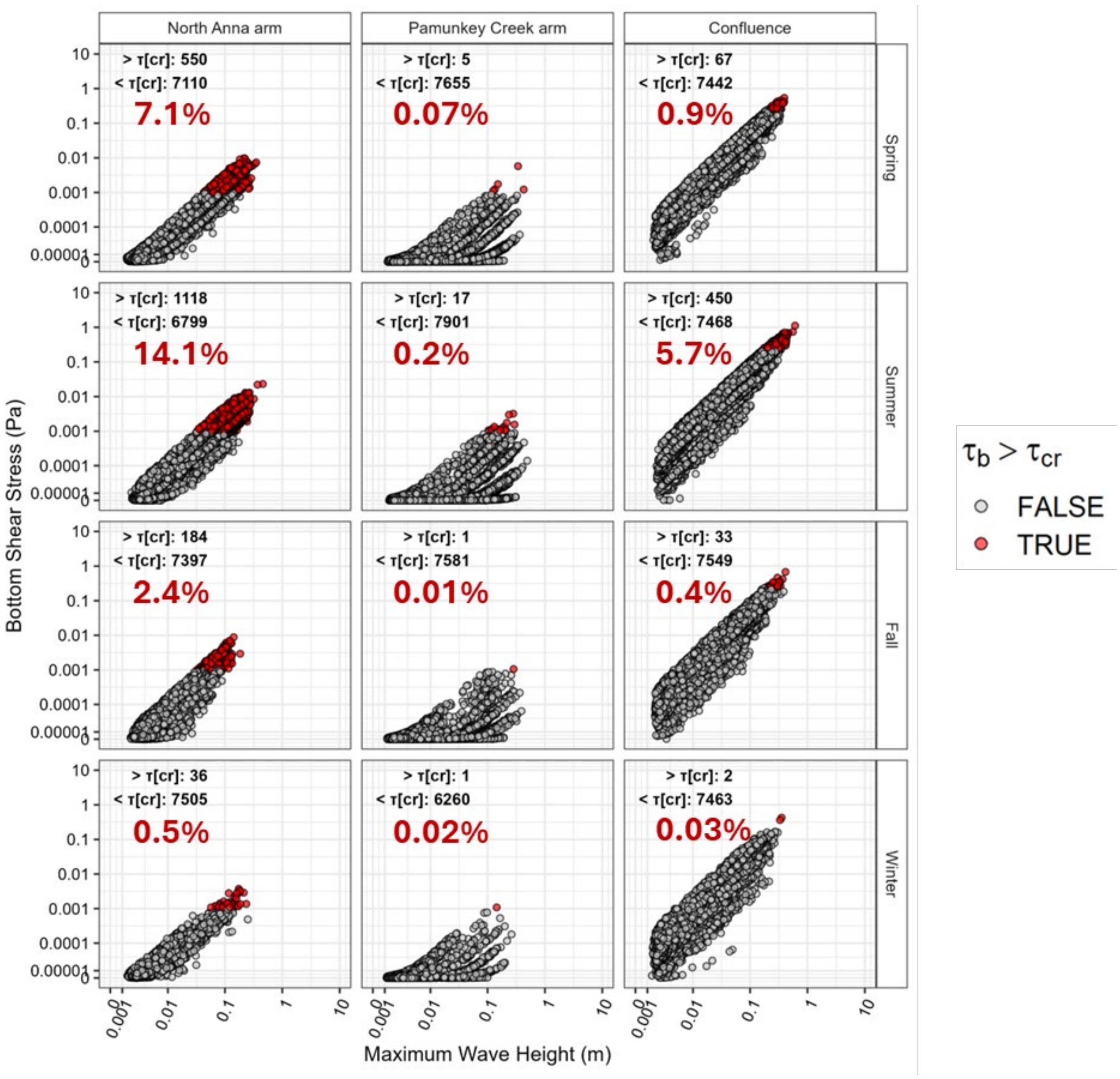

Figure 24. Bottom shear stress versus maximum wave height by station and season across calendar year 2024. Data points represent 15-minute interval bottom shear stress and maximum wave height data. Gray points indicate that the bottom shear stress was less than or equal to the critical shear stress (i.e., no sediment resuspension) and red points indicate that bottom shear stress was greater than the critical shear stress (i.e., sediment resuspension). Data from Vande Pol and others (2026).

In the North Anna arm, most of the days in spring (87.9 percent) and summer (94.7 percent) contained at least one sediment-resuspending wave, while 50 and 19.8 percent of the days contained at least one sediment-resuspending wave in fall and winter, respectively (Figure 25). The Confluence experienced 21.1, 84, 15.6, and 2.2 percent of days with at least one sediment-resuspending wave in spring, summer, fall, and winter, respectively. At the Pamunkey Creek arm, 5.5, 16, 1.1, and 1.3 percent of days had at least one sediment-resuspending wave in spring, summer, fall, and winter, respectively.

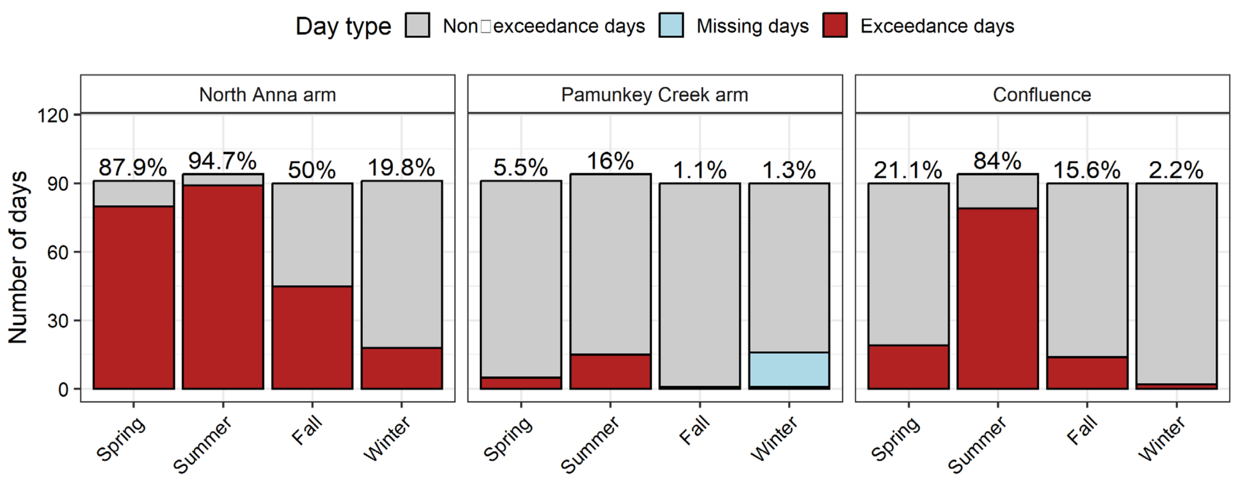

Figure 25. The proportion of days in each season and at each station in which at least one wave was generated that could resuspend lake-bottom sediment (i.e., lake-bottom shear stress was greater than critical shear stress). Refer to Table 1 for additional station information.

At all stations, sediment-resuspending waves were generally experienced during low wind speed conditions over the study period, with the most of those waves occurring with average wind speeds of 8 km/h or less (Figure 26). Based on the 5-minute wind speed data (n = 140,560), wind speeds greater than or equal to 12 km/h accounted for approximately 2.5 percent of measurements.

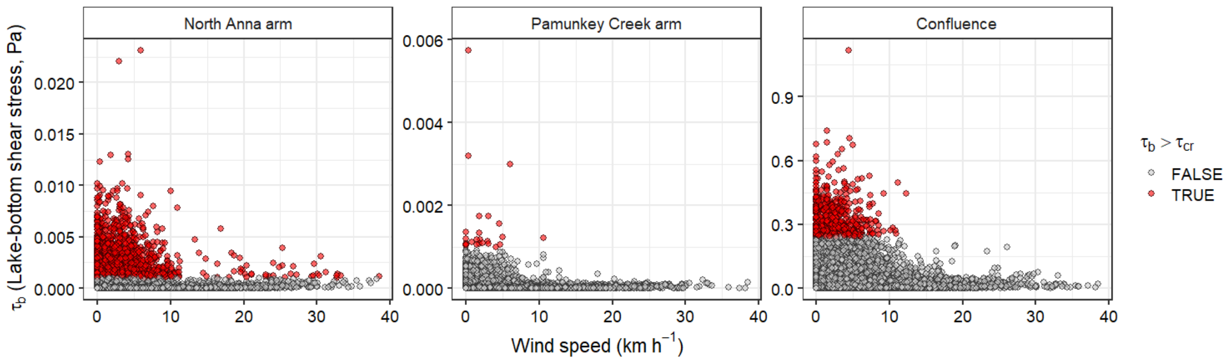

Figure 26. Graphs showing the 15-minute interval lake-bottom shear stress versus average wind speed. Red points show waves where lake-bottom shear stress was greater than critical shear stress and grey points when a wave that were less than or equal to critical shear stress. Refer to Table 1 for additional station information.

During the two wave-action water-quality sampling events, that is, high residential occupancy and boating activity (HROB) and low residential occupancy and boating activity (LROB), the frequency of the sediment-resuspending waves differed among the stations during HROB and were similar among stations during LROB. During the HROB sampling day, 16 sediment-resuspending waves (41 percent) were recorded at the North Anna arm, zero waves were recorded at the Pamunkey Creek arm, and 1 wave (2.6 percent) was recorded at the Confluence (Figure 27). During the LROB sampling day, there was only 1 sediment-resuspending wave (2.6 percent) at the North Anna arm, and none occurred at the Pamunkey

Creek arm or the Confluence. The North Anna arm was the only station that observed a substantial difference in the number of sediment resuspending waves, with 16 times as many in HROB compared to LROB (Figure 27).

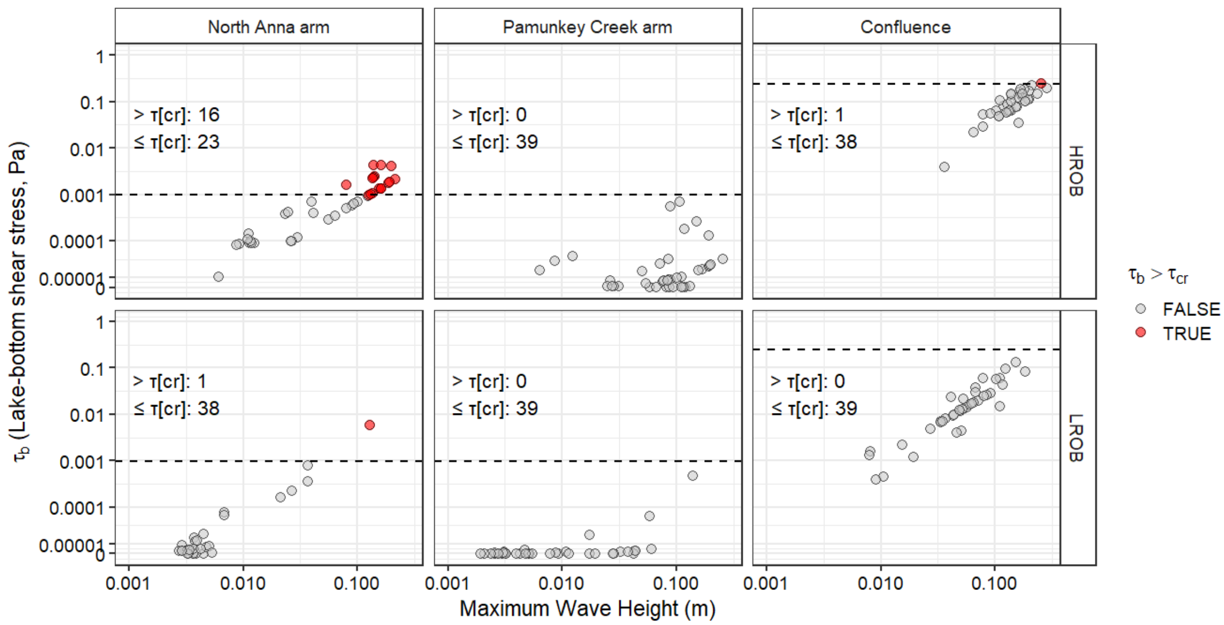

Figure 27. Plots of 15-minute interval lake-bottom shear stress versus maximum wave heights by station during the high residential occupancy and boating activity (HROB) and low residential occupancy and boating activity (LROB) water quality sampling events. The dashed lines represented the critical shear stress value for each station. Grey points represent wave were estimated to not resuspend lake bed sediments and red points represent waves that were estimated to resuspend lake bed sediments. Refer to Table 1 for additional station information.

Hourly discrete measurements of suspended sediment concentration (SSC) were highest at the North Anna arm during HROB sampling event, with a median ± standard deviation of 24 mg/L ± 6.8 mg/L (Figure 28). The SSC values were significantly lower during the LROB event at the North Anna arm, with a p-value of 0.00008, and median concentration ± standard deviation of 9.9 mg/L ± 0.9 mg/L. SSCs during the HROB sampling event were more variable and were 2 to 4 times higher than SSCs during the LROB sampling event.

At the Confluence, median ± standard deviations were 5 mg/L ± 3 and 4.3 mg/L ± 0.7 during the HROB and LROB sampling events, respectively. A non-significant p-value (≥0.05) was yielded between HROB and LROB SSC values, meaning the central tendencies of the datasets are similar. The HROB sampling event experienced more than twice as much variability compared to the LROB sampling event.

At the Pamunkey Creek arm, median ± standard deviations were 8.4 mg/L ± 1 and 12.4 mg/L ± 1.3 during the HROB and LROB sampling events, respectively. A significant p-value of 0.0004 was yielded between HROB and LROB SSC values, meaning the central tendencies of the datasets differ. The LROB sampling event had a higher median than the HROB sampling event.

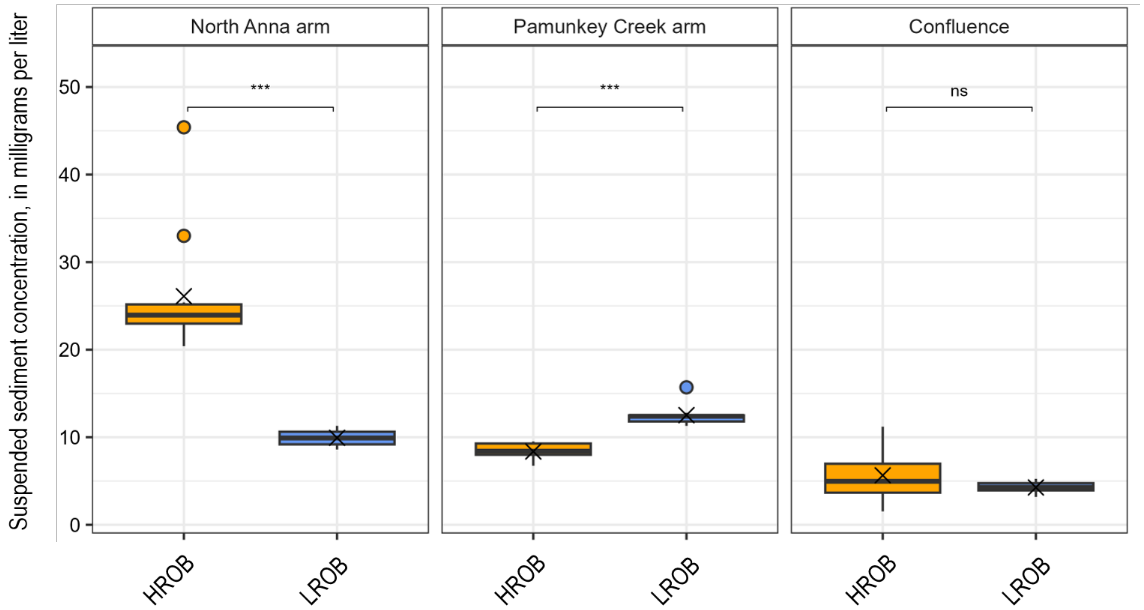

Figure 28. Boxplots of suspended sediment concentrations during the high residential occupancy and boating activity (HROB) and low residential occupancy and boating activity (LROB) water quality sampling events. [* indicates a significant results with p-values ranging from <0.01-0.05, ** indicates a significant result with p-values ranging from <0.001-0.01 , *** indicates a significant result with p-values <0.001, ns indicates a non-significant result with p-values ≥ 0.05]. Refer to Table 1 for additional station information.

Temperature Stratification and Hypoxia

Thermal stratification occurred during 4 of the 5 seasonal synoptics at Lake Anna. All synoptic sampling locations stratified at least one time (n = 30), with 23 stations stratifying once, 12 stations stratifying twice, and one station stratifying four times. Stratification was most widespread during the Spring 2024 synoptic, in which 29 of 30 (97 percent) of the synoptic sampling stations exhibited stratification (Figure 29). The Fall and Winter of 2023 were vertically homogenous and thus were not stratified. During the summer of 2023, only 1 of 30 (3 percent) sampling stations were thermally stratified. The station closest to the North Anna arm routine monitoring station stratified the most frequently, during four of the five synoptics.

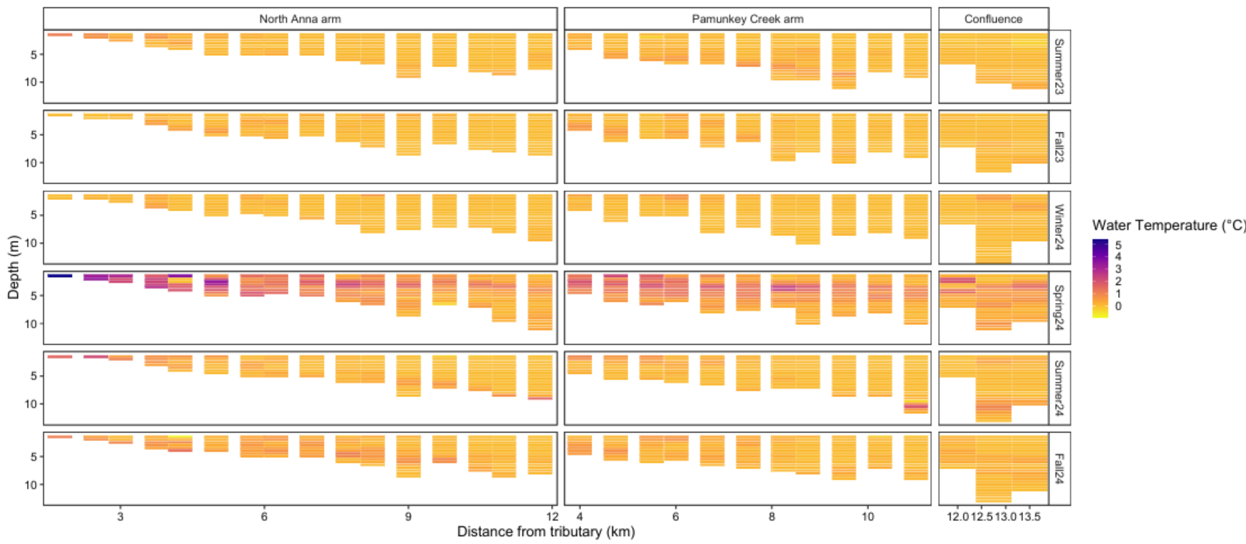

Figure 29. Differences in water temperature per meter of vertical profile plotted as a function of depth and longitudinal distance from the mouth of the tributary for the North Anna arm, Pamunkey Creek arm, and Confluence across six sampling periods (Summer 2023, Fall 2023, Winter 2024, Spring 2024, Summer 2024, and Fall 2024). The y-axis is depth, with 0 m at the surface of the lake. Refer to Table 4 for additional station information.

Hypoxia was observed during spring (2024) and summer (2023 and 2024) sampling periods (Figure 30). Synoptic events were absent during the fall and winter surveys. Hypoxia was identified at 15 synoptic sampling locations; 3 stations were hypoxic once, 10 stations were hypoxic twice, and 2 stations were hypoxic three times.

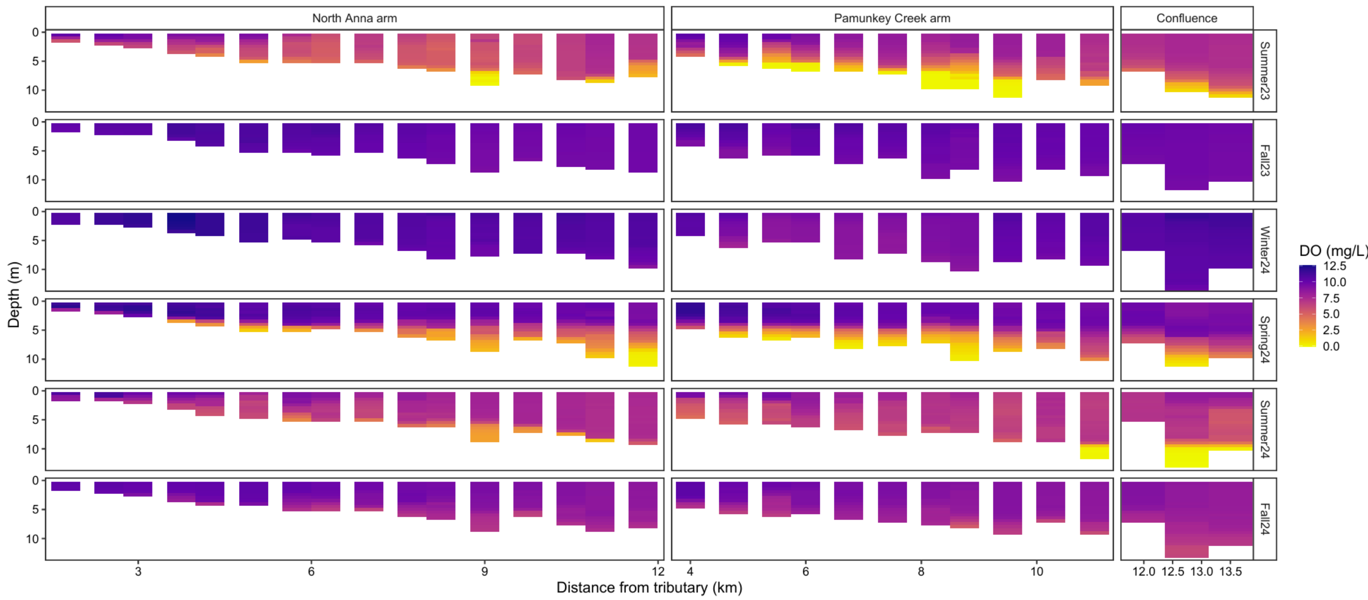

Figure 30. Dissolved oxygen (DO) profiles plotted as a function of depth and longitudinal distance from the mouth of the tributary for the North Anna arm, Pamunkey Creek arm, and Confluence across six sampling periods (summer 2023, Fall 2023, Winter 2024, Spring 2024, Summer 2024, and Fall 2024). The black line indicates areas of hypoxic conditions. The y-axis is the depth, with 0 m at the surface of the lake. Refer to Table 4 for additional station information.

During the summer 2023 synoptic survey, 12 of 30 measured stations (40 percent) had hypoxia, ranging from 0.5 to 29 percent of the water column. Hypoxic conditions were recorded at 13 of the 30 stations during the spring 2024 synoptic survey, ranging from 0 to 31 percent of the water column. Of these 13 stations, 10 measured hypoxia in less than 5 percent of the water column, with 7 measuring hypoxia on the water-lakebed interface. During the summer of 2024 synoptic survey, hypoxic conditions were recorded at 4 stations, ranging from hypoxia at the water-lakebed interface to 28 percent of the water column.

The three arms differed in the extent and frequency of hypoxia. The North Anna arm (Figure 3, map numbers 1-16) recorded hypoxic conditions at 7 of the 96 sampling events (7 percent) at 4 of the 16 stations. For 6 of the 7 hypoxia events, the water was hypoxic in less than 10 percent of the water column. During the Summer of 2023, hypoxia at map number 12 (Figure 3) began 2.3 m above the water-lakebed interface, comprising about 25 percent of the water column. The Pamunkey Creek arm (Figure 3, map numbers 18–28) recorded hypoxic conditions at 17 of the 66 sampling events (26 percent) at 9 of the 11 synoptic sampling locations. 11 of the 17 water column events measured were less than 10 percent hypoxic and less than 0.5 m in the water column. The remaining six stations had hypoxic conditions in greater than 10 percent of the water column, ranging from 13 to 29 percent of the water column. The total depth of hypoxia at each station ranged from 0 m, directly on the water-lakebed interface, to 2.8 m above the lakebed sediments. The Confluence stations comprised map numbers 17, 29, and 30 (Figure 3). There was hypoxia identified at Station 29 and 30. Hypoxia was measured at map number 29 (Figure 3) during the summer 2023, spring 2024, and summer 2024 synoptic events, with hypoxia ranging from 10 to 31 percent of the water column. At map number 30 (Figure 3), hypoxia was measured only at the water-lake bed interface.

There were 13 times when there was both hypoxia and thermal stratification in summer (2023 and 2024) and spring (2024). There was one instance during the summer of 2023 on the Pamunkey Creek arm at Station 20. The most profiles with both hypoxia and thermal stratification occurred during the Spring of 2024 sampling event. During this event, there were 3 locations on the North Anna arm (map numbers 6, 12, and 15; Figure 3), 7 locations on the Pamunkey Creek arm (map numbers 19–21 and 23–26; Figure 3), and one station on the Confluence (map number 29; Figure 3). The summer of 2024 had two instances of both hypoxia and thermal stratification: location 28 on the Pamunkey Creek arm, and location 30 nearest to the Confluence continuous monitoring location (Figure 3).

In-Lake Near Shore Transects

Absolute abundances across phyla were higher during the high-occupancy period than during the low-occupancy period, with abundances 22 times higher at the agricultural transect, 71 times higher at the forest transect, and 5 times higher at the residential transect. Cyanobacteria had the greatest relative abundance across all three transects during both periods. During the low-occupancy period, cyanobacteria accounted for 61 percent of the abundance at the agricultural and forest transects and 65 percent of the abundance at the residential transect. During the high-occupancy period, cyanobacteria accounted for 99 percent of the abundance at the agricultural transect and 98 percent of the abundance at the forest and residential transects.

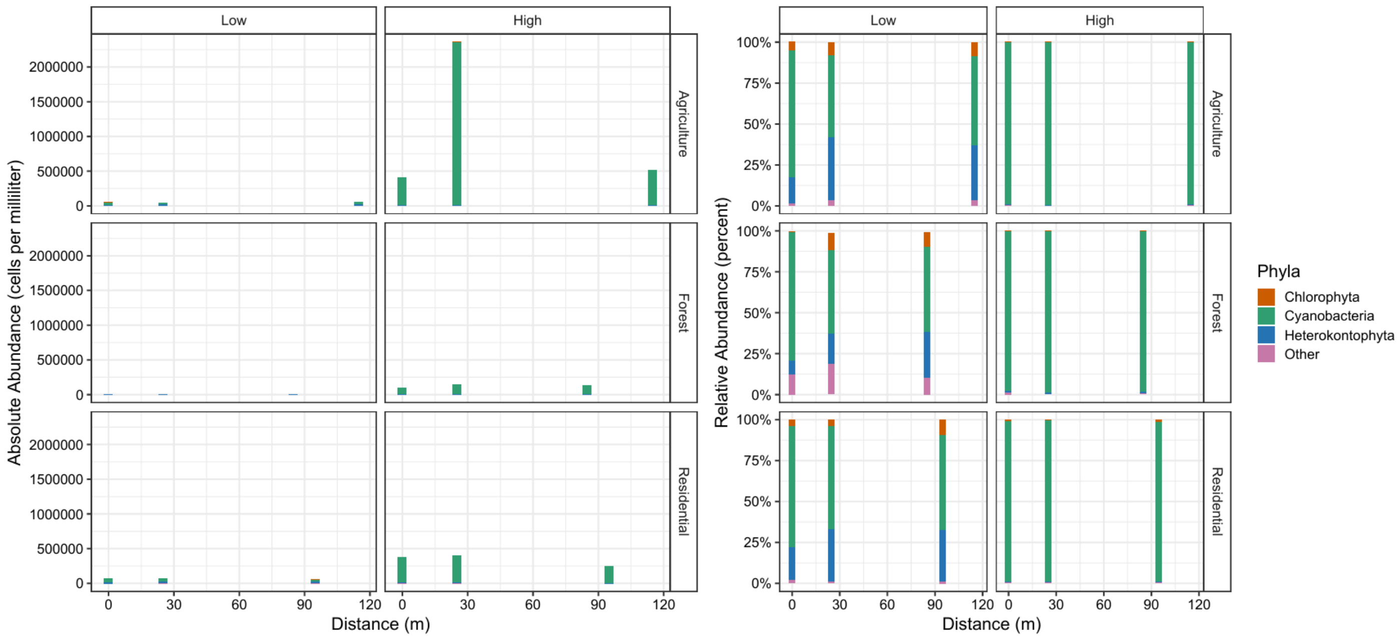

Figure 31. Absolute abundance and relative abundance of phyla for agricultural, residential, and forested land use during low- and high-occupancy periods from the lake shore at 0 m to the mid-channel. Sample collected along the transect during the low-occupancy period were collected on 4/30/2024 and 5/01/2024. Sample collected along the transect during the high occupancy period were collected on 8/13/2024. Refer to Table 3 for additional station information.

Absolute abundances across pTOX cyanobacteria were higher during the high-occupancy period than the low-occupancy period: 1,632 times higher at the agricultural transect, 3,316 times higher at the forest transect, and 58 times higher at the residential transect. Cell counts ranged from 109,449 to 1,077,772 cells per milliliter during the high-occupancy period. The agricultural transect had the highest combined cell counts across the three transect locations (Figure 31).

Aphanizomenon had the highest relative abundant taxa in the low-occupancy periods: 100 percent of the taxonomic community at the agricultural and forested transects and 62 percent of the taxonomic community in the residential transect (Figure 32). The residential transect had the greatest taxonomical community difference, with 5 genera identified. During the high-occupancy time, the most abundant genus at all three stations was *Raphidiopsis*, which represented 98 percent of the taxonomic composition at the agricultural transect and 90 percent of the taxonomic composition at the residential and forest transect.

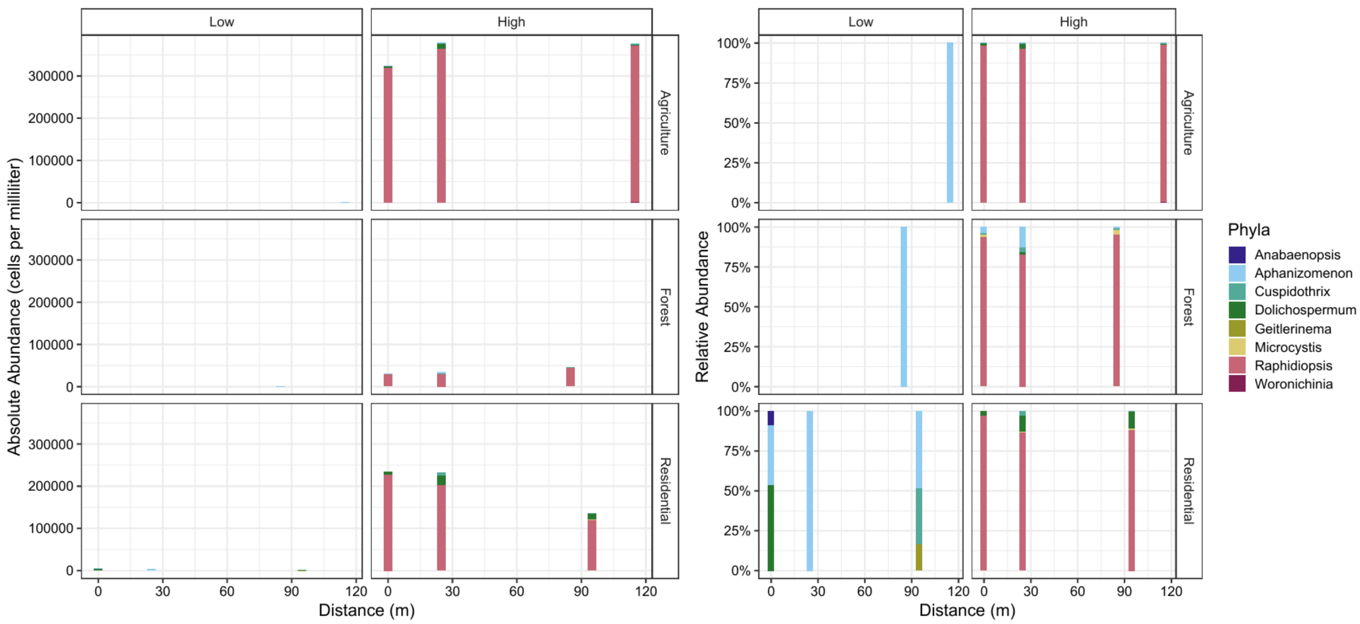

Figure 32. Absolute abundance and relative abundance of pTOX for agricultural, residential, and forested land use during low- and high-occupancy periods. Sample collected along the transect during the low-occupancy period were collected on 4/30/2024 and 5/01/2024. Sample collected along the transect during the high occupancy period were collected on 8/13/2024. Refer to Table 3 for additional station information.

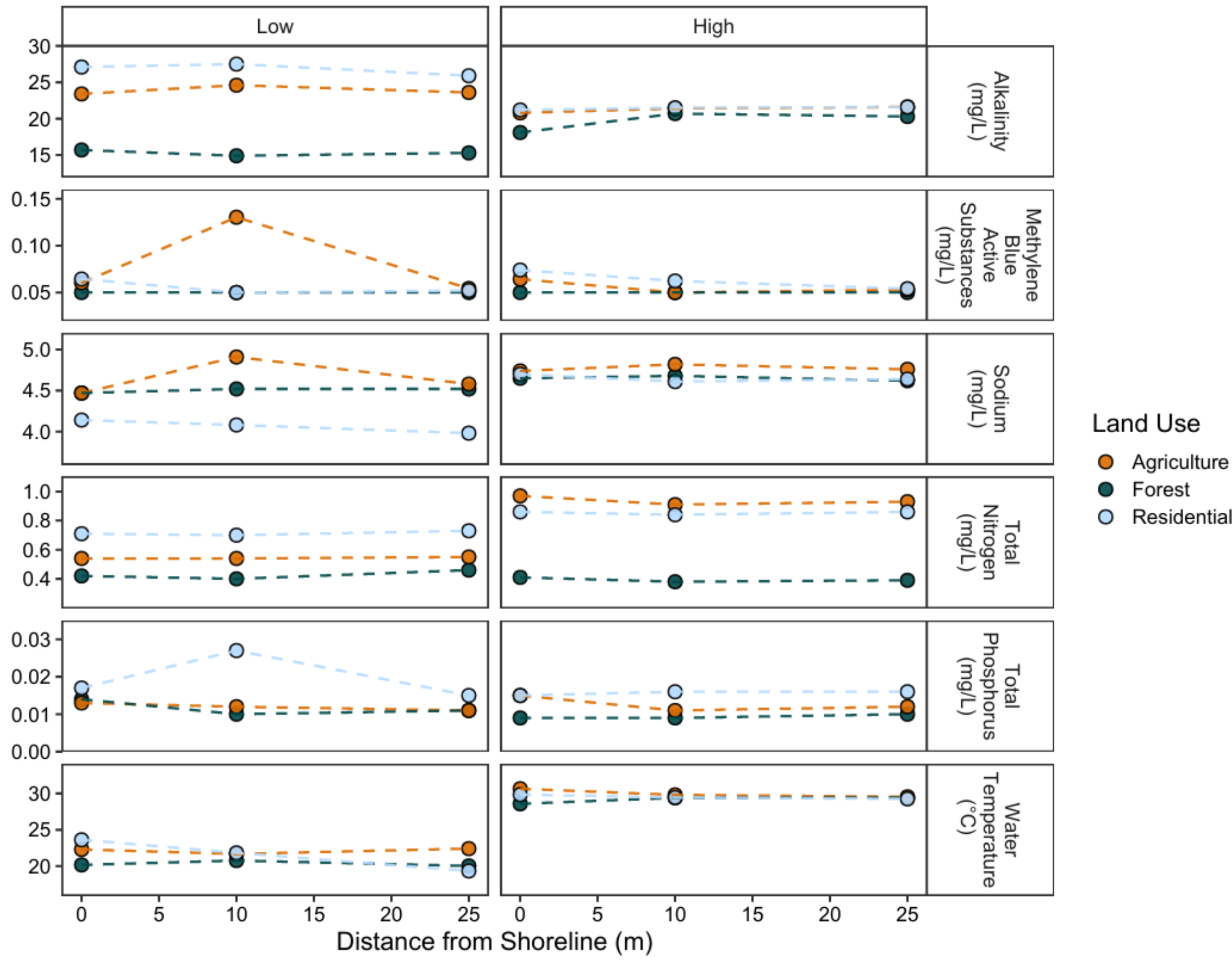

Figure 33. Graphs showing the total concentrations for agricultural, residential, and forested land use during low- and high-occupancy periods across the transects. The x-axis represents the distance from shoreline. Sample collected along the transect during the low-occupancy period were collected on 4/30/2024 and 5/01/2024. Sample collected along the transect during the high occupancy period were collected on 8/13/2024. Refer to Table 3 for additional station information.

Among the drivers identified from the CRF and GAM analysis, alkalinity, Na, TN, TP, and WT were collected during the near shore sampling days (Figure 33). Most of the drivers showed limited and inconsistent variations with distance from the shoreline across the two occupancy periods, with standard deviations of 0.21–1.40 mg/L for alkalinity, 0.03–0.23 mg/L for Na, 0.01–0.03 mg/L for TN, 0.00–0.01 mg/L for TP, and 0.30–2.15°C for WT (Appendix Table 3.2). Water temperature had the greatest range in standard deviation, which is likely attributable to differences in seasonal temperature conditions.

Alkalinity concentrations were relatively stable with distance from shoreline but differed among land-use types. During the low-occupancy period, median alkalinity was lowest at the forested transect (15.3 mg/L), compared with 23.6 mg/L at the agricultural transect and 27.1 mg/L at the residential transect. MBAS concentrations also showed limited variation with distance from the shoreline, with the highest concentration occurring at 10 m on the agricultural transect during the low-occupancy period (0.13 mg/L). Sodium concentrations remained relatively stable with distance from shoreline but slightly differed among land-use types during the low-occupancy period. TN concentrations were relatively stable across shoreline distances but differed among land-use types. During high occupancy, the forested transect had the lowest median TN concentration (0.39 mg/L), compared with 0.93 mg/L at the agricultural transect and 0.86 mg/L at the residential transect. TP showed the least variation among the measured constituents. However, an elevated TP concentration was observed at 10 m on the residential transect during low occupancy.

Synthesis of Cyanobacterial Bloom and Nutrient Dynamics Over Space and Time

Algal blooms began forming in May, peaking in late July and early August, and began declining in October. The dominant phyla at all three lakes stations are cyanobacteria, which can produce toxins. The composition of the potentially toxigenic genera was evaluated, and the dominant bloom-forming genera was *Raphidiopsis*, with *Aphanizomenon* growing earlier in the season. This finding supports findings of previous studies in which *Aphanizomenon* grows best in high light and ample nutrient conditions with a lower temperature tolerance, allowing the genera to proliferate first during the growing season (Tsujimura and others, 2001; Underwood and others, 2024). Of the three stations routinely sampled, the North Anna arm had the highest taxonomic richness, and the Confluence had the least taxonomic richness. This spatial pattern is typical of reservoirs (Rock and others, 2025a). The North Anna arm and the Pamunkey Creek arm are located in the riverine zone of the Lake Anna reservoir, which is characterized by higher turbidity, nutrients, and productivity (Rock and others, 2025a). The Confluence station represents the transitional zone between the riverine zone and the lacustrine zone (Rock and others, 2025a).

Although there were high cell counts (>100,000 cells per mL) of potentially toxigenic cyanobacteria genera, low concentrations of toxins were observed, with most of the samples below the detection limit, with only 30, 41, and 10 percent of the samples having toxin detections at the North Anna arm, Pamunkey Creek arm, and Confluence, respectively. The mechanisms of and reason for toxin production are not well understood (Omidi and others, 2018). Currently, toxin production is known to be a secondary metabolism, so inorganic nitrogen demands must be higher than the quota needed for cyanobacteria primary metabolism (growth and reproduction) in non-diazotrophic taxa, like *Microcystis* (Gobler and others, 2016). Toxin production for diazotrophic taxa, like *Aphanizomenon*, was shown to increase in nutrient limited conditions; however, more studies would be needed to confirm and expand the understanding of diazotrophic genera (Gomaa and Carmichael, 2023). Additionally, mixed assemblages of non-toxic and toxic strains of cyanobacteria could result from the lower toxin production in Lake Anna (Chorus and Welker, 2021b).

The relations between chlorophyll-a and TN, DIN, TP, OP, and TN:TP were evaluated to determine if nutrient enrichment is associated with algal biomass. At the tributary stations, TN and TP explained similar proportions of variance of chlorophyll-a, ranging from 20 to 48 percent, whereas DIN and OP explained less variance, ranging from less than 1 percent to 43 percent, with increasing relations. Most of the samples at the North Anna River were co-limited (66 percent) for TN and TP, and at Pamunkey Creek, 62 percent of the samples were N-limited. At the lake stations, TN and TP concentrations were positively related to chlorophyll-a concentrations. However, at the North Anna arm and the Pamunkey Creek arm, concentrations of inorganic nutrients DIN and OP were negatively related to chlorophyll-a concentrations. This result indicates that the inorganic nutrients are rapidly consumed by the algal biomass and converted to organic forms of the nutrients, which contributes to the overall increase in TN. TN:TP ratios indicate that 90.3, 83.3, and 55.2 percent of collected samples were co-limited at the North Anna arm, Pamunkey Creek arm, and Confluence stations, respectively. In general, eutrophic lakes tend to have lower TN:TP ratios and are more N-deficient, often leading to N and P co-limitation (Zhou and others, 2022). However, internal lake processes—such as denitrification, nitrogen fixation, sedimentation, and sediment resuspension—can also modify TN:TP ratios (Zhou and others, 2022). Low TN:TP ratios favor cyanobacteria dominance in lakes (Zhou and others, 2022), and certain genera, such as *Raphidiopsis*, exhibit higher growth rates in N-limited conditions and are highly adapted to low dissolved inorganic phosphorus concentrations (Burford and others, 2023; Recknagel and others, 2019).

Early warning statistical models that utilize continuously measured parameters such as temperature, dissolved oxygen, chlorophyll, phycocyanin and others could provide near real-time data of lake conditions and potentially provide early indication of an algal bloom as demonstrated in studies such as Tassone and others, 2026, Buelo and others (2022), and Ortiz and others (2020). Early indication of an algal bloom could provide managers with time to proactively manage lakes experiencing blooms.

Synthesis of *Raphidiopsis* Traits and Capabilities on the Key Drivers

The genus *Raphidiopsis* was the dominant pTOX cyanobacteria throughout the study period in Lake Anna. The prevalence of *Raphidiopsis* at Lake Anna can be attributed to its highly adaptive physiological, genetic, and molecular traits, allowing this genus to outcompete similar taxa in the environment (Alvarez Dalinger and others, 2026).

There is growing evidence that lakes are becoming increasingly alkaline and eutrophic, and that shifts in pH and dissolved inorganic carbon (DIC) strongly influence cyanobacterial bloom proliferation and dynamics (Raven and others, 2020; Shapiro, 1997; Verspagen and others, 2014). Alkalinity was identified as a key driver in all modeled scenarios except the pTOX excluding *Raphidiopsis* model, and cell counts increased with increasing alkalinity. Like most cyanobacteria, *Raphidiopsis* possesses a robust carbon concentrating mechanism (CCM) which allows an efficient uptake of bicarbonate to CO_2 for photosynthesis (Vilar and Molica, 2020). Through this process, cyanobacteria raise the CO_2 concentration around Ribulose-1,5-bisphosphate carboxylase/oxygenase (RuBisCo) by actively transporting DIC for uptake to balance photosynthesis and respiration rates. Culture experiments by Vilar & Molica (2020) showed that a strain (ITEP-A) of *Raphidiopsis* has been identified to have genes that predominately use BicA, a sodium dependent bicarbonate transporter that has a high-flux rate. This allows for rapid uptake of bicarbonate into the cell membrane in high pH (alkaline) waters such as was found in Lake Anna, supporting a more rapid growth than cyanobacteria genera that might depend on low-flux CO_2 conversion system which could not take advantage of the DIC saturation (Vilar and Molica, 2020). Few studies have examined the influence of sodium on cyanobacterial growth and dominance in freshwater lakes; however, sodium is a required nutrient in nitrogenase activity in nitrogen-fixing cyanobacteria, such as *Raphidiopsis*, and can enhance nutrient efficiency, reduce losses of fixed organic matter, and increase phosphorus uptake in non-nitrogen fixing cyanobacteria (de Oliveira and Dantas, 2019; Seale and others, 1987).

Phosphorus acquisition in *Raphidiopsis* contrasts with its CCM strategy; under low P concentrations, *Raphidiopsis* can rapidly absorb and store phosphate to maintain a competitive advantage under limited P conditions (Shen and others, 2025). Interestingly, total phosphorus was only identified as a key driver in the pTOX excluding *Raphidiopsis* model and exhibited a monotonic decreasing pattern, indicating that as the total phosphorus concentrations increased, total cell counts of non-*Raphidiopsis* genera decreased. This pattern could be indicative of senescence during seasonal succession from non-*Raphidiopsis* genera in the spring to *Raphidiopsis* in June through December (Zhang and others, 2019). Kinetic studies on strains of *Raphidiopsis* demonstrated a high affinity for P uptake, exceeding other cyanobacteria and eukaryotic phytoplankton groups in culture (Isvánovics and others, 2000). This high affinity was also observed in Shi and others, (2022), with the high affinity phosphate bonding protein being upregulated when in P stress conditions. In cultured populations, different strains of *Raphidiopsis* responded differently to P availability, synthesizing DIP at different growth stages and expressing varying phosphate acquisition genes (Willis and others, 2019).

Total nitrogen was a key driver in all 5 biological response models, exhibiting a general pattern showing that increasing concentrations of total nitrogen corresponded with increasing algal biomass or production. Cyanobacteria have a higher N requirement than eukaryotic algae because of their phycobiliprotein accessory pigments (Beaulieu and others, 2013), and previous studies have documented a close association between cyanobacteria abundance and TN (Beaulieu and others, 2013). Along with the CCM and phosphorus acquisition advantages, *Raphidiopsis* is a diazotrophic cyanobacteria. When cellular nitrogen storage is below metabolic requirements, diazotrophs can synthesize inert atmospheric nitrogen from the atmosphere into ammonia for biosynthesis (Seefeldt and others, 2020; Xiao and others, 2026). Lake Anna becoming DIN limited system during the summer allows diazotrophic cyanobacteria to upregulate the nif (nitrogen fixation) genes so the production of the nitrogenase enzyme may begin (Xiao and others, 2026). Notably, nitrogen fixation is an expensive anaerobic metabolism that requires a large amount of ATP for the enzyme nitrogenase to catalyze the process (Glass and others, 2010; Xiao and others, 2026) even when enzyme cofactors like Molybdenum (Mo) and/or Iron (Fe) are available. Heterocyst formation provides an anaerobic zone that protects nitrogenase (an oxygen inhibited enzyme) allowing nitrogen fixation to occur in oxygenated waters (Glass and others, 2010). Nitrogen fixation has a high energy cost; therefore, *Raphidiopsis* is unlikely to counterbalance total DIN limitation in a system but could outcompete other cyanobacteria and phytoplankton groups in a system of low DIN periods in warmer months (Xiao and others, 2026). However, determining whether cyanobacteria were fixing nitrogen in Lake Anna was beyond the scope of this study.

Water temperature was identified as a driver in all five models and the most significant predictor in four of the five models. Throughout all the models, the increasing water temperature increased algal biomass and growth. Warmer water temperatures affect many biological processes, such as metabolism, photosynthesis, respiration, growth, reproduction, and the interactions among species (Carey and others, 2012; Walls and others, 2018). Cyanobacteria have a higher water temperature tolerance than other algae and can result in a shift in the phytoplankton community from green algae to cyanobacteria (Carey and others, 2012). In particular, *Raphidiopsis* had wide optimal growth temperature range, between 15 to 35 °C, with a preference of temperatures above 23°C (Alvarez Dalinger and others, 2026).

There is currently less literature highlighting the importance of suspended sediment, wind speed, and micronutrients on *Raphidiopsis* growth and proliferation. At Lake Anna, suspended sediment was identified as a key driver in the chlorophyll-a, cyanobacteria, and *Raphidiopsis* models, with monotonic increasing trends as concentrations increased. No studies were found at time of publication which associated *Raphidiopsis* blooms to increased suspended sediment, but the entrainment of sediments in the water column can facilitate the delivery of nutrients to the phytoplankton communities, reduce light availability, and, in turn, sustain the algal community in shallow lakes such as Lake Anna (Ortiz and others, 2026). *Raphidiopsis* has been shown to tolerate very low light conditions (Mehnert and others, 2012; Wu and others, 2023). Suspended sediment concentration can increase due to delivery from the tributaries or wave action from boats or high wind speeds and is explored further in the "Synthesis of Sources of the Drivers at Lake Anna, Virginia" section. However, phytoplankton are sensitive to wind-induced disturbances, which can reduce cyanobacteria surface scums (Moreno-Ostos and others, 2009). Wind speeds greater than 12.7 km/hr were identified as a driver of pTOX excluding

Raphidiopsis model. Wind speeds greater than 10.8 km/hr can result in cyanobacteria colonies entrained throughout the entire mixed layer (Wu and others, 2015).

Micronutrients such as copper, iron, molybdenum, and nickel were identified as key drivers in the models, are essential components of metalloenzymes that catalyze primary production and nutrient transformations, and can be limiting or co-limiting factors in aquatic ecosystems (Costello and others, 2026). These micronutrients have not been studied for *Raphidiopsis*, but there are studies synthesizing the importance of micronutrients on cyanobacteria (Facey and others, 2019b). Copper and iron exhibited a decreasing monotonic response for both the cyanobacteria and pTOX model. Copper is an essential nutrient in the electron transport chain and photosynthesis; however, at higher concentrations, copper can be toxic to cyanobacteria and is used in algaecide (Facey and others, 2019b; Kelly and others, 2021). Iron functions as a cofactor of enzymes, supports detoxification of reactive oxygen species, contributes to the electron transport chain, chlorophyll-a synthesis, respiration, nitrogen fixation, and photosynthesis (Facey and others, 2019a). However, the decreasing relation could be due to uptake by algal biomass during the growing season and a return to ambient conditions after senescence occurred. Molybdenum was identified as a key driver in all models except the pTOX model, exhibiting different patterns with increasing concentrations. At Mo concentrations greater than 2.20 ug/L, there was increased cell counts and biomass for chlorophyll-a, cyanobacteria, and *Raphidiopsis,* and lower cell counts of pTOX, excluding *Raphidiopsis*. At concentrations less than 2 µg/L of Mo, concentrations are insufficient for nitrogen fixation by heterocystous cyanobacteria such as *Raphidiopsis* (Facey and others, 2019a). Therefore, the increased concentrations of Mo could allow for the assimilation of inorganic nitrogen (Facey and others, 2019a). The pTOX excluding *Raphidiopsis* had the opposite patterns, indicate this genus is not capable of nitrogenase or nitrate reductase. The last micronutrient identified as a driver was nickel, with a decreasing trend in the chlorophyll-a and Raphidiopsis model and a variable pattern in the cyanobacteria model. Nickel is required for cellular development but can be toxic and affect photosynthesis at high concentrations (Martínez-Ruiz and Martínez-Jerónimo, 2016).

The competitive traits outlined above align with the environmental conditions at Lake Anna. Although Lake Anna is considered co-limited by nitrogen and phosphorus, TP was not a primary driver of the *Raphidiopsis* model, while TN was a primary driver of the model. However, *Raphidiopsis* has a high affinity for DIP uptake and can store P in low-P conditions across generations. While *Raphidiopsis* is a diazotroph, fixing nitrogen from the atmosphere is energetically expensive; therefore, the genus likely relies on sources from internal and external loads. *Raphidiopsis* has a competitive advantage in Lake Anna's warm, alkaline waters with nutrient co-limitation. In addition to *Raphidiopsis'* robust CCM, this genus is adapted to tolerate mixed to low-light conditions (Mehnert and others, 2012; Wu and others, 2023) that would allow increased proliferation as DIN and DIP decrease in the summer (Briand and others, 2004).

Synthesis of Sources of the Drivers at Lake Anna, Virginia

Findings from this 19-month study on Lake Anna identified 11 statistically significant drivers of algal blooms from the biological response models: total nitrogen, total phosphorus, alkalinity, sodium, water temperature, suspended sediment concentrations, wind speed, copper, iron, molybdenum, and nickel. External and internal sources of these drivers were evaluated to determine potential sources and processes contributing to algal biomass and bloom initiation, persistence, and decline. Although only a few potential sources and drivers were investigated, additional factors could be contributing to algal bloom responses within the Lake Anna watershed.

Measured tributary drivers included TN, TP, alkalinity, Na, WT, and SSC, with the sources of nitrate identified using nitrogen and oxygen stable isotopes. The concentrations of alkalinity and Na were higher during baseflow conditions than during storm events. The tributaries of Lake Anna deliver highly alkaline water to the western arms of the lake. A growing body of literature suggests that this delivery of highly alkaline water might allow for rapid uptake of bicarbonate into *Raphidiopsis* by providing a carbon source and allowing for the genus to proliferate and potentially decrease toxicity (Vilar and Molica, 2020). The influence of Na to cyanobacteria proliferation is poorly understood in the freshwater reservoir literature; however, there is evidence that Na is essential for fixing nitrogen (de Oliveira and Dantas, 2019) and can enhance nutrient uptake efficiency, reduce losses of fixed organic matter, and increase phosphorus uptake in non-nitrogen fixing cyanobacteria species (Seale and others, 1987). Recent evidence also indicates that sodium ion may increase photosynthetic efficiency (Tsujii and others, 2025).

Stable isotopes of nitrogen and oxygen indicate that manure and human waste are the dominant sources of nitrogen in the North Anna River watershed and that soil nitrogen was the largest source in the Pamunkey Creek watershed. Manure and human waste in the watershed could be sourced through many potential avenues such as livestock operations, biosolids application on fields, septic systems, and wildlife (Hyer and others, 2016). Soil nitrogen was estimated as the largest proportion of nitrogen at Pamunkey Creek and the second largest proportion at North Anna River, indicating that nitrogen from all sources are accumulated and stored in soil and transported to the streams at variable rates through the soil (Kendall and others, 2007).

Concentrations of suspended sediment, TN, and TP were higher during storms than during baseflow conditions, and estimated loads were primarily exported to Lake Anna during storm events primarily from mid-November 2023 through January 2024. The timing of suspended sediment, TN, and TP loads to Lake Anna throughout the study period did not correspond with timings of with bloom initiation, growth, or persistence. Rather, there is an inverse relation between load delivery and cell counts of the algal community which indicates that a consistent, external load delivery from the tributaries throughout the growing season is not needed for algal biomass initiation and growth and that Lake Anna may function as a sink for some externally derived constituents. This finding is consistent with findings from Kohlhaas and others (2026) that the lake is a net accumulator of metals and metalloids from nine of the tributaries.

Lakebed sediments can function as both sinks and sources of nutrients and other constituents to be remobilized and returned to the water column through chemical, physical, and biological processes (Kirol and others, 2024; Shaughnessy and others, 2019). Drivers Fe, Na, Cu, Ni, Mo and nitrate were identified in the lakebed sediment, with values ranging from 0.72 to 31,000 mg/kg. Findings demonstrate that although lakes can act as sinks for nutrients, nutrients are not necessarily permanently buried in lakebed sediments. Instead, internal lake processes can remobilize nutrients and other constituents from sediments, returning them to the water column where they can continue to participate in nutrient cycling and support primary production.

Waves that have enough energy to resuspend lakebed sediment occurred most frequently at the shallow North Anna arm station and at all stations during the summer months (July, August, and September). The Pamunkey Creek arm had fewer sediment resuspending waves in comparison to the North Anna arm and the Confluence, potentially because the Pamunkey Creek arm is deeper and located within a no-wake zone. Most of the waves were resuspended during wind speeds less than 8 km/h, which indicates that the waves responsible for resuspension were not primarily generated by winds but originated from another source, such as boating activity. Wake boats and similar watercraft have been shown to generate waves with sufficient downward energy capable of reaching the lake bed and resuspending sediments (Beachler and Hill, 2003; Hofmann and others, 2011; Houser, 2010). Motorized boats have the potential to generate a downward propagating wave that can resuspend lake-bottom sediments and transverse waves at the surface of the wave, which can erode the shoreline (Bauer and others, 2002; Bilkovic and others, 2019; Castillo and others, 2000; Ortiz and others, 2026). The downward-propagating wave resuspends bed sediments and can cause a disruption to the thermocline (Boegman and others, 2003; Lorke, 2007). The resuspension of sediments can contribute to a positive feedback loop, in which waves resuspend bed sediments, increase macro- and micro-nutrient availability, reduce water clarity, and can sustain or increase algal biomass (Adams and others, 2016; Egertson and others, 2004).

In this study, waves that resuspended lake-bottom sediments were estimated to occur at rates that could keep them in suspension for hours to days, especially during the warmer months of a typical growing season, likely contributing to internal nutrient loading in Lake Anna. Boat wakes are the most likely source of these sediment resuspending waves. Although not directly measured or analyzed in this study, future studies could fill gaps in knowledge to quantify shoreline erosion and thermocline disruptions at Lake Anna because the presence of lakebed sediment resuspension provides at least some evidence that these other processes may be occurring.

During periods when external nutrient loading is reduced, internal nutrient loading from hypoxia and thermal stratification can provide a source of macro- and micronutrients to algal biomass (Facey and others, 2026). Thermal stratification can promote hypoxia and anoxia by separating the hypolimnion from atmospheric and photosynthetically derived oxygen, creating strong redox conditions that release N, P, and other bioavailable macro- and micronutrients from the sediment into the hypolimnion (Facey and others, 2026; Weinke and Biddanda, 2019). During mixing, the nutrients are delivered and can stimulate the production of algal biomass and can sustain the biomass for years to decades (Defeo and others, 2024; Facey and others, 2026).

In shallow, polymictic lakes, such as Lake Anna, episodic and intermittent stratification and hypoxia can result in a pulsed nutrient source (Facey and others, 2026). Weak temperature gradients can form because of daytime solar heating and breakdown throughout the night (Pernica and Wells, 2012). This episodic thermal stratification promotes sediment anoxia and internal nutrient loading, releasing the pool of dissolved P, ammonium, and Fe^{2+} into the photic zone (Antunes and others, 2015). The episodic release of nutrients will favor taxonomy that can uptake and store nutrient sources quickly (Facey and others, 2026). For example, the release of phosphorus from the sediments can lower the TN:TP ratios and promote a shift towards cyanobacteria dominance to the genera that can fix nitrogen from the atmosphere (Defeo and others, 2024; Rock and others, 2025b). Although the presence and the co-occurrence of hypoxic conditions and thermal stratification were confirmed at Lake Anna, temporal resolution is insufficient to quantify the duration of these events and the releases of macro- and micronutrients into the water column.

In the near-shore transect study, the chemical constituents of the water column showed no distance-from-shore gradient, indicating that the water quality is uniform for distances up to 25 m from the shoreline,. Differences in water column nutrients were observed across land uses and locations within Lake Anna. The conversion of forested land to agricultural or residential uses along the shoreline have the potential to increase the water temperature, which could, in turn, increase the proliferation of algal biomass (Doubek and others, 2015). Doubek and others (2015) found that increasing agriculture and developed land use around lake shorelines was positively associated with total phytoplankton biovolume, cyanobacterial biovolume, and cyanobacteria dominance. Agricultural runoff may contribute increased nutrient runoff, while developed areas may increase the water temperature from warmer air-water temperature exchange, both of which can stimulate algal biomass proliferation (Doubek and others, 2015). Some differences in water quality and algal community were observed between land uses but were not large enough to provide clear evidence that a particular land use type or residential occupancy rate was contributing to algal bloom proliferation.

Summary of HAB Initiation, Proliferation, and Decline

Algal blooms of potentially toxigenic cyanobacteria, such as *Raphidiopsis*, are prevalent in the western Lake Anna reservoir in central Virginia. In the Commonwealth of Virginia, an algal bloom is considered a harmful algal bloom, or HAB, when toxins are present and at a level of detection that can harm humans when ingested. Algal bloom advisories due to high cell counts of potentially toxigenic algal biomass have been issued for the western, riverine portion of the reservoir since 2018, when Virginia revised the HAB monitoring framework. In 2023, the U.S. Geological Survey began a study in cooperation with Virginia Department of Environmental

Quality (DEQ) to collect and analyze biological, chemical, physical, and meteorological data in the western Lake Anna reservoir and tributaries to determine the factors contributing to algal biomass initiation, persistence, and decline. This study included year-round monitoring and data collection from May 2023 through December 2024. This report (1) presents a characterization of the algal community, biomass, and toxin production at three stations on Lake Anna; (2) identifies key drivers that could be contributing to algal biomass, proliferation, and decline; and (3) explains the potential sources of the key drivers from external and internal loading. During this study, discrete and continuous water-quality, meteorological, biological, and hydrological data were collected.

Cyanobacteriota is the dominant phylum at all three stations from June through December in 2023 and 2024 in western Lake Anna. Eight potentially toxigenic genera were identified, including *Anabaenopsis*, *Aphanizomenon*, *Chrysosporum*, *Cuspidothrix*, *Dolichospermum*, *Microcystis*, *Raphidiopsis*, and *Woronichinia*. There is a succession of potentially toxigenic genera, with richness of pTOX cyanobacteria higher in the early spring followed by dominance of *Raphidiopsis* in the later summer and through November. However, toxin concentrations were either non-detectable or below the Virginia Department of Health's threshold.

Due to the low toxin concentrations at the lake, we aimed to identify the key drivers of algal biomass. A conditional random forest and generalized additive modeling framework was developed to identify both the important and predictive drivers of the western Lake Anna reservoir. Multiple models were evaluated to determine if there are similar drivers of the bloom at different biological groupings, including total algal biomass model (chlorophyll-a), cyanobacteria model (cells per milliliter), pTOX genera (cells per milliliter), *Raphidiopsis* (cells per milliliter), and pTOX genera excluding *Raphidiopsis* (cells per milliliter). Eleven drivers were identified from the five models: total nitrogen, total phosphorus, alkalinity, copper, iron, molybdenum, nickel, sodium, suspended sediment concentrations, wind speed, and water temperature. However, these drivers do not explain an equal amount of variance in each of the biological response models. Total nitrogen and water temperature were identified as key drivers in all of the models, with water temperature explaining the greatest amount of variance in four of the five models.

Potential external and internal sources of the algal bloom drivers were investigated. External sources include drivers from the tributaries and potential lake-shore sources. Internal loading sources included quantifying bed sediments, active resuspension of bed sediments from wave action, and passive resuspension or release of macro- and micronutrients through thermal stratification and hypoxia. Over the study period, the largest external loads of nutrients and sediment were delivered to Lake Anna from the tributaries during winter storm events. Lakes are sinks for tributaries; however, the nutrients can either settle in the bed sediment or remain suspended. While this study was not designed to determine the fate of the external loads, the concentrations of drivers were elevated in the bed sediments. As water temperatures increased, cell counts of potentially toxigenic genera increased throughout the study area. *Aphanizomenon* cell counts increased at all three stations across Lake Anna during the spring months and *Raphidiopsis* dominated from June through December. During the spring and summer, episodic thermal stratification and hypoxia could provide a source of macro-and micronutrients to the algal bloom. Further, wave action increased during the summer, resuspending sediments into the water column. The waves were occurring when there were low wind speeds, indicating that the waves could be from boats. These sediments could be releasing weakly bound nutrients into the water column that provide key nutrients for algal growth and proliferation. The algal community at Lake Anna is responding primarily to longer-term environmental signals rather than single inflow events.

This report provides insights into the algal blooms that were experienced in Lake Anna over the 19-month study period. The lake and watershed conditions, algal community, and toxins were characterized, drivers were identified, and potential sources of those drivers were evaluated. Blooms have been identified in most years since 2018 and bloom-forming taxa can produce toxins. Several proactive management strategies could be considered help mitigate toxic algal blooms in Lake Anna: (1) monitoring systems that provides early warning indication of an algal bloom; (2) continuous monitoring instruments that measure pigments, such as chlorophyll and phycocyanin, and could provide near real-time estimations of lake algal conditions; (3) Early warning statistical models that utilize these continuously measured parameters to provide early indication of algal blooms.

Appendix 1. Sampling Methods and Analytes

Appendix Table 1.1. Description of discrete samples collected and analyzed to characterize the algal community, cell abundance, and toxin production from the discrete samples collected in Lake Anna, central Virginia. More information is found at U.S. Geological Survey (2026) and Vande Pol and others (2026).

[USGS, U.S. Geological Survey; ID, Identifier; DCLS, Division of Consolidated Laboratory Services; ODU, Old Dominion University]

USGS station number	Analyte category	Analyte	Laboratory
01670144, 01670209, 016702576	Photosynthetic Pigments	Chlorophyll-A	DCLS
	Algal	Algal Community Algal Cell Counts	ODU
	Toxins	Anatoxins Cylindrospermopsin Microcystins Nodularin	ODU

Appendix Table 1.2. Description of discrete samples collected and analyzed to characterize the drivers from Lake Anna discrete monitoring stations. More information is found at U.S. Geological Survey (2026).

[USGS, U.S. Geological Survey; ID, Identifier; DCLS, Division of Consolidated Laboratory Services; ODU, Old Dominion University]

USGS station number	Analyte Category	Analyte	Laboratory
01670144, 01670209, 016702576	Nutrients and Sediment	Turbidity	DCLS
		Total Suspended Solids	
		Volatile Suspended Solids	
		Fixed Suspended Solids	
		Total Nitrogen	
		Particulate Nitrogen	
		Total Dissolved Nitrogen	
		Total Dissolved Phosphorus	
		Particulate Phosphorus	
		Particulate Inorganic Carbon	
		Particulate Carbon	
		Dissolved Organic Carbon	
		Total Phosphorus	
		Dissolved Ammonia Nitrogen	
		Dissolved Nitrite	
		Dissolved Nitrate	
		Nitrite + Nitrate	
		Dissolved Orthophosphorus	
		Dissolved Silica	
		Suspended Sediment Concentration	
		Suspended Sediment -percent <0.0625 mm	
	Major Ions	Total Alkalinity	
		Dissolved Nitrate	
		Dissolved Calcium	
		Dissolved Magnesium	
		Dissolved Sodium	
		Dissolved Potassium	
		Dissolved Chloride	
		Dissolved Sulfate	
	Photosynthetic Pigments	Pheophytin	
		Chlorophyll A	
	Biomass	Biomass as Ash-Free Dry Weight	

	Aluminum
	Antimony
	Arsenic
	Barium
	Beryllium
	Cadmium
	Calcium
	Chromium
	Copper
	Hardness
	Iron
	Lead
Metals and Trace Elements	Magnesium
	Manganese
	Mercury
	Molybdenum
	Nickel
	Potassium
	Selenium
	Silver
	Sodium
	Strontium
	Thallium
	Uranium
	Vanadium
	Zinc

Appendix Table 1.3. Description of discrete samples collected and analyzed to identify potential sources of drivers from the tributaries. More information is found at U.S. Geological Survey (2026).

[USGS, U.S. Geological Survey; ID, Identifier; DCLS, Division of Consolidated Laboratory Services; RSIL, Reston Stable Isotope Laboratory]

USGS station number	Analyte category	Analyte	Laboratory
01670200, 016701405	Nutrients and Sediment	Turbidity	DCLS
		Total Suspended Solids	
		Volatile Suspended Solids	
		Fixed Suspended Solids	
		Total Nitrogen	
		Particulate Nitrogen	
		Total Dissolved Nitrogen	
		Total Dissolved Phosphorus	
		Particulate Phosphorus	
		Particulate Inorganic Carbon	
		Particulate Carbon	
		Dissolved Organic Carbon	
		Total Phosphorus	
		Dissolved Ammonia Nitrogen	
		Dissolved Nitrite	
		Dissolved Nitrate	
		Nitrite + Nitrate	
		Dissolved Orthophosphorus	
		Dissolved Silica	
		Suspended Sediment Concentration	
		Suspended Sediment -percent <0.0625 mm	
	Major Ions	Total Alkalinity	
		Dissolved Nitrate	
		Dissolved Calcium	
		Dissolved Magnesium	
		Dissolved Sodium	
		Dissolved Potassium	
		Dissolved Chloride	
		Dissolved Sulfate	
	Photosynthetic Pigments	Pheophytin	
		Chlorophyll A	
	Stable Isotopes of Nitrate	$^{15}N/^{14}N$	USGS RSIL
		$^{18}O/^{16}O$	

Appendix Table 1.4. Description of discrete samples collected and analyzed to identify potential sources of drivers from the near-shore transects. More information is found at U.S. Geological Survey (2026) and Vande Pol and others (2026).

[USGS, U.S. Geological Survey; ID, Identifier; DCLS, Division of Consolidated Laboratory Services; USGS NWQL, U.S. Geological Survey National Water Quality Laboratory; USGS RSIL, U.S. Geological Survey Reston Stable Isotope Laboratory; ODU, Old Dominion University]

USGS station number	Analyte category	Analyte	Laboratory
380606077495601, 380606077495602, 380606077495605, 380606077495605, 380756077523901, 380756077523903, 380756077523801, 380756077523801, 380642077534801, 380642077534702, 380642077534704, 360634077541201	Nutrients and Sediment	Turbidity	DCLS
		Total Suspended Solids	
		Volatile Suspended Solids	
		Fixed Suspended Solids	
		Total Nitrogen	
		Particulate Nitrogen	
		Total Dissolved Nitrogen	
		Total Dissolved Phosphorus	
		Particulate Phosphorus	
		Particulate Inorganic Carbon	
		Particulate Carbon	
	Major Ions	Specific Conductance	
		pH	
		Total Alkalinity	
		Dissolved Nitrate	
		Dissolved Calcium	
		Dissolved Magnesium	
		Dissolved Sodium	
		Dissolved Potassium	
		Dissolved Chloride	
		Dissolved Sulfate	
		End Point pH	
	Wastewater Indicator	Methylene-Blue Active Substances	USGS NWQL
	Stable Isotopes of Nitrate	$^{15}N/^{14}N$	USGS RSIL
		$^{18}O/^{16}O$	
	Algal	Algal Community	ODU
		Algal Cell Counts	
380606077495601, 380606077495605, 380606077495605, 380603077495801, 380756077523901, 380756077523801, 380756077523801, 380809077531901, 380642077534801, 380642077534704, 360634077541201	Toxins	Anatoxin	ODU
		Cylindrospermopsin	
		Microcystin	
		Saxitoxin	

Appendix Table 1.5. Description of discrete samples collected and analyzed to identify potential sources of drivers from the bed sediments. More information is found at U.S. Geological Survey (2026).

Appendix Table 1.5. Description of discrete samples collected and analyzed to identify potential sources of drivers from the bed sediments.
[USGS, U.S. Geological Survey; ID, Identifier]

USGS station number	Analyte category	Analyte	Analytical method	Laboratory
Reference Table 3 for the USGS station numbers	Nutrients	Nitrogen as bottom material	USEPA Method 351.2 and 353.2 (Agency, 1993; O'Dell, 1993)	RTI
		Phosphorus as bottom material	SM 4500-P F (Standard Methods Online)	
		Carbon as bottom material	Kahn, 1988	
	Metals and Trace Elements	Iron Manganese Mercury Cadmium Lead Cobalt Chromium Copper Zinc	USEPA Method 200.7 – water (EPA, 1994)	

Appendix 2. Variance Explained by Each Driver

Appendix Table 2.1. Model results of the five generalized additive models used to identify the drivers of algal biomass, cyanobacteria concentration, pTOX genera, *Raphidiopsis*, and pTOX excluding *Raphidiopsis* using discrete data collected from Lake Anna, Virginia, 2023–2024.The parameters included in each model were identified using conditional random forest and generalized additive models. Superscripted values next to each parameter indicated the variance explained by each parameter. The R^2 value indicates the total variance explained by each model. Station information for the stations included in these models is found in Table 1. Data used in these models are available at USGS Water Data for the Nation (U.S. Geological Survey, 2026).

[WT, water temperature; TN, total nitrogen; Ni, nickel; Alk, Alkalinity; Mo, Molybdenum; SSC, suspended sediment concentration; Cu, copper; Fe, iron; Na, sodium; WS, wind speed; TP, total phosphorus]

Model	Parameters	R^2
Algal Biomass	$WT^{.266}$, $TN^{0.262}$, $Ni^{0.191}$, $Alk^{0.127}$, $Mo^{0.048}$, $SSC^{0.043}$	93.7
Cyanobacteria	$Ni^{0.188}$, $TN^{0.182}$, $WT^{0.109}$, $Alk^{0.10}$, $Mo^{0.076}$, $Cu^{0.054}$, $Fe^{0.039}$, $SSC^{0.039}$	78.7
pTOX	$WT^{.331}$, $Alk^{0.159}$, $TN^{0.088}$, $Na^{0.073}$, $Fe^{0.043}$, $Cu^{0.037}$	73.1
Raphidiopsis	$WT^{.215}$, $Alk^{0.207}$, $TN^{0.118}$, $Mo^{0.054}$, $Ni^{0.053}$, $SSC^{0.047}$	69.4
pTOX excluding *Raphidiopsis*	$WT^{.133}$, $TN^{0.119}$, $WS^{.102}$, $Mo^{0.094}$, $TP^{0.049}$	49.7

Appendix 3. Data Tables for the Sources of Drivers

Appendix Table 3.1. Summary of the median analyte concentrations of the Lake Anna bed sediment within the North Anna River arm, Pamunkey Creek arm, Confluence, and the entire lake. Refer to Table 4 for additional site information.

[n, number of observations; mg/kg, milligrams per kilograms]

Analyte	Median (mg/kg) ± Standard Deviation (mg/kg)			
	North Anna River arm (n = 16)	Pamunkey Creek arm (n = 11)	Confluence (n = 3)	Entire study area (n = 30)
Fe	33,000 ± 16,792	31,000 ± 14,550	13,000 ± 14,908	31,000 ± 15,790
K	2,250 ± 1,065	2,800 ± 1,120	1,100 ± 980	2,250 ± 1,083
Ca	1,100 ± 426	900 ± 528	630 ± 535	1,000 ± 467
Na	155 ± 175	87 ± 75	37 ± 31	84.5 ± 147
Cu	22 ± 11	23 ± 16	21 ± 23	22.5 ± 14
Ni	12.5 ± 5	12 ± 8	7 ± 8	12 ± 6
Mo	1.3 ± 1	0.86 ± 1	0.18 ± 2	1.25 ± 1
Nitrate	0.8 ± 2	0.43 ± 0	0.5 ± 0	0.72 ± 1

Appendix Table 3.2. Summary of the median and standard deviation for the near-shore transects during low- and high-occupancy periods across agricultural, forested, and residential land uses. Refer to Table 3 for additional information.

[TN, total nitrogen; Alk, alkalinity; Na, sodium; WT; water temperature; MBAS, methylene-blue active substances; TP, total phosphorus; Med, Median; SD, standard deviation]

		Milligram per liter										Degrees C	
		TN		Alk		Na		TP		MBAS		WT	
Occupancy	Land Use	Med	SD	Med	SD	Med	SD	Med	SD	Med	SD	Med	SD
Low	Agriculture	0.54	0.01	23.6	0.64	4.58	0.23	0.01	0.00	0.06	0.04	22.30	0.40
High	Agriculture	0.93	0.03	21.4	0.42	4.76	0.04	0.01	0.00	0.05	0.01	29.80	0.58
Low	Forest	0.42	0.03	15.3	0.40	4.52	0.03	0.01	0.01	0.05	0.00	20.18	0.39
High	Forest	0.39	0.02	20.3	1.40	4.65	0.03	0.01	0.00	0.05	0.00	29.40	0.49
Low	Residential	0.71	0.02	27.1	0.83	4.08	0.08	0.02	0.00	0.05	0.01	21.84	2.15
High	Residential	0.86	0.01	21.5	0.21	4.64	0.05	0.02	0.00	0.06	0.01	29.44	0.30

References Cited

ABRAXIS Anatoxin-a ELISA Microtiter Plate, 2023a, Product No. 520060 accessed January 27, 2023, at, https://www.goldstandarddiagnostics.us/media/18008/ifu-21-057-rev-04-abraxis-anatoxin-a-elisa_520060.pdf.

ABRAXIS Microcystins-ADDA ELISA Microtiter Plate, 2023b, Product No. 520011 accessed January 27, 2023, at, https://www.goldstandarddiagnostics.us/media/17860/ifu-21-052-rev-05-abraxis-microcystins-adda-elisa_520011.pdf.

ABRAXIS Saxitoxin (PSP) ELISA Microtiter Plate, 2023c, Product No. 52255B accessed January 26, 2023, at, https://www.goldstandarddiagnostics.us/media/17882/ifu-21-081-rev-04-abraxis-saxitoxin-elisa_52255b.pdf.

ABRAXIS Cylindrospermopsin ELISA Microtiter Plate, 2023d, Product No. 522011 accessed January 26, 2023, at, https://www.goldstandarddiagnostics.us/media/17867/ifu-21-059-rev-03-abraxis-cylindrospermopsin-elisa_522011.pdf.

Adams, M., Hovey, R., Hipsey, M., Bruce, L., Chisalberti, M., Lowe, R., Gruber, R., Ruiz-Montoya, L., Maxwell, P., Callaghan, D., Kendrick, G., and O'Brien, K., 2016, Feedback between sediment and light for seagrass: Where is it important? Limnology and Oceanography, p. 1937–1955, at https://doi.org/10.1002/lno.10319.

Agency, U.E.U.S.E.P., 1993, Method 351.2, revision 2.0: Determination of total Kjeldahl nitrogen by semi-automated colorimetry:

Alvarez Dalinger, F.S., Laureano, L.V., Moraña, L.B., Borja, C.N., Sanchéz, M.L., and Lozano, V.L., 2026, Drivers of the Worldwide Distribution of Raphidiopsis raciborskii: Evidence from

Experimental to Field Studies: Limnological Review, v. 26, no. 2, p. 13, at https://doi.org/10.3390/limnolrev26020013.

Anthony, J.L., and Downing, J.A., 2003, Physical Impacts of Wind and Boat Traffic on Clear Lake, Iowa, USA: Lake and Reservoir Management, v. 19, no. 1, p. 1–14, at https://doi.org/10.1080/07438140309353984.

Antunes, J.T., Leão, P.N., and Vasconcelos, V.M., 2015, Cylindrospermopsis raciborskii: review of the distribution, phylogeography, and ecophysiology of a global invasive species: Frontiers in Microbiology, v. 6, accessed August 15, 2026, at https://doi.org/10.3389/fmicb.2015.00473.

Arbizu, P.M., 2026, pmartinezarbizu/pairwiseAdonis: accessed August 14, 2026 at https://github.com/pmartinezarbizu/pairwiseAdonis.

Barr, M.N., 2018, Evaluation of whole-water churn splitters for suspended-sediment sample collection and analysis: U.S. Geological Survey 2018–5126, accessed August 7, 2026, at Scientific Investigations Report, at https://doi.org/10.3133/sir20185126.

Bauer, B.O., Lorang, M.S., and Sherman, D.J., 2002, Estimating Boat-Wake-Induced Levee Erosion using Sediment Suspension Measurements: Journal of Waterway, Port, Coastal, and Ocean Engineering, v. 128, no. 4, p. 152–162, at https://doi.org/10.1061/(ASCE)0733-950X(2002)128:4(152).

Beachler, M.M., and Hill, D.F., 2003, Stirring up Trouble? Resuspension of Bottom Sediments by Recreational Watercraft: Lake and Reservoir Management, v. 19, no. 1, p. 15–25, at https://doi.org/10.1080/07438140309353985.

Beaulieu, M., Pick, F., and Gregory-Eaves, I., 2013, Nutrients and water temperature are significant predictors of cyanobacterial biomass in a 1147 lakes data set: Limnology and Oceanography, v. 58, no. 5, p. 1736–1746, at https://doi.org/10.4319/lo.2013.58.5.1736.

Beaver, J.R., Tausz, C.E., Scotese, K.C., Pollard, A.I., and Mitchell, R.M., 2018, Environmental factors influencing the quantitative distribution of microcystin and common potentially toxigenic cyanobacteria in U.S. lakes and reservoirs: Harmful Algae, v. 78, p. 118–128, at https://doi.org/10.1016/j.hal.2018.08.004.

Bilkovic, D.M., Mitchell, M.M., Davis, J., Herman, J., Andrews, E., King, A., Mason, P., Tahvildari, N., Davis, J., and Dixon, R.L., 2019, Defining boat wake impacts on shoreline stability toward management and policy solutions: Ocean & Coastal Management, v. 182, p. 104945, at https://doi.org/10.1016/j.ocecoaman.2019.104945.

Boegman, L., Imberger, J., Ivey, G.N., and Antenucci, J.P., 2003, High-frequency internal waves in large stratified lakes: Limnology and Oceanography, v. 48, no. 2, p. 895–919, at https://doi.org/10.4319/lo.2003.48.2.0895.

Bouffard, D., Ackerman, J.D., and Boegman, L., 2013, Factors affecting the development and dynamics of hypoxia in a large shallow stratified lake: Hourly to seasonal patterns: Water Resources Research, v. 49, no. 5, p. 2380–2394, at https://doi.org/10.1002/wrcr.20241.

Briand, J.-F., Leboulanger, C., Humbert, J.-F., Bernard, C., and Dufour, P., 2004, Cylindrospermopsis Raciborskii (cyanobacteria) Invasion at Mid-Latitudes: Selection, Wide Physiological Tolerance, Orglobalwarming? Journal of Phycology, v. 40, no. 2, p. 231–238, at https://doi.org/10.1111/j.1529-8817.2004.03118.x.

Burford, M.A., Willis, A., Xiao, M., Prentice, M.J., and Hamilton, D.P., 2023, Understanding the relationship between nutrient availability and freshwater cyanobacterial growth and abundance: Inland Waters, v. 13, no. 2, p. 143–152, at https://doi.org/10.1080/20442041.2023.2204050.

Busse, L.B., Simpson, J.C., and Cooper, S.D., 2006, Relationships among nutrients, algae, and land use in urbanized southern California streams: Canadian Journal of Fisheries and Aquatic Sciences, v. 63, no. 12, p. 2621–2638, at https://doi.org/10.1139/f06-146.

Carey, C.C., Ibelings, B.W., Hoffmann, E.P., Hamilton, D.P., and Brookes, J.D., 2012, Eco-physiological adaptations that favour freshwater cyanobacteria in a changing climate: Water Research, v. 46, no. 5, p. 1394–1407, at https://doi.org/10.1016/j.watres.2011.12.016.

Castillo, J.M., Luque, C.J., Castellanos, E.M., and Figueroa, M.E., 2000, Causes and consequences of salt-marsh erosion in an Atlantic estuary in SW Spain: Journal of Coastal Conservation, v. 6, no. 1, p. 89–96, at https://doi.org/10.1007/BF02730472.

Charles, D.F., Knowles, C., and Davis, R.S., 2002, Protocols for the analysis of algal samples collected as part of the US Geological Survey National Water-Quality Assessment Program: Patrick Center for Environmental Research Report, no. 02–06, at.

Chorus, I., and Welker, M. (Eds.), 2021a, Toxic Cyanobacteria in Water: A Guide to Their Public Health Consequences, Monitoring and Management, 2: CRC Press, London, 858 pp.

Chorus, I., and Welker, M. (Eds.), 2021b, Toxic Cyanobacteria in Water: A Guide to Their Public Health Consequences, Monitoring and Management, 2: CRC Press, London, 858 pp.

Commonwealth of Virginia, 2021, Harmful Algae Blooms in Virginia:, 47 pp.

Costello, D.M., Akinnifesi, O.J., Schipper, R.C., Kostick, P., Stoll, J.T., Tiegs, S.D., Marcarelli, A.M., Entrekin, S.A., Bier, R.L., Capps, K.A., and Fletcher, D.E., 2026, Anaemic Streams: Iron and Essential Trace Metals Frequently Limit Primary Producer Biomass: Ecology Letters, v. 29, no. 3, p. e70357, at https://doi.org/10.1111/ele.70357.

Defeo, S., Beutel, M.W., Rodal-Morales, N., and Singer, M., 2024, Sediment release of nutrients and metals from two contrasting eutrophic California reservoirs under oxic, hypoxic and anoxic conditions: Frontiers in Water, v. 6, accessed April 2, 2026, at https://doi.org/10.3389/frwa.2024.1474057.

Delwiche, K., Gu, J., Hemond, H., and Preheim, S.P., 2020, Vertical transport of sediment-associated metals and cyanobacteria by ebullition in a stratified lake: Biogeosciences, v. 17, no. 12, p. 3135–3147, at https://doi.org/10.5194/bg-17-3135-2020.

Department of Environmental Quality, 2021, Harmful Algal Blooms in Virginia: Virginia General Assembly RD411.

Dodds, W.K., Bouska, W.W., Eitzmann, J.L., Pilger, T.J., Pitts, K.L., Riley, A.J., Schloesser, J.T., and Thornbrugh, D.J., 2008, Eutrophication of U.S. Freshwaters: Analysis of Potential Economic Damages: Environmental Science & Technology, v. 43, no. 1, p. 12–19, at https://doi.org/10.1021/es801217q.

Doubek, J.P., Carey, C.C., and Cardinale, B.J., 2015, Anthropogenic land use is associated with N-fixing cyanobacterial dominance in lakes across the continental United States: Aquatic Sciences, v. 77, no. 4, p. 681–694, at https://doi.org/10.1007/s00027-015-0411-x.

Egertson, C.J., Kopaska, J.A., and Downing, J.A., 2004, A Century of Change in Macrophyte Abundance and Composition in Response to Agricultural Eutrophication: Hydrobiologia, v. 524, no. 1, p. 145–156, at https://doi.org/10.1023/B:HYDR.0000036129.40386.ce.

EPA, U., 1994, Method 200.7: determination of metals and trace elements in water and wastes by inductively coupled plasma-atomic emission spectrometry: US EPA Cincinnati, OH, USA.

Eslick-Huff, P., and Puls, K., 2025, wren (version 1.0.0): accessed June 10, 2026 at https://code.usgs.gov/water/stats/wren.

Facey, J.A., Apte, S.C., and Mitrovic, S.M., 2019a, A Review of the Effect of Trace Metals on Freshwater Cyanobacterial Growth and Toxin Production: Toxins, v. 11, no. 11, p. 643, at https://doi.org/10.3390/toxins11110643.

Facey, J.A., Apte, S.C., and Mitrovic, S.M., 2019b, A Review of the Effect of Trace Metals on Freshwater Cyanobacterial Growth and Toxin Production: Toxins, v. 11, no. 11, p. 643, at https://doi.org/10.3390/toxins11110643.

Facey, J.A., Karapoulios, E., and Köhler, J., 2026, Short-term thermal stratification induces hypoxia-related nutrient pulses which reshapes cyanobacterial dynamics in a shallow lake: Harmful Algae, v. 158, p. 103162, at https://doi.org/10.1016/j.hal.2026.103162.

Fenberg, P.B., Menge, B.A., Raimondi, P.T., and Rivadeneira, M.M., 2015, Biogeographic structure of the northeastern Pacific rocky intertidal: the role of upwelling and dispersal to drive patterns: Ecography, v. 38, no. 1, p. 83–95, at https://doi.org/10.1111/ecog.00880.

Feng, L., Wang, Y., Hou, X., Qin, B., Kutser, T., Qu, F., Chen, N., Paerl, H.W., and Zheng, C., 2024a, Harmful algal blooms in inland waters: Nature Reviews Earth & Environment, v. 5, no. 9, p. 631–644, at https://doi.org/10.1038/s43017-024-00578-2.

Feng, L., Wang, Y., Hou, X., Qin, B., Kutser, T., Qu, F., Chen, N., Paerl, H.W., and Zheng, C., 2024b, Harmful algal blooms in inland waters: Nature Reviews Earth & Environment, v. 5, no. 9, p. 631–644, at https://doi.org/10.1038/s43017-024-00578-2.

Filbee-Dexter, K., and Scheibling, R.E., 2017, The present is the key to the past: linking regime shifts in kelp beds to the distribution of deep-living sea urchins: Ecology, v. 98, no. 1, p. 253–264, at https://doi.org/10.1002/ecy.1638.

Gautreau, E., Volatier, L., Nogaro, G., Gouze, E., and Mermillod-Blondin, F., 2020, The influence of bioturbation and water column oxygenation on nutrient recycling in reservoir sediments: Hydrobiologia, v. 847, no. 4, p. 1027–1040, at https://doi.org/10.1007/s10750-019-04166-0.

Gerhardt, S., and Schink, B., 2005, Redox Changes of Iron Caused by Erosion, Resuspension and Sedimentation in Littoral Sediment of a Freshwater Lake: Biogeochemistry, v. 74, no. 3, p. 341–356, at https://doi.org/10.1007/s10533-004-4725-3.

Glass, J.B., Wolfe-Simon, F., Elser, J.J., and Anbar, A.D., 2010, Molybdenum—nitrogen co-limitation in freshwater and coastal heterocystous cyanobacteria: Limnology and Oceanography, v. 55, no. 2, p. 667–676, at https://doi.org/10.4319/lo.2010.55.2.0667.

Gobler, C.J., Burkholder, J.M., Davis, T.W., Harke, M.J., Johengen, T., Stow, C.A., and Van de Waal, D.B., 2016, The dual role of nitrogen supply in controlling the growth and toxicity of cyanobacterial blooms: Harmful Algae, v. 54, p. 87–97, at https://doi.org/10.1016/j.hal.2016.01.010.

Gomaa, M.N., and Carmichael, W.W., 2023, The Role of Heterocysts in Cyanotoxin Production during Nitrogen Limitation: Toxins, v. 15, no. 10, p. 611, at https://doi.org/10.3390/toxins15100611.

Gorney, R.M., Graham, J.L., and Murphy, J.C., 2023a, The "H," "A," and "B" of a HAB: A definitional framework: Lakeline, v. 43, no. 2, p. 7–11, at.

Gorney, R.M., June, S.G., Stainbrook, K.M., and Smith, A.J., 2023b, Detections of cyanobacteria harmful algal blooms (cyanoHABs) in New York State, United States (2012–2020): Lake and Reservoir Management, v. 39, no. 1, p. 21–36, at https://doi.org/10.1080/10402381.2022.2161436.

Graham, J.L., Dubrovsky, N.M., and Eberts, S.M., 2016, Cyanobacterial harmful algal blooms and U.S. Geological Survey science capabilities: U.S. Geological Survey 2016–1174, 1–12 pp., accessed September 22, 2025, at Open-File Report, at https://doi.org/10.3133/ofr20161174.

Granger, J., Sigman, D.M., Rohde, M.M., Maldonado, M.T., and Tortell, P.D., 2010, N and O isotope effects during nitrate assimilation by unicellular prokaryotic and eukaryotic plankton cultures: Geochimica et Cosmochimica Acta, v. 74, no. 3, p. 1030–1040, at https://doi.org/10.1016/j.gca.2009.10.044.

Greene, W., 2008, Functional forms for the negative binomial model for count data: Economics Letters, v. 99, no. 3, p. 585–590, at https://doi.org/10.1016/j.econlet.2007.10.015.

Griffith, A.W., and Gobler, C.J., 2020, Harmful algal blooms: A climate change co-stressor in marine and freshwater ecosystems: Harmful Algae, v. 91, p. 101590, at https://doi.org/10.1016/j.hal.2019.03.008.

Harvey, D.T., and Hanson, B.A., 2024, A Comparison of Functions for PCA: p. 14, at.

Helsel, D.R., Hirsch, R.M., Ryberg, K.R., Archfield, S.A., and Gilroy, E.J., 2020, Statistical methods in water resources: U.S. Geological Survey 4-A3, accessed August 30, 2026, at Techniques and Methods, at https://doi.org/10.3133/tm4A3.

Hofmann, H., Lorke, A., and Peeters, F., 2011, Wind and ship wave-induced resuspension in the littoral zone of a large lake: Water Resources Research, v. 47, no. 9, accessed April 22, 2026, at https://doi.org/10.1029/2010WR010012.

Hothorn, T., Seibold, H., and Zeileis, A., 2025, partykit: A Toolkit for Recursive Partytioning (version 1.2-24): accessed February 4, 2026 at https://cran.r-project.org/web/packages/partykit/index.html.

Hothorn, T., and Zeileis, A., 2011, partykit: A Toolkit for Recursive Partytioning: accessed January 7, 2026, at https://doi.org/10.32614/CRAN.package.partykit.

Houser, C., 2010, Relative Importance of Vessel-Generated and Wind Waves to Salt Marsh Erosion in a Restricted Fetch Environment: Journal of Coastal Research, v. 26, no. 2, p. 230–240, at.

Hyer, K.E., Denver, J.M., Langland, M.J., Webber, J.S., Böhlke, J.K., Hively, W.D., and Clune, J.W., 2016, Spatial and temporal variation of stream chemistry associated with contrasting geology and land-use patterns in the Chesapeake Bay watershed—Summary of results from

Smith Creek, Virginia; Upper Chester River, Maryland; Conewago Creek, Pennsylvania; and Difficult Run, Virginia, 2010–2013: U.S. Geological Survey 2016–5093, 1–211 pp., accessed March 5, 2026, at Scientific Investigations Report, at https://doi.org/10.3133/sir20165093.

Igwaran, A., Kayode, A.J., Moloantoa, K.M., Khetsha, Z.P., and Unuofin, J.O., 2024, Cyanobacteria Harmful Algae Blooms: Causes, Impacts, and Risk Management: Water, Air, & Soil Pollution, v. 235, no. 1, p. 71, at https://doi.org/10.1007/s11270-023-06782-y.

Iiames, J.S., Salls, W.B., Mehaffey, M.H., Nash, M.S., Christensen, J.R., and Schaeffer, B.A., 2021, Modeling Anthropogenic and Environmental Influences on Freshwater Harmful Algal Bloom Development Detected by MERIS Over the Central United States: Water Resources Research, v. 57, no. 10, p. e2020WR028946, at https://doi.org/10.1029/2020WR028946.

Isvánovics, V., Shafik, H.M., Présing, M., and Juhos, S., 2000, Growth and phosphate uptake kinetics of the cyanobacterium, Cylindrospermopsis raciborskii (Cyanophyceae) in throughflow cultures: Freshwater Biology, v. 43, no. 2, p. 257–275, at https://doi.org/10.1046/j.1365-2427.2000.00549.x.

Ji, X., Shu, L., Chen, W., Chen, Z., Shang, X., Yang, Y., Dahlgren, R.A., and Zhang, M., 2022, Nitrate pollution source apportionment, uncertainty and sensitivity analysis across a rural-urban river network based on δ15N/δ18O-NO3− isotopes and SIAR modeling: Journal of Hazardous Materials, v. 438, p. 129480, at https://doi.org/10.1016/j.jhazmat.2022.129480.

Kahn, L., 1988, Determination of total organic carbon in sediment: United States Environmental Protection Agency, Region II, Environmental Services Division, Monitoring Management Branch, Edison, NJ, at.

Karlson, B., Godhe, A., Cusack, C., and Bresnan, E., 2010, Intergovernmental Oceanographic Commission Manuals and Guides 55 MICROSCOPIC AND MOLECULAR METHODS FOR QUANTITATIVE PHYTOPLANKTON ANALYSIS, *in*, p. 5–12.

Kelly, L.T., Champeaud, M., Beuzenberg, V., Goodwin, E., Verburg, P., and Wood, S.A., 2021, Trace metal and nitrogen concentrations differentially affect bloom forming cyanobacteria of the genus Dolichospermum: Aquatic Sciences, v. 83, no. 2, p. 34, at https://doi.org/10.1007/s00027-021-00786-8.

Kendall, C., Elliot, E., and Wankel, S., 2007, Tracing Anthropogenic Inputs of Nitrogen to Ecosystems. In Stable Isotopes in Ecology and Environmental Science: 375–449 pp.

Kirol, A.P., Morales-Williams, A.M., Braun, D.C., Marti, C.L., Pierson, O.E., Wagner, K.J., and Schroth, A.W., 2024, Linking Sediment and Water Column Phosphorus Dynamics to Oxygen, Temperature, and Aeration in Shallow Eutrophic Lakes: Water Resources Research, v. 60, no. 1, p. e2023WR034813, at https://doi.org/10.1029/2023WR034813.

Kohlhaas, R.T., Schroeder, S.E., and Richardson, J.B., 2026, Phosphorus and potentially toxic elements in stream waters, sediments, mine tailings, and pines across Lake Anna watershed, VA, USA, and biochar-lime remediation: Environmental Science and Pollution Research, v. 33, no. 3, p. 800–821, at https://doi.org/10.1007/s11356-025-37328-w.

Komárek, J., 2008, Cyanoprokaryota, Teil 1 / Part 1: Chroococcales, 1: Süßwasserflora von Mitteleuropa, Spektrum Akademischer Verlag Heidelberg, 548 pp.

Komárek, J., 2013, Süßwasserflora Von Mitteleuropa, Bd. 19/3: Cyanoprokaryota: 3. Teil / 3rd Part: Heterocytous Genera (Hardcover), 1: Süßwasserflora von Mitteleuropa, Springer Spektrum, 1131 pp.

Komárek, J., and Anagnostidis, K., 2005, Süßwasserflora von Mitteleuropa, Bd. 19/2: Cyanoprokaryota, 1: Süßwasserflora von Mitteleuropa, Spektrum Akademischer Verlag Heidelberg, 759 pp.

Lee, J., Rai, P.K., Jeon, Y.J., Kim, K.-H., and Kwon, E.E., 2017, The role of algae and cyanobacteria in the production and release of odorants in water: Environmental Pollution, v. 227, p. 252–262, at https://doi.org/10.1016/j.envpol.2017.04.058.

Leiker, B.M., Abel, J.R., Graham, J.L., Foster, G.M., King, L.R., Stiles, T.C., and Buley, R.P., 2021, Spatial and temporal variability of nutrients and algae in the Republican River and Milford Lake, Kansas, June through November 2017 and May through November 2018: U.S. Geological Survey 2020–5135, accessed February 23, 2026, at Scientific Investigations Report, at https://doi.org/10.3133/sir20205135.

Levshina, N., 2020, Conditional Inference Trees and Random Forests, *in* Paquot, M. and Gries, S.Th. eds., A Practical Handbook of Corpus Linguistics: Springer International Publishing, Cham, p. 611–643.

Loftin, K.A., Meyer, M.T., Rubio, F., Kamp, L., Humphries, E., and Whereat, E., 2008, Comparison of two cell lysis procedures for recovery of microcystins in water samples from silver lake in Dover, Delaware, with microcystin producing cyanobacterial accumulations: U.S. Geological Survey 2008–1341, accessed August 12, 2026, at Open-File Report, at https://doi.org/10.3133/ofr20081341.

Lorke, A., 2007, Boundary mixing in the thermocline of a large lake: Journal of Geophysical Research: Oceans, v. 112, no. C9, accessed April 22, 2026, at https://doi.org/10.1029/2006JC004008.

Martínez-Ruiz, E.B., and Martínez-Jerónimo, F., 2016, How do toxic metals affect harmful cyanobacteria? An integrative study with a toxigenic strain of *Microcystis aeruginosa* exposed to nickel stress: Ecotoxicology and Environmental Safety, v. 133, p. 36–46, at https://doi.org/10.1016/j.ecoenv.2016.06.040.

Mason, C., and Soroka, A., 2026, Nitrogen, phosphorus, and suspended-sediment loads and trends measured at the Chesapeake Bay River Input Monitoring stations: Water years 1985-2025: ScienceBase, accessed June 10, 2026, at https://doi.org/https://doi.org/10.5066/P13B4M8S.

Mehnert, G., Rücker, J., Nicklisch, A., Leunert, F., and Wiedner, C., 2012, Effects of thermal acclimation and photoacclimation on lipophilic pigments in an invasive and a native cyanobacterium of temperate regions: European Journal of Phycology, v. 47, no. 2, p. 182–192, at https://doi.org/10.1080/09670262.2012.683496.

Metje, N., 2001, Sediment suspension under water waves:

Miller, S.A., Webber, J.S., Jastram, J.D., and Aguilar, M.F., 2023, Using high-frequency monitoring data to quantify city-wide suspended-sediment load and evaluate TMDL goals: Environmental Monitoring and Assessment, v. 195, no. 11, p. 1372, at https://doi.org/10.1007/s10661-023-11905-3.

Mishra, S., Stumpf, R.P., Schaeffer, B.A., and Werdell, P.J., 2023, Recent changes in cyanobacteria algal bloom magnitude in large lakes across the contiguous United States: Science of The Total Environment, v. 897, p. 165253, at https://doi.org/10.1016/j.scitotenv.2023.165253.

Moreno-Ostos, E., Cruz-Pizarro, L., Basanta, A., and George, D.G., 2009, The influence of wind-induced mixing on the vertical distribution of buoyant and sinking phytoplankton species: Aquatic ecology, v. 43, no. 2, p. 271–284, at.

Moy, N.J., Dodson, J., Tassone, S.J., Bukaveckas, P.A., and Bulluck, L.P., 2016, Biotransport of Algal Toxins to Riparian Food Webs: Environmental Science & Technology, v. 50, no. 18, p. 10007–10014, at https://doi.org/10.1021/acs.est.6b02760.

Mrdjen, I., Fennessy, S., Schaal, A., Dennis, R., Slonczewski, J.L., Lee, S., and Lee, J., 2018, Tile Drainage and Anthropogenic Land Use Contribute to Harmful Algal Blooms and Microbiota Shifts in Inland Water Bodies: Environmental Science & Technology, v. 52, no. 15, p. 8215–8223, at https://doi.org/10.1021/acs.est.8b03269.

Murphy, J.C., Gorney, R.M., Lucas, L.A., Zwart, J.A., and Graham, J.L., 2025, A systematic literature review of forecasting and predictive models of harmful algal blooms in flowing waters: p. 2025.09.29.679270, accessed August 6, 2026, at https://doi.org/10.1101/2025.09.29.679270.

Myrhaug, D., Wang, H., and Holmedal, L., 2024, Revisiting wave friction factors for rough turbulent flow: OCEANOLOGIA, v. 66, no. 3, accessed March 25, 2026, at https://doi.org/10.5697/NMCX3016.

Niu, C., Zhai, T., Zhang, Q., Wang, H., and Xiao, L., 2021, Research Advances in the Analysis of Nitrate Pollution Sources in a Freshwater Environment Using δ15N-NO3− and δ18O-NO3−:

International Journal of Environmental Research and Public Health, v. 18, no. 22, accessed March 25, 2026, at https://doi.org/10.3390/ijerph182211805.

Nürnberg, G.K., 2004, Quantified Hypoxia and Anoxia in Lakes and Reservoirs: The Scientific World Journal, v. 4, no. 1, p. 276509, at https://doi.org/10.1100/tsw.2004.5.

O'Dell, J., 1993, Method 353.2, Revision 2.0: Determination of nitrate-nitrite nitrogen by automated colorimetry: Environmental Monitoring Systems Laboratory, US Environmental Protection Agency, Cincinnati, Ohio, at.

Odhiambo, B.K., Brown, V., Armentrout, G., Giancarlo, L.C., and Wegner, C., 2013, Sediment trace metals and PCB input history in Lake Anna, Virginia, USA: Environmental Earth Sciences, v. 69, no. 6, p. 2103–2117, at https://doi.org/10.1007/s12665-013-2500-2.

Odhiambo, B.K., and Ricker, M.C., 2012, Spatial and isotopic analysis of watershed soil loss and reservoir sediment accumulation rates in Lake Anna, Virginia, USA: Environmental Earth Sciences, v. 65, no. 1, p. 373–384, at https://doi.org/10.1007/s12665-011-1098-5.

Oksanen, J., Simpson, G.L., Blanchet, F.G., Kindt, R., Legendre, P., Minchin, P.R., O'Hara, R.B., Solymos, P., Stevens, M.H.H., Szoecs, E., Wagner, H., Barbour, M., Bedward, M., Bengtsson, H., and others, 2026, vegan: Community Ecology Package (version 2.7-5): accessed August 14, 2026 at https://cran.r-project.org/web/packages/vegan/index.html.

de Oliveira, F.H.P.C., and Dantas, Ê.W., 2019, Sodium and nitrate favor the steady state of cyanobacteria in a semiarid ecosystem: Acta Scientiarum. Biological Sciences, v. 41, p. 47924, at.

Omidi, A., Esterhuizen-Londt, M., and Pflugmacher, S., 2018, Still challenging: the ecological function of the cyanobacterial toxin microcystin – What we know so far: Toxin Reviews, v. 37, no. 2, p. 87–105, at https://doi.org/10.1080/15569543.2017.1326059.

O'Neil, J.M., Davis, T.W., Burford, M.A., and Gobler, C.J., 2012, The rise of harmful cyanobacteria blooms: The potential roles of eutrophication and climate change: Harmful Algae, v. 14, p. 313–334, at https://doi.org/10.1016/j.hal.2011.10.027.

Ortiz, D.A., Blackburn, S.R., Daulton, T., Kovar, B., Meyer, M.W., Pralle, C.E., and Stanley, E.H., 2026, Wake boats and lakes: physical, ecological, and policy implications: Lake and Reservoir Management, v. 42, no. 1, p. 15–35, at https://doi.org/10.1080/10402381.2025.2578757.

Paerl, H.W., Fulton, R.S., Moisander, P.H., and Dyble, J., 2001, Harmful Freshwater Algal Blooms, With an Emphasis on Cyanobacteria: The Scientific World Journal, v. 1, no. 2, p. 139109, at https://doi.org/10.1100/tsw.2001.16.

Paerl, H.W., and Otten, T.G., 2013, Harmful Cyanobacterial Blooms: Causes, Consequences, and Controls: Microbial Ecology, v. 65, no. 4, p. 995–1010, at https://doi.org/10.1007/s00248-012-0159-y.

Palshin, N., Zdorovennova, G., Efremova, T., Bogdanov, S., Terzhevik, A., and Zdorovennov, R., 2021, Dissolved oxygen stratification in a small lake depending on water temperature and density and wind impact: IOP Conference Series: Earth and Environmental Science, v. 937, no. 3, p. 032019, at https://doi.org/10.1088/1755-1315/937/3/032019.

Parker, C.R., and Voshell Jr., J.R., 1983, Production of filter-feeding Trichoptera in an impounded and a free-flowing river: Canadian Journal of Zoology, v. 61, no. 1, p. 70–87, at https://doi.org/10.1139/z83-008.

Parnell, A.C., Inger, R., Bearhop, S., and Jackson, A.L., 2010, Source Partitioning Using Stable Isotopes: Coping with Too Much Variation: PLOS ONE, v. 5, no. 3, p. e9672, at https://doi.org/10.1371/journal.pone.0009672.

Pernica, P., and Wells, M., 2012, Frequency of episodic stratification in the near surface of Lake Opeongo and other small lakes: Water Quality Research Journal, v. 47, no. 3–4, p. 227–237, at https://doi.org/10.2166/wqrjc.2012.001.

Phillips, K., 2017, Lake Anna Map: at, https://www.sycamoreshoalspoa.com/index.php/documents/document-list/82-lake-anna-map-and-information/file.

Porter, A.J., 2025, Spatiotemporal patterns in urban nutrient and suspended sediment loads and stream response to watershed management implementation: Environmental Monitoring and Assessment, v. 197, no. 4, p. 497, at https://doi.org/10.1007/s10661-025-13917-7.

R Core Team, 2025, (version 4.5.2): at https://www.R-project.org/.

Rantz, S., 1982, Measurement and computation of streamflow: Report 2175, at https://doi.org/10.3133/wsp2175.

Raven, J.A., Gobler, C.J., and Hansen, P.J., 2020, Dynamic CO2 and pH levels in coastal, estuarine, and inland waters: Theoretical and observed effects on harmful algal blooms: Harmful Algae, v. 91, p. 101594, at https://doi.org/10.1016/j.hal.2019.03.012.

Recknagel, F., Zohary, T., Rücker, J., Orr, P.T., Branco, C.C., and Nixdorf, B., 2019, Causal relationships of *Raphidiopsis* (formerly *Cylindrospermopsis*) dynamics with water temperature and N:P-ratios: A meta-analysis across lakes with different climates based on inferential modelling: Harmful Algae, v. 84, p. 222–232, at https://doi.org/10.1016/j.hal.2019.04.005.

Robertson, T., 2025, An Overview of the Lake Anna Harmful Algal Bloom Study: Lake Anna Research Summit, accessed August 16, 2026, at https://www.louisacounty.gov/DocumentCenter/View/11701/Reference_F_DEQ_Study_2025.

Rock, L.A., Fetzer, W.W., Patterson, L.S., Sillen, S.J., Steg, R., Walters, A.W., and Collins, S.M., 2025a, Spatiotemporal drivers of water quality and phytoplankton communities in a cyanobacteria-dominated reservoir provide management insights: Environmental Monitoring and Assessment, v. 197, no. 7, p. 795, at https://doi.org/10.1007/s10661-025-14258-1.

Rock, L.A., Fetzer, W.W., Patterson, L.S., Sillen, S.J., Steg, R., Walters, A.W., and Collins, S.M., 2025b, Spatiotemporal drivers of water quality and phytoplankton communities in a cyanobacteria-dominated reservoir provide management insights: Environmental Monitoring and Assessment, v. 197, no. 7, p. 795, at https://doi.org/10.1007/s10661-025-14258-1.

Salmon, R., 2008, Introduction to ocean waves: Scripps Institution of Oceanography, University of California, San Diego, at.

Sauer, V.B., and Turnipseed, D.P., 2010, Stage measurement at gaging stations: U.S. Geological Survey 3-A7, accessed August 7, 2026, at Techniques and Methods, at https://doi.org/10.3133/tm3A7.

Schulte, N.O., Carlisle, D.M., and Spaulding, S.A., 2022, Natural and anthropogenic influences on benthic cyanobacteria in streams of the northeastern United States: Science of The Total Environment, v. 826, p. 154241, at https://doi.org/10.1016/j.scitotenv.2022.154241.

Seabird Scientific, 2018, SUNA V2 manual: accessed August 15, 2026, at, https://www.seabird.com/products/suna-v2.

Seale, D.B., Boraas, M.E., and Warren, G.J., 1987, Effects of sodium and phosphate on growth of cyanobacteria: Water Research, v. 21, no. 6, p. 625–631, at https://doi.org/10.1016/0043-1354(87)90072-8.

Seefeldt, L.C., Yang, Z.-Y., Lukoyanov, D.A., Harris, D.F., Dean, D.R., Raugei, S., and Hoffman, B.M., 2020, Reduction of Substrates by Nitrogenases: Chemical Reviews, v. 120, no. 12, p. 5082–5106, at https://doi.org/10.1021/acs.chemrev.9b00556.

Shapiro, J., 1997, The role of carbon dioxide in the initiation and maintenance of blue-green dominance in lakes: Freshwater Biology, v. 37, no. 2, p. 307–323, at https://doi.org/10.1046/j.1365-2427.1997.00164.x.

Shaughnessy, A. r., Sloan, J. j., Corcoran, M. j., and Hasenmueller, E. a., 2019, Sediments in Agricultural Reservoirs Act as Sinks and Sources for Nutrients over Various Timescales: Water Resources Research, v. 55, no. 7, p. 5985–6000, at https://doi.org/10.1029/2018WR024004.

Shen, W., Yang, H., Ding, G., Li, B., Gan, X., Yuan, Z., Wang, L., and Zhang, W., 2025, Response of the Invasive Cyanobacterium Raphidiopsis raciborskii to Iron and Phosphorus Concentrations in the Habitat: Effects on Growth and Cellular Phosphorus Distribution: Diversity, v. 17, no. 6, p. 386, at https://doi.org/10.3390/d17060386.

Shi, J., Ou-yang, T., Yang, S., Zhao, L., Ji, L., and Wu, Z., 2022, Transcriptomic responses to phosphorus in an invasive cyanobacterium, Raphidiopsis raciborskii: Implications for nutrient management: Harmful Algae, v. 111, p. 102150, at https://doi.org/10.1016/j.hal.2021.102150.

Snow, D., 2018, Nitrate-N Isotope Results and Interpretation:

Sokal, R.R., and Rohlf, F.J., 1995, Biometry: Macmillan.

Standard Methods Online Standard Methods for the Examination of Water and Wastewater: accessed August 1, 2026 at http://standardmethods.org/.

Stauffer, B.A., Bowers, H.A., Buckley, E., Davis, T.W., Johengen, T.H., Kudela, R., McManus, M.A., Purcell, H., Smith, G.J., Vander Woude, A., and Tamburri, M.N., 2019, Considerations in Harmful Algal Bloom Research and Monitoring: Perspectives From a Consensus-Building Workshop and Technology Testing: Frontiers in Marine Science, v. 6, accessed April 8, 2026, at https://doi.org/10.3389/fmars.2019.00399.

Sterner, R.W., 2008, On the Phosphorus Limitation Paradigm for Lakes: International Review of Hydrobiology, v. 93, no. 4–5, p. 433–445, at https://doi.org/10.1002/iroh.200811068.

Storm User’s Manual for the CAAS Cube, 2021, accessed January 4, 2023, at https://doi.org/CAASCB-0006.A.

Strobl, C., Boulesteix, A.-L., Zeileis, A., and Hothorn, T., 2007, Bias in random forest variable importance measures: Illustrations, sources and a solution: BMC Bioinformatics, v. 8, no. 1, p. 25, at https://doi.org/10.1186/1471-2105-8-25.

Tang, C., Li, Y., He, C., and Acharya, K., 2020, Dynamic behavior of sediment resuspension and nutrients release in the shallow and wind-exposed Meiliang Bay of Lake Taihu: Science of The Total Environment, v. 708, p. 135131, at https://doi.org/10.1016/j.scitotenv.2019.135131.

Tao, M., Xie, P., Chen, J., Qin, B., Zhang, D., Niu, Y., Zhang, M., Wang, Q., and Wu, L., 2012, Use of a Generalized Additive Model to Investigate Key Abiotic Factors Affecting Microcystin Cellular Quotas in Heavy Bloom Areas of Lake Taihu: PLOS ONE, v. 7, no. 2, p. e32020, at https://doi.org/10.1371/journal.pone.0032020.

Tassone, S.J., Foster, B.M., Maas, C.M., and Jastram, J.D., 2026, Ecosystem Metabolism as an Early Warning Indicator of Lake Algal Blooms: accessed August 28, 2026, at, https://eartharxiv.org/repository/view/13537/.

Things to Do at Lake Anna Lake Anna, accessed August 16, 2026 at https://lakeanna.com/things-to-do/.

Tsujii, M., Kobayashi, A., Kano, A., Kera, K., Takagi, T., Nagata, N., Kojima, S., Hikosaka, K., Oguchi, R., Sonoike, K., Azai, C., Inagaki, T., Ishimaru, Y., and Uozumi, N., 2025, Na + -driven pH regulation by Na+/H+ antiporters promotes photosynthetic efficiency in cyanobacteria: Plant Physiology, v. 197, no. 1, p. kiae562, at https://doi.org/10.1093/plphys/kiae562.

Tsujimura, S., Ishikawa, K., and Tsukada, H., 2001, Effect of temperature on growth of the cyanobacterium Aphanizomenon flos-aquae in Lake Biwa and Lake Yogo: Phycological Research, v. 49, no. 4, p. 275–280, at https://doi.org/10.1046/j.1440-1835.2001.00255.x.

Tukey, J.W., 1953, The problem of multiple comparisons:

U. S. Geological Survey, 2019, StreamStats: accessed August 6, 2026 at https://streamstats.usgs.gov/ss/.

U. S. Geological Survey, 2024, Annual NLCD Collection 1 Science Products:at https://doi.org/https://doi.org/10.5066/P94UXNTS.

U. S. Geological Survey, 2026, Water Data for the Nation: accessed August 7, 2026 at https://waterdata.usgs.gov/.

Underwood, J.C., Hall, N.C., Mumford, A.C., Harvey, R.W., Bliznik, P.A., and Jeanis, K.M., 2024, Relation between the relative abundance and collapse of Aphanizomenon flos-aquae and microbial antagonism in Upper Klamath Lake, Oregon: FEMS Microbiology Ecology, v. 100, no. 5, p. fiae043, at https://doi.org/10.1093/femsec/fiae043.

U.S. Army Corps of Engineers, 2024, National Inventory of Dams: National Inventory of Dams, accessed July 23, 2024 at https://nid.sec.usace.army.mil/#/dams/system/VA177002/summary.

U.S. Geological Survey, 2015, National Field Manual for the Collection of Water-Quality Data. U.S. Geological Survey Techniques of Water-Resources Investigations, Book 9: Report 09, at https://doi.org/10.3133/twri09.

U.S. Geological Survey, 2026, USGS Water Data for the Nation: U.S. Geological Survey National Water Information System database: accessed August 16, 2026 at https://waterdata.usgs.gov/.

Verspagen, J.M.H., Waal, D.B.V. de, Finke, J.F., Visser, P.M., Donk, E.V., and Huisman, J., 2014, Rising CO2 Levels Will Intensify Phytoplankton Blooms in Eutrophic and Hypertrophic Lakes: PLOS ONE, v. 9, no. 8, p. e104325, at https://doi.org/10.1371/journal.pone.0104325.

Vilar, M.C.P., and Molica, R.J.R., 2020, Changes in pH and dissolved inorganic carbon in water affect the growth, saxitoxins production and toxicity of the cyanobacterium *Raphidiopsis raciborskii* ITEP-A1: Harmful Algae, v. 97, p. 101870, at https://doi.org/10.1016/j.hal.2020.101870.

Virginia Department of Health, 2021, Guidance for Cyanobacteria Bloom Recreational Advisory Management: Virginia Department of Health, accessed March 12, 2026.

Wagner, R.J., Jr, R.W.B., Oblinger, C.J., and Smith, B.A., 2006, Guidelines and standard procedures for continuous water-quality monitors station operation, record computation, and data reporting: Techniques and Methods 1-D3, 51 pp.

Walls, J.T., Wyatt, K.H., Doll, J.C., Rubenstein, E.M., and Rober, A.R., 2018, Hot and toxic: Temperature regulates microcystin release from cyanobacteria: Science of The Total Environment, v. 610–611, p. 786–795, at https://doi.org/10.1016/j.scitotenv.2017.08.149.

Wasko, C., and Guo, D., 2022, Understanding event runoff coefficient variability across Australia using the hydroEvents R package: Hydrological Processes, v. 36, no. 4, p. e14563, at https://doi.org/10.1002/hyp.14563.

Wehr, J., and Sheath, R., 2015, Freshwater Algae of North America: Ecology and Classification, 2: 1066 pp.

Weinke, A.D., and Biddanda, B.A., 2019, Influence of episodic wind events on thermal stratification and bottom water hypoxia in a Great Lakes estuary: Journal of Great Lakes Research, v. 45, no. 6, p. 1103–1112, at https://doi.org/10.1016/j.jglr.2019.09.025.

Wetzel, R.G., 2001, Limnology: Lake and River Ecosystems: Gulf Professional Publishing, 1023 pp.

Willis, A., Chuang, A.W., Dyhrman, S., and Burford, M.A., 2019, Differential expression of phosphorus acquisition genes in response to phosphorus stress in two Raphidiopsis raciborskii strains: Harmful Algae, v. 82, p. 19–25, at https://doi.org/10.1016/j.hal.2018.12.003.

Wiltsie, D., Schnetzer, A., Green, J., Vander Borgh, M., and Fensin, E., 2018, Algal Blooms and Cyanotoxins in Jordan Lake, North Carolina: Toxins, v. 10, no. 2, p. 92, at https://doi.org/10.3390/toxins10020092.

Wood, S., 2025, mgcv: Mixed GAM Computation Vehicle with Automatic Smoothness Estimation (version 1.9-4): accessed February 16, 2026 at https://cran.r-project.org/web/packages/mgcv/index.html.

Wu, T., Qin, B., Brookes, J.D., Shi, K., Zhu, G., Zhu, M., Yan, W., and Wang, Z., 2015, The influence of changes in wind patterns on the areal extension of surface cyanobacterial blooms in a large shallow lake in China: Science of The Total Environment, v. 518–519, p. 24–30, at https://doi.org/10.1016/j.scitotenv.2015.02.090.

Wu, W., Wang, S.S.Y., and Jia, Y., 2000, Nonuniform sediment transport in alluvial rivers Transport de sédiments non uniformes en rivière alluviale:

Wu, Z., Yang, S., and Shi, J., 2023, Overview of the distribution and adaptation of a bloom-forming cyanobacterium Raphidiopsis raciborskii: integrating genomics, toxicity, and ecophysiology: accessed August 15, 2026 at https://www.proquest.com/openview/f6ebbb478b4d5f3629441322016527c7/1?pq-origsite=gscholar&cbl=54339.

Xiao, M., Burford, M.A., Frassl, M.A., Willis, A., Roberts, M.E., and Hamilton, D.P., 2026, Nitrogen fixation is driven by cellular nitrogen stores in a diazotrophic cyanobacterium: Evidence from culture experiments and model validation: Limnology and Oceanography, v. 71, no. 2, p. e70326, at https://doi.org/10.1002/lno.70326.

Yamashita, K., Yamazaki, Y., Bai, Y., Takahashi, T., Imamura, F., and Cheung, K.F., 2022, Modeling of sediment transport in rapidly-varying flow for coastal morphological changes caused by tsunamis: Marine Geology, v. 449, p. 106823, at https://doi.org/10.1016/j.margeo.2022.106823.

Yang, J., Holbach, A., Wilhelms, A., Krieg, J., Qin, Y., Zheng, B., Zou, H., Qin, B., Zhu, G., Wu, T., and Norra, S., 2020, Identifying spatio-temporal dynamics of trace metals in shallow eutrophic lakes on the basis of a case study in Lake Taihu, China: Environmental Pollution, v. 264, p. 114802, at https://doi.org/10.1016/j.envpol.2020.114802.

Yellow Springs Instruments, 2017, EXO user manual— Advanced water quality monitoring platform: Revision G, 154 pp., accessed May 1, 2026, at https://www.ysi.com/File%20Library/Documents/Manuals/EXO-User-Manual-Web.pdf.

Zhang, S., Wang, W., and Chang, J., 2019, The Contribution of Cyanobacteria Bloom Decline to Phosphorus in Water Column of Dianchi Lake, China: Polish Journal of Environmental Studies, v. 28, no. 5, p. 3513–3520, at https://doi.org/10.15244/pjoes/94217.

Zhou, J., Han, X., Brookes, J.D., and Qin, B., 2022, High probability of nitrogen and phosphorus co-limitation occurring in eutrophic lakes: Environmental Pollution, v. 292, p. 118276, at https://doi.org/10.1016/j.envpol.2021.118276.